

**Underground Injection Control
Carbon Sequestration
Class VI Permit Application**

**APPLICATION NARRATIVE
40 CFR 146.82(a)**

**NexGen Carbon Oklahoma, LLC
Vanguard CCS Hub**

June 2025

Table of Contents

List of Figures	4
List of Tables	7
List of Equations	8
Acronyms and Abbreviations	9
1.0 Project Background and Contact Information	13
1.1 Project Goals, Partners, and Collaborators	19
1.2 Project Timeframe	19
1.3 Proposed Injection Mass/Volume and CO ₂ Source	20
1.4 Injection Depth Waver and or Aquifer Exemption.....	22
1.5 List of Permits or Construction Approvals Well Drilling, Completion and P&A.....	22
1.6 List of State, Tribe, Territory Contacts.....	22
2.0 Site Characterization.....	24
2.1 Regional Geology, Hydrogeology, and Local Structural Geology [40 CFR 146.82(a)(3)(vi)]	27
2.1.1 Tectonic and Structural History	34
2.1.2 Stratigraphy	43
2.1.3 General Hydrogeology	70
2.2 Maps and Cross Sections of the AoR [40 CFR 146.82(a)(2), 146.82(a)(3)(i)]	87
2.2.1 Map of the Area of Review.....	87
2.2.2 Maps of the Injection and Confining Zones	90
2.2.3 Cross Sections Through the AoR.....	97
2.3 Faults and Fractures [40 CFR 146.82(a)(3)(ii)].....	98
2.3.1 Faults and Fractures in the Area of Review	98
2.3.2 Literature Review.....	98
2.3.3 Seismic Data	98
2.3.4 Well Data	100
2.4 Injection and Confining Zone Details [40 CFR 146.82(a)(3)(iii)]	110
2.4.1 Data on the Injection Zone.....	112
2.4.2 Data on the Confining Zones	131
2.5 Geomechanical and Petrophysical Information [40 CFR 146.82(a)(3)(iv)].....	163
2.5.1 Fractures.....	163
2.5.2 Pore Pressure.....	163
2.5.3 Stress	163
2.5.4 Ductility	166
2.5.5 Rock Strength.....	166
2.3.1 In-Situ Fluid Properties.....	166

2.3.2 Geothermal Gradient.....	166
2.6 Seismic History [40 CFR 146.82(a)(3)(v)].....	166
2.6.1 Summary of Seismic History and Available Data	166
2.6.2 Seismic Risk.....	171
2.7 Hydrologic and Hydrogeologic Information [40 CFR 146.82(a)(3)(vi), 146.82(a)(5)]	177
2.7.1 Hydrostratigraphy and Underground Sources of Drinking Water.....	177
2.7.2 Springs	180
2.7.3 Water Wells Within the Area of Review	180
2.8 Geochemistry [40 CFR 146.82(a)(6)].....	181
2.8.1 Fluid Chemistry	181
2.8.2 Solid Phase Geochemistry	185
2.9 Other Information (Including Surface Air and/or Soil Gas Data, if Applicable)	191
2.10 Site Suitability [40 CFR 146.83]	191
2.10.1 Structural and Tectonic Suitability	191
2.10.2 Storage Reservoir Suitability (Injection Zone)	191
2.11 References.....	194
3.0 AoR and Corrective Action	204
4.0 Financial Responsibility	205
5.0 Injection Well Construction.....	206
6.0 Pre-Operational Logging and Testing.....	207
7.0 Injection Well Operation 40 CFR 146.82(7) & (10)	208
8.0 Testing and Monitoring	209
9.0 Injection Well Plugging.....	210
10.0 Post-Injection Site Care (PISC) and Site Closure.....	211
11.0 Emergency and Remedial Response.....	212
12.0 Injection Depth Waiver and Aquifer Exemption Expansion	213

LIST OF FIGURES

Figure 1.1—Injection well locations.....	14
Figure 1.2—Injection well locations, AoR boundary, and CO ₂ plume outlines.....	16
Figure 1.3—Cross-section showing modeled CO ₂ concentration and the extent of the plume.....	18
Figure 2.1—Major tectonic features of Oklahoma	28
Figure 2.2—Regional cross-sections	29
Figure 2.3—Gravity map of the Midcontinent Region.....	31
Figure 2.4—Detailed stratigraphy of the Cambrian through Middle Pennsylvanian in western Osage County, Oklahoma	33
Figure 2.5—Map of Midcontinent Rift extending from Grenville Front to northeastern Kansas	35
Figure 2.6—Precambrian basement map of northeastern Oklahoma	36
Figure 2.7—Southern Oklahoma Aulacogen.....	38
Figure 2.8—Known and inferred faults basement faults in northeastern Oklahoma	40
Figure 2.9—Contoured surface of Mississippian Limestone across the Labette Fault within the Vanguard CCS Hub AoR.....	41
Figure 2.10—Stratigraphy and geophysical log response for the Paleozoic section.....	44
Figure 2.11—Representative vintage composite petrophysical log for the area of the Vanguard CCS Hub AoR.....	45
Figure 2.12—Geologic map of Oklahoma showing regional outcrop patterns.....	46
Figure 2.13—Detailed geologic map of Osage County.....	47
Figure 2.14—Basement structure for northern Oklahoma	50
Figure 2.15—Distribution of the Arbuckle aquifer	52
Figure 2.16—Thickness of Arbuckle Group carbonate in Osage County	54
Figure 2.17—Thickness of Arbuckle Group in northern Oklahoma	55
Figure 2.18—Seismic profile A -A' from Kolawale et al., 2019 and profile H – H' from Elebiju et al., 2011.....	56
Figure 2.19—Seismic profiles F-F' and G-G' from Elebiju et al., 2011	57
Figure 2.20—Petrophysical log showing radiogenic beds in dolomite toward the base of the Arbuckle Group	59
Figure 2.21—Structure of the Arbuckle Group in northern Oklahoma.....	60
Figure 2.22—Thickness of the Simpson Group in northern Oklahoma	62
Figure 2.23—Structure of the Woodford Shale in northern Oklahoma.....	63
Figure 2.24—Thickness of the Woodford Shale in northern Oklahoma	64
Figure 2.25—Geologic map of Osage County and parts of adjacent counties.....	69
Figure 2.26—The location of the proposed Project Vanguard CCS Hub AoR	72
Figure 2.27—Map from Oklahoma Water Resources Board (OWRB).....	74
Figure 2.28—Position of the Vanguard CCS Hub AoR	76
Figure 2.29—Transition of water chemistry in the Vamoosa-Ada aquifer	80
Figure 2.30—Cross section A-A' in T.25N., R.6E. to R.8E.	81
Figure 2.31—Cross section B-B' in T.26N., R.6E. to R.8E.....	82
Figure 2.32—Location of the proposed Vanguard CCS Hub AoR	84
Figure 2.33—Image of vintage wireline log.....	86
Figure 2.34—Area of Review basemap.....	89
Figure 2.35—Cross-section T – T' showing the thickness of subunits in the Arbuckle Group.....	91

Figure 2.36—Cross-section NE-SW showing gamma-ray and density-neutron porosity log profiles and petrophysical properties of Simpson Group shale, Woodford Shale and lower Mississippian Limestone confining zones	93
Figure 2.37—Thickness of the combined Simpson shale and Woodford Shale to form the Simpson-Woodford confining zone	94
Figure 2.38—Thickness of the lower Mississippian Limestone confining unit relative to the AoR.....	95
Figure 2.39—Cross-section R-R' showing resistivity characteristics of the Woodford Shale-Simpson Group shale and lower Mississippian Limestone confining zones	96
Figure 2.40—Portion of the central part of the Vanguard CCS Hub AoR	101
Figure 2.41—Seismic line that transects the Vanguard CCS Hub AoR.....	102
Figure 2.42—Strike plots of conductive natural fractures.....	104
Figure 2.43—Strike plot of faults interpreted for the Shaw 5A-8 and Hickory Creek Dome 2A-22.....	105
Figure 2.44—Vertical distribution of fractures across the lower Mississippian Limestone confining zone	107
Figure 2.45—Strike plot of drilling induced fractures in the Shaw 5A-8	108
Figure 2.46—State of stress in Oklahoma and southern Kansas	109
Figure 2.47—Stratigraphic nomenclature and biostratigraphy for the Arbuckle Group	113
Figure 2.48—Block diagrams showing (A) the regional depositional setting for Arbuckle carbonates and (B) the hypothetical depositional model	114
Figure 2.49—Initial (A) and main (B) stages of karst development from Lynch (1990).....	115
Figure 2.50—Regional karst environments	116
Figure 2.51—Cross section and enlarged sections of petrophysical logs.....	117
Figure 2.52—Lateral extent of Arbuckle and equivalent Cambro-Ordovician carbonates across North America	118
Figure 2.53—Pressure-depth gradients for the Arbuckle Group from drill-stem tests and static fluid levels	120
Figure 2.54—Core photographs of the Cotter Dolomite in the upper Arbuckle	123
Figure 2.55—Comparison of dissolution and karst features to density and neutron porosity.....	124
Figure 2.56—Dissolution and karst features in the Upper Arbuckle Group injection zone	125
Figure 2.57—Dissolution and karstic features in the Upper Arbuckle Group injection zone	128
Figure 2.58—Thickness of shale in the Simpson Group	132
Figure 2.59—Thickness of the Woodford Shale confining unit in the area of the Vanguard CCS Hub AoR	133
Figure 2.60—Stratigraphic relationship between the Arbuckle injection zone, Woodford Shale-Simpson Shale confining zone, lower Mississippian confining zone.....	134
Figure 2.61—Thickness of the lower Mississippian Limestone confining unit based on gamma-ray, density-neutron porosity and microresistivity curves	135
Figure 2.62—Cross section R-R'	137
Figure 2.63—Wireline log responses and porosity and permeability measurements.....	141
Figure 2.64—Seismic section through Blackland field	143
Figure 2.65—Gas chromatograph and porosity logs for the Bird Creek 2A-15 well.....	144
Figure 2.66—Evidence of a vertical permeability barrier in the Arbuckle Group	146
Figure 2.67—Flow baffles in the middle and lower Arbuckle Group	147
Figure 2.68—Salinity data (left) and isotopic data (right) from Wellington field, Kansas	148
Figure 2.69—Open-hole geophysical logs and microresistivity formation image across the Woodford Shale	151

Figure 2.70—Open-hole geophysical logs and microresistivity formation image across the lower Mississippian Limestone confining zone.....	153
Figure 2.71—Total rock powder X-ray diffraction spectrum of Woodford Shale from Noble County, Oklahoma	155
Figure 2.72—Geophysical log sections across the upper Arbuckle Group, Simpson Group and lower Mississippian Limestone.....	157
Figure 2.73—Whole rock powdered sample x-ray diffraction mineralogy of the light gray to green shale in the Simpson Group	159
Figure 2.74—Mineralogy of the Cotter Dolomite, upper Arbuckle Group	161
Figure 2.75—Locations of historic 1897 to 2002 earthquakes in Oklahoma	168
Figure 2.76—Seismic events >1.0 M for Osage County and adjacent areas.....	170
Figure 2.77—Correlation of earthquake moment magnitudes (Mw) to known and inferred faults from Hu (2019)	173
Figure 2.78—National Seismic Hazard Model (2023) map	175
Figure 2.79—Simplified seismicity hazard map	176
Figure 2.80—Location of most of the AoR on the drainage divide between the Salt Creek and Bird Creek/Hominy Creek drainage basins	181
Figure 2.81—Regional distribution of salinity in the Arbuckle aquifer	190

LIST OF TABLES

Table 2.1—Site characterization summary.....	26
Table 2.2—Maps, Cross Sections and Other Figures Through the AoR.....	97
Table 2.3—Seismic surveys and published seismic profiles, Osage County, Oklahoma.....	99
Table 2.4—Geologic characteristics of the proposed Vanguard CCS Hub Site.....	111
Table 2.5—Eaton's (1969) method estimated fracture gradients for the Lower Mississippian and Woodford Shale confining zones based on the uncertainty range of Poisson's ratio for each zone derived from dipole sonic logs in the Conservancy 11-3W well.	165
Table 2.6—Seismic Events for Osage County from the Oklahoma Geological Survey Earthquake Catalog	169
Table 2.7—Seismic Events >1.0 M from the United States Geological Survey (USGS) Earthquake Catalog for Osage County between February 2013 and February 2025. Event numbers correspond to numbers shown on Figure 2.76.	169
Table 2.8—Summary table of measured and calculated TDS values for formation waters from relevant zones within a 6-mile buffer of the Vanguard CCS Hub AoR.	183
Table 2.9—Salinity Measurements from Water Samples, Osage County, Oklahoma	184
Table 2.10—Measured XRD mineralogy Upper Arbuckle injection zone from Lynch (1990).....	185

LIST OF EQUATIONS

Equation 2.1—Bulk density.....	164
Equation 2.2—Eaton's method (Eaton, 1969) calculation for estimating fracture gradient.	164
Equation 2.3—R _w calculated from R _t and porosity	177
Equation 2.4—conversion of R _w to NaCl salinity.	178
Equation 2.5—calculation of formation temperature using AMST and BHT.....	178
Equation 2.6—calculation of resistivity of mud filtrate (R _{mf}) at formation temperature (T _f).....	178
Equation 2.7—calculation equivalent water resistivity (R _{we}) from spontaneous potential (SP)	178
Equation 2.8—conversion of R _{we} is to R _w	179
Equation 2.9—Archie equation for calculating water saturation S _w	182
Equation 2.10—CO ₂ storage volume calculation (after Bachu 2006).....	193

ACRONYMS AND ABBREVIATIONS

Note: All terms are written as used in the text.

°	degrees
%	percent
µmho	micromhos
µS	microSiemens
2D	two dimensional
A	
AOI	area of interest
AoR	Area of Review
API	American Petroleum Institute
ATSM	American Society for Testing and Materials
AWRI	Annis Water Resources Institute
B	
bbl	barrel(s)
Bcf	billion cubic feet
bgs	below ground surface
BHP	bottomhole pressure
BHT	bottomhole temperature
BOP	blowout preventer
C	
CBL	cement bond log
CCS	carbon capture and storage
CCUS	carbon capture, utilization, and storage
CEJST	Climate and Economic Justice Screening Tool
CFR	Code of Federal Regulations
CO ₂	carbon dioxide (may also refer to other carbon oxides)
CRA	corrosion resistant alloy
D	
DIC	dissolved inorganic carbon
DITF	drilling-induced tensile fractures
DOC	dissolved organic carbon
DOE	Department of Energy
E	
ECOS	Environmental Conservation Online System
EHS	environmental, health and safety
EJ	environmental justice
ELAN	elemental analysis
EOS	equation of state

EPA	Environmental Protection Agency
ERP	emergency response plan
ERRP	emergency and remedial response plan
ESHIA	Environmental, Social and Health Impact Assessment
F	
F	Fahrenheit
FMI	formation microimager
ft	feet/foot
ft/D	feet per day
ft/mile	feet per mile
ft ² /D	square feet per day
ft ³ /sec	cubic feet per second
G	
g/cm ³	grams per cubic centimeter
gpm	gallons per minute
GR	gamma ray
GSDT	Geologic Sequestration Data Tool
H	
HHRA	Human Health Risk Assessment
I	
IEA	International Energy Agency
in.	inch
L	
lbfm	pound mass
lbf	pound force
M	
Ma	million years
mD	millidarcy
MD	measured depth
MDT	Modular Formation Dynamics Tester
MEM	mechanical earth model
mg/L	milligrams per litter
MICP	mercury injection capillary pressure
MIRU	move in and rig up
MIT	mechanical integrity test
MM	million
MMCF	million cubic feet
Mt	megatonne/million metric tons
Mt/yr	million metric tons per year
Mta	million metric tons per annum
mV	millivolt

N

NexGen	NexGen Carbon Oklahoma, LLC
NHD	National Hydrography Dataset
NMR	Nuclear Magnetic Resonance
NPDES	National Pollutant Discharge Elimination System

O

OCWP	Oklahoma Comprehensive Water Plan
OD	outside diameter
ohm-m / Ω m	ohm meters – unit of resistivity
OSHA	Occupational Safety and Health Administration

P

P&A	plug and abandon
PGA	peak ground acceleration
PISC	post-injection site care
PLSS	Public Land Survey System
POD	point of diversion
P _p	pore pressure
ppm	parts per million
psi	pounds per square inch
psi/ft	pounds per square inch per foot
psig	pounds per square inch gauge

R

RCA	routine core analysis
RCRA	Resource Conservation and Recovery Act
RHOB	bulk density log
Rmf	resistivity of mud filtrate
Rw	resistivity of connate water

S

SCADA	supervisory control and data acquisition
SCAL	special core analyses
sc-CO ₂	supercritical carbon dioxide
SCP	State Cleanup Program
SEM	scanning electron microscope
SHmax	maximum horizontal stress
SHmin	minimum horizontal stress
SP	spontaneous potential
SRT	step-rate test
SS	subsea
SSTVD	subsea true vertical depth
Sv	vertical stress
SWD	saltwater disposal

T

t	tonne / metric ton
TCS	triaxial compressive strength
TD	total depth
TDS	total dissolved solids
ThruBit™	SLB through-the-bit logging - an openhole logging tool that is deployed from within drill string for difficult logging jobs
TVD	true vertical depth
TVDSS	true vertical depth subsea

U

UIC	Underground Injection Control
US	United States
USDW	Underground Source of Drinking Water
USFWS	U.S. Fish & Wildlife Service
USGS	U.S. Geological Survey
UST	underground storage tanks

W

WHP	wellhead pressure
wt%	weight percent

X

XRD	X-ray diffraction
XRF	X-ray fluorescence

1.0 PROJECT BACKGROUND AND CONTACT INFORMATION

NexGen Carbon Oklahoma, LLC (“NexGen”) is a privately owned Oklahoma-based limited liability company which was principally established to develop a carbon dioxide (CO₂) capture and permanent storage (CCS) project in northern Oklahoma: the Vanguard CCS Hub (the “Project”). The Project is designed to mitigate the detrimental consequences of industrial CO₂ emissions. NexGen is owned equally by NexGen Carbon Solutions, LLC and Prairie Carbon Solutions, LLC. The parent companies of both owners have decades of prior experience in exploration and development of hydrocarbons in northeastern Oklahoma. NexGen owns pipeline easements and rights of way comprising over 650 miles within the Project area.

The proposed CO₂ storage site is located in Osage County, in northeastern Oklahoma (**Figure 1.1**). Initially, NexGen will develop the first phase of the project (“Phase 1”). Phase 1 encompasses approximately 75,000 acres of contiguous carbon storage leases which NexGen has acquired. The surface lands above the proposed storage leases are primarily used for ranching and conservation. At such time that the Class VI permits are approved and issued, the full development of Phase 1 will proceed. This will entail the following: (i) construction of an extensive CO₂ pipeline system to transport the CO₂, in a supercritical state, from the emission sites to the storage sites; (ii) drilling and completion of ten (10) injection and ten (10) above-zone and seven (7) in-zone monitoring wells; and (iii) construction of capture facilities located at nearby industrial CO₂ emitters. The CO₂ will be transported from the emission sites through the pipeline system and injected for permanent storage. The operational area for the sequestration sites covers several townships in Osage County and covers an Area of Review (“AoR”) of 137 sq miles.

Claimed as PBI

Figure 1.1—Injection well locations (Vanguard I-1, Vanguard I-2, Vanguard I-3, Vanguard I-4, Vanguard I-5, Vanguard I-6, Vanguard I-8, Vanguard I-9, Vanguard I-10, Vanguard I-12) and NexGen's phase 1 land position.

The expected maximum daily injection rate for each well is 18 million cubic ft per day (MMcf/D) of CO₂, which translates to approximately 350,000 metric tons per year (Mta) per injection well. It is anticipated that the CO₂ injection period for Phase 1 will be 20 years, and the total permanent quantity of CO₂ stored will be approximately 71 million metric tons (Mt) collectively from the 10 injection wells. It is intended that Phase 1 of the Project will be fully operational in 2028, capturing, transporting, and storing CO₂ at volumes up to 3.5 Mta collectively.

The Project is designed to operate within safe geomechanical limits, maintaining injection pressures below 90% of the fracture gradient at the top of the Arbuckle Group. Injection wells target the upper 60% of the Arbuckle, to avoid low permeability zones in the lower 40% and to minimize the risk of induced seismicity. The Arbuckle, approximately 950 ft thick, consists primarily of carbonate rocks from the Upper Cambrian and Lower Ordovician, capped by multiple impermeable confining units including the Woodford Shale and lower Mississippian Limestone, with an average thickness of 80 ft. These units provide containment, while additional formations above the lower Mississippian offer tertiary confinement. NexGen will deploy above-zone monitoring wells to ensure confining integrity, in-zone wells to monitor the pressure front, and USDW wells to detect CO₂ contamination and seismic activity. Additionally, 2D seismic monitoring will track plume growth during and after injection.

The Project's area of review (AoR) represents the area where USDWs may be at increased risk due to the Project, as determined through modeling and simulation. The design indicates that 90 percent of the frac gradient will never be reached during the injection period. The preliminary size of the AoR for the entire phase 1 project site is approximately 88,000 acres. The spacing for each injector well is expected to be 3,000 acres or more. The AoR was modeled using the critical pressure threshold calculation, based on the characteristics of the USDWs, the injection zone and the maximum differential pressure occurring at the end of injection. Based on modeling and simulation results, the expected maximum subaerial extent of the CO₂ plume within the Arbuckle Group is approximately 55,000 acres and the expected critical pressure boundary of the entire AoR encompasses approximately 77,000 acres (**Figure 1.2**). Following 224 the rilling, coring, sampling and logging of a stratigraphic test well(s), the geologic model and simulation will be updated and revised to provide a better estimate of the AoR impacts.

Claimed as PBI

Figure 1.2—Injection well locations, AoR boundary, and CO₂ plume outlines ($\geq 2\%$ concentration in 2146).

The selection of the proposed Project site was based on a culmination of several relevant factors that indicated the location to be an ideal candidate for a commercial CCS project. Both the confining layers and the targeted injection zone are regionally extensive and possess the necessary properties to safely contain the injected CO₂ and displaced formation fluids. Furthermore, there is minimal faulting, and seismic activity in the area has been negligible. NexGen has identified, evaluated, and classified all 218 artificial penetrations (APs) penetrating the upper confining units within the AoR.

The potential conduits related to these APs within the AoR will be evaluated, and as required, mitigated through appropriate corrective measures. Well plugging, well construction, and operational parameters for this Project are designed to protect Underground Sources of Drinking Water (“USDW”), prevent surface releases, and inject at rates that will not fracture the storage reservoir or the confining units and/or induce seismicity. Available data indicates that the AoR is rooted in igneous granites of Precambrian age and there are no known transmissive faults within the AoR. The Project site is in an area of Oklahoma where only modest seismic events have been detected. Present USDW withdrawals within the AoR are from only five (5) shallow groundwater wells that are 100 and 254 ft deep, respectively (see *Section 3*). These wells service only domestic users. Importantly, according to the Oklahoma Water Resources Board there are no water source wells in northwest Osage County that provide water for human consumption.

The general topographic relief within the AoR is at an elevation between 1,000 and 1,100 ft above sea level. The area is mainly grasslands, with minimal relief and sparse forestland. The facilities for the site will be located exclusively on private land leased to NexGen.

A schematic cross-section diagram (**Figure 1.3**) depicts the ten (10) proposed injection wells and their associated CO₂ plumes at site closure in 2146. The Project site will be owned and operated by NexGen. NexGen will continuously monitor operations both at the surface and subsurface and provide collected data to the Environmental Protection Agency (EPA) within prescribed times and formats. Permitting and oversight for this project will be through the EPA, unless the State of Oklahoma is granted primacy over Class VI permitting.

Claimed as PBI

Figure 1.3—Cross-section showing modeled CO₂ concentration and the extent of the plume ($\geq 2\%$ saturation) at the end of PISC (site closure).

The State of Oklahoma plans to establish a carbon hub in the area of the planned CO₂ storage site; NexGen intends to work closely with the State of Oklahoma and the Oklahoma Corporation Commission as a coordinated participant.

Project Contact Information:

NexGen Oklahoma, LLC
600 Rockmead Drive, Suite 112
Kingwood, TX 77339
817-239-2686
marcthomas@nexgencarbonsolutions.com

Amended plans or demonstrations per this permit application shall be submitted to the UIC Program Director as follows:

1. Within one year of an Area of Review (AoR) reevaluation
2. Following any significant changes to the facility, such as addition of monitoring wells or newly permitted injection wells within the AoR, on a schedule determined by the Underground Injection Control (UIC) Program Director, or
3. When required by the UIC Program Director.

1.1 Project Goals, Partners, and Collaborators

NexGen Carbon Oklahoma, LLC (“NexGen”) plans to partner with industrial CO₂ emitters from the refining, fertilizer and cement manufacturing sectors to address CO₂ emissions at their source. NexGen will focus on demonstrating the feasibility and scalability of CCS technology to capture, transport and permanently store approximately 71 million tons of CO₂ over a 20-year injection period.

- Warrior Exploration & Production LLC & Prairie Carbon Solutions LLC
- Stanford Center for Carbon Storage
- Oklahoma Geologic Survey
- University of Oklahoma
- Baker Hughes Company
- Koch Energy Services
- SLB-Aker Carbon Capture
- ION Clean Energy
- Burns & McDonnell
- Quanta Services

1.2 Project Timeframe

2024

- Initiated project by verifying pore space ownership, conducting comparative market analysis and leasing of 75,000 acres.
- Initiated discussions with commercial, research & academic, engineering & technology partners, industrial emitters and the Osage Nation.

- Prepare Class VI Permit Application

2025–2026

- Submit Class VI application, accounting for EPA Region 6 concerns.
- Initiate Front End Engineering and Design (“FEED”) work scope for carbon capture, transportation and storage with engineering & technology vendors.
- Execute agreements with industrial emitters.
- Drill and evaluate a stratigraphic well test, update geologic and computational models.
- Accommodate and modify Class VI application to address additional EPA Region 6 concerns required for approval.

2027–2028

- Execute engineering, procurement and construction agreements with carbon capture, transportation and storage vendors.
- Obtain required permits for construction and installation of carbon capture, transportation and storage project components.
- Construct and install carbon capture, transportation and storage project components.
- Initiate carbon capture, transportation and storage activities.

1.3 Proposed Injection Mass/Volume and CO₂ Source

CO₂ Pipelines

The pipeline and stations shall be designed and constructed in accordance with all applicable Federal, State and local laws and regulations; in accordance with all permits; in accordance with the latest edition of the basic codes, standards and permits listed below.

Design & Construction Basis

Code	Title
API Spec. 5L	American Petroleum Institute: Specification for Line Pipe
API RP 1102	American Petroleum Institute: Steel Pipelines Crossing Railroads and Highways
API Std. 1104	American Petroleum Institute: Welding of Pipelines and Related Facilities
API Std. 1130	American Petroleum Institute: Computational Pipeline Modeling for Liquid Pipelines
NACE.P0169	National Association of Corrosion Engineers: Control of External Corrosion on Underground or Submerged Metallic Piping Systems
NACE.P0177	National Association of Corrosion Engineers: Mitigation of Alternating Current and Lightning Effects on Metallic Structures and Corrosion Control Systems
NACE MR0175	National Association of Corrosion Engineers: Control of External Corrosion on Underground or Submerged Metallic Piping Systems
ISO 15589-1	Petroleum and natural gas industries – Cathodic protection of pipeline transportation systems – Part 1: On-land Pipelines
ISO 15589-2	Petroleum and natural gas industries – Cathodic protection of pipeline transportation systems – Part 2: Offshore Pipelines
ISO 27913	Carbon Dioxide Capture, transportation and Geological Storage - Pipeline Transportation Systems
API Spec. 6D	American Petroleum Institute: Specification for Pipeline Valves (Gate, Plug, Ball and Check Valves)
ASME B16.5	American Society of Mechanical Engineers: Pipe Flanges and Flanged Fittings
ASME B16.9	American Society of Mechanical Engineers: Factory-Made Wrought Steel Butt Welding Fittings
MSS-SP-44	Manufacturers Standardization Society: Steel Pipeline Flanges
MSS-SP-75	Manufacturers Standardization Society: Specification for High Test Wrought Butt-Welding Fittings
MSS-SP-97	Manufacturers Standardization Society: Integrally Reinforced Forged Branch Outlet Fittings – Socket Welding, Threaded, and Butt-Welding Ends
49 CFR 195	Transportation of Hazardous Liquids by Pipeline
Federal, State, and Local	County Highway Department Pipeline Crossing /Encroachment Permit
Federal, State, and Local	NPDES General Permit for temporary hydrotest discharge activities
Federal, State, and Local	NDPDES General Permit for Stormwater Discharges Associated with Construction Activity

1.4 Injection Depth Waver and or Aquifer Exemption

CCS Equipment

The CCS Equipment shall be designed and constructed in accordance with all applicable Federal, State and local laws and regulations; in accordance with all permits; in accordance with the latest edition of the basic codes, standards and permits.

Design & Construction Basis

1.3.1. Stripper Contactor Vessels: The Stripper Contactor vessels will be designed, fabricated, inspected, tested, stamped, and certified in full compliance with ASME section VIII, Div. 1.

1.3.2. CO₂ Absorber Contactor Vessels: The CO₂ Absorber Contactor vessels will generally be designed and constructed in accordance with ASME Section VIII, Div. 1 to the extent applicable to these vessels. These vessels, which have a design pressure just over ambient and are open to the atmosphere, will not be code stamped and will not require Authorized Inspector involvement. The reinforcement at the inlet duct will be designed using either the breech opening analysis rules in ASME STS-1 or using finite element analysis (FEA) with stress categorization and acceptance based on ASME Section VIII, Div 2 procedures, but with Div 1 basic design factors. API-650 and/or API-620 will be referenced for guidelines on detailing of the vessel floor, which are not provided in ASME Section VIII.

1.3.3. Direct Contact Cooler Vessels: The DCC vessels will be designed and constructed on the same basis as described above for the Absorber vessels. The top, round-to-square transition and outlet duct will be designed using FEA using applicable design by analysis procedures described

1.5 List of Permits or Construction Approvals Well Drilling, Completion and P&A

Well drilling, completion and P&A shall be designed and constructed in accordance with all applicable Federal, State and local laws and regulations; in accordance with all permits; in accordance with the latest edition of the basic codes, standards and permits.

Design & Construction Basis

EPA 40 CFR

OCC Title 165 Chapter 10 (Drilling/Complete) and Subchapter 11 (P&A) regulations.

1.6 List of State, Tribe, Territory Contacts

Oklahoma Department Environmental Quality
Office of Business & Regulatory Affairs
Lloyd Kirk
405-702-7105

Oklahoma Secretary of Energy & Environment
Brandy Wreath
405-522-7099

Plan revision number: 0
Plan revision date: 6/24/2025

Oklahoma Commissioner of Corporation Commission
Brian Bingman
405-521-2211

Oklahoma Area III Commissioner Conservation Commission
Grant Victor
918-257-1213

Osage Nation
Director Department of Natural Resources
Craig Walker
918-287-5531

GSDT Submission - Project Background and Contact Information

GSDT Module: Project Information Tracking

Tab(s): General Information tab; Facility Information and Owner/Operator Information tab

Please use the checkbox(es) to verify the following information was submitted to the GSDT:

Required project and facility details *[40 CFR 146.82(a)(1)]*

2.0 SITE CHARACTERIZATION

The site characterization included within this application will demonstrate that NexGen Carbon Oklahoma, LLC's (NexGen) proposed Vanguard CCS Hub (the "Project") is ideally situated for the permanent geologic storage of CO₂. These reasons include, but are not limited to:

- The upper and middle section of the Arbuckle Group is an ideal injection zone of laterally continuous, thick (500 to 600 ft) carbonate with intervals of high-porosity (10–12%), and high-permeability (10s to > 1,000 millidarcy) dolomitic limestone with occasional thin sandstone and shale beds. The Vanguard CCS Hub is expected to sequester 350,000 metric tons per year, per injection well for a total of approximately 71 million tons (Mt) over 20 years.
- The Arbuckle Group lies beneath a sequence of geologic layers that effectively isolate it from the Vamoosa-Ada aquifer, the lowermost Underground Source of Drinking Water ("USDW"). The primary confining unit, the combined shale beds of the Simpson Group and Devonian Woodford Shale, consists of low-permeability shale and mudstone. The secondary confining unit, the low-permeability lower Mississippian Limestone, lies above the Simpson Group and Woodford Shale. Overlying these confining units are thick Pennsylvanian shales that further enhance isolation.
- The Arbuckle Group and confining units are not structurally complex. The formations have a gentle local and regional structural dip with few identified faults or geologic hazards within the modeled plume/pressure front extent ("Area of Review" or "AoR").
- Water samples indicate that the Arbuckle is saline (approximately 115,000 to 140,000 mg/L), with no economically recoverable hydrocarbon resources within the gross injection interval within the AoR.
- The injection and monitoring wells will be designed to prevent fluids from migrating to USDWs.
- The operator, NexGen Carbon Oklahoma, LLC, will control the pore space occupied by the modeled plume.

The Site Characterization provides text, tables, and figures to fulfill the requirements of 40 CFR §146.82(a)(2), (3), (5), and (6). It provides information on regional and local geology, hydrogeology and hydrostratigraphy, geologic structure, and detailed characterization of lithology, mineralogy, geochemistry, and reservoir and geomechanical properties of the confining and injection zones.

Data, information, and interpretations described in this section are summarized in the following text, demonstrating the Vanguard CCS Hub and AoR to be geologically and hydrologically favorable for the permanent storage of CO₂:

- The extent and structure of the Cherokee Platform, along with its tectonic setting, make it an ideal location for CO₂ storage. Much of the platform consists of relatively simple structures with shallow dips (less than one degree within the AoR). Recent faulting is absent from the injection and upper confining zones. No significant seismic hazards are present in the AoR (*Sections 2.1, 2.3*).
- The regional geologic setting is well constrained due to thousands of wellbore penetrations from petroleum exploration and production that began in 1901 within the area (*Section 2.2*).
- Within the AoR, the Cambrian-Ordovician Arbuckle Group is an excellent reservoir for injection with high porosity (average 7%) and permeability (geometric mean: 26 mD). (*Sections 2.4.1, 2.5*).
- Within the AoR, the Arbuckle Group is highly saline with no economic quantities of hydrocarbons (*Sections 2.1.3.6, 2.8.1*).

- The Arbuckle Group is encountered at adequate depths for pressures and temperatures favorable for storing supercritical CO₂, thousands of ft below currently exploited groundwater aquifers and the lowermost USDW (*Sections 2.4.1, 2.7*).
- The Arbuckle Group is laterally extensive with no known stratigraphically or structurally trapped oil and gas within the AoR. Faulting within the AoR and the surrounding area is tectonic, and karst collapse in origin. Faults related to karst/collapse appear to sole-out within the upper Arbuckle and are detached from the lower Arbuckle and underlying granitic basement. While the top of the Arbuckle and the primary confinement interval (Woodford and Simpson Shale) appear to have occasional noticeable fault offset on seismic in the northern part of AoR (both tectonic and karst/collapse related), pressure and salinity data indicate isolation of the upper Mississippian Chat reservoir from the Arbuckle aquifer across geologic time. Interpretation and mapping of the GAM_Miss_SecondaryConfinementTophorizon demonstrates little to no fault offset, suggesting potential fault leakage risks above the secondary confinement zone could be considered minimal.
- The Arbuckle Group has the pore volume to store many times more CO₂ than proposed by this Project (*Section 2.10.2.1*).
- The Arbuckle Group is vertically bound by the combination of shale in the Simpson Group and the Woodford Shale that forms a laterally continuous upper confining layer consisting of approximately 4 to 60 ft of low permeability shale and mudstone. Additional vertical confinement is provided by the lower Mississippian Limestone, the secondary upper confining zone. Thick, laterally continuous, shales in the Pennsylvanian section provide tertiary vertical isolation between the Arbuckle and lowermost USDW (*Sections 2.4.2, 2.10.2*).
- As the Arbuckle Group is an open saline aquifer, CO₂ would be confined vertically by the overlying Simpson Group shale-Woodford Formation and lower Mississippian zone while lateral confinement would initially occur via residual and solubility trapping and then ultimately via mineral trapping (Xu et al., 2001; Bachu and Adams, 2003; Bachu, 2006; Saadatpoor et al., 2010; Kampman et al., 2014; Ajayi et al., 2019) (*Sections 2.2.2, 2.10.2*). Separating the injection and storage interval from the basement will be achieved by a series of low-porosity, low-permeability dolomite beds that form flow baffles that impede and ultimately block the downward flow of injectate.
- No detrimental geochemical interactions are expected between the injectate and the formations or formation fluids. This expectation will be confirmed via future core and fluid analyses along with geochemical modeling (*Section 2.8*).

This site characterization is based on a comprehensive review of publicly available data, including geologic maps, reports, and data repositories, supplemented by public record requests. References are appropriately cited throughout, and a list of all citations with links to where the source can be downloaded or acquired is provided in **List of Cited References_OsageHub.xlsx**. Additional proprietary and public site-specific data, including well records, geophysical logs, and 3D seismic surveys, were acquired and incorporated into this permit application.

A guide of detailed site characterization discussions is provided in Table 2.1.

Plan revision number: 0

Plan revision date: 6/24/2025

Table 2.1—Site characterization summary.

CFR	Section Title	Section No.	Sub-Section Title	Sub-Section No.
40 CFR 146.82(a)(3)(iii)	Regional Geology, Hydrology, and Local Structural Geology	2.1	Tectonic and Structural History	2.1.1
			Stratigraphy	2.1.2
			General Hydrogeology	2.1.3
40 CFR 146.82(a)(2), 146.82(a)(3)(i)	Maps and Cross Sections of the Area of Review	2.2	Map of Area of Review	2.2.1
			Structure Maps of the Injection and Confining Zones	2.2.2
			Cross Sections Through the AoR	2.2.3
40 CFR 146.82(a)(3)(ii)	Faults and Fractures	2.3	Literature Review	2.3.1
			Seismic Data	2.3.2
			Well Data	2.3.3
40 CFR 146.82(a)(3)(iii)	Injection and Confining Zone Details	2.4	Data on the Injection Zone	2.4.1
			Data on the Confining Zone(s)	2.4.2
			Fractures	2.5.1
			Pore Pressure	2.5.2
40 CFR 146.82(a)(3)(iv)	Geomechanical and Petrophysical Information	2.5	Stress	2.5.3
			Ductility	2.5.4
			Rock Strength	2.5.5
			In-Situ Fluid Properties	2.5.6
			Geothermal Gradient	2.5.7
40 CFR 146.82(a)(3)(v)	Seismic History	2.6	Summary of Seismic History and Available Data	2.6.1
			Seismic Risk	2.6.2
40 CFR 146.82(a)(3)(vi), 146.82(a)(5)	Hydrologic and Hydrogeologic Information	2.7	Hydrostratigraphy and Underground Sources of Drinking Water	2.7.1
			Springs	2.7.2
			Water Wells Within the AoR	2.7.3
40 CFR 146.82(a)(6)	Geochemistry	2.8	Fluid Chemistry	2.8.1
			Solid Phase Geochemistry	2.8.2
			Geochemical Modeling	2.8.3
-	Other Information	2.9	Not Applicable	-
			Structural and Tectonic Suitability	2.10.1
40 CFR 146.83	Site Suitability	2.10	Storage Reservoir Suitability (Injection Zone)	2.10.2
			Confining Zone Suitability	2.10.3

2.1 Regional Geology, Hydrogeology, and Local Structural Geology [40 CFR 146.82(a)(3)(vi)]

The proposed Vanguard CCS Hub (the “Project”) geologic storage site (the “Site” or the “Project Area”) is situated on the southwestern flank of the Cherokee Basin, within the Cherokee Platform of northeastern Oklahoma (**Figure 2.1**). The Cherokee Platform is bounded by significant structural features including the Ozark Uplift, Bourbon Arch, Nemaha Ridge, Arbuckle Uplift, and the Arkoma Basin. Regionally, the geology consists of Paleozoic formations that dip gently to the southwest, influenced by the surrounding uplifts and ridges (**Figure 2.2**).

Plan revision number: 0

Plan revision date: 6/24/2025

Claimed as PBI

Figure 2.1—Major tectonic features of Oklahoma and the position of the NexGen Carbon Oklahoma: Project Vanguard CCS AoR on the Cherokee Platform in Osage County, northeastern Oklahoma. Cross-sections W-E and S-N are shown in **Figure 2.2**.

Plan revision number: 0

Plan revision date: 6/24/2025

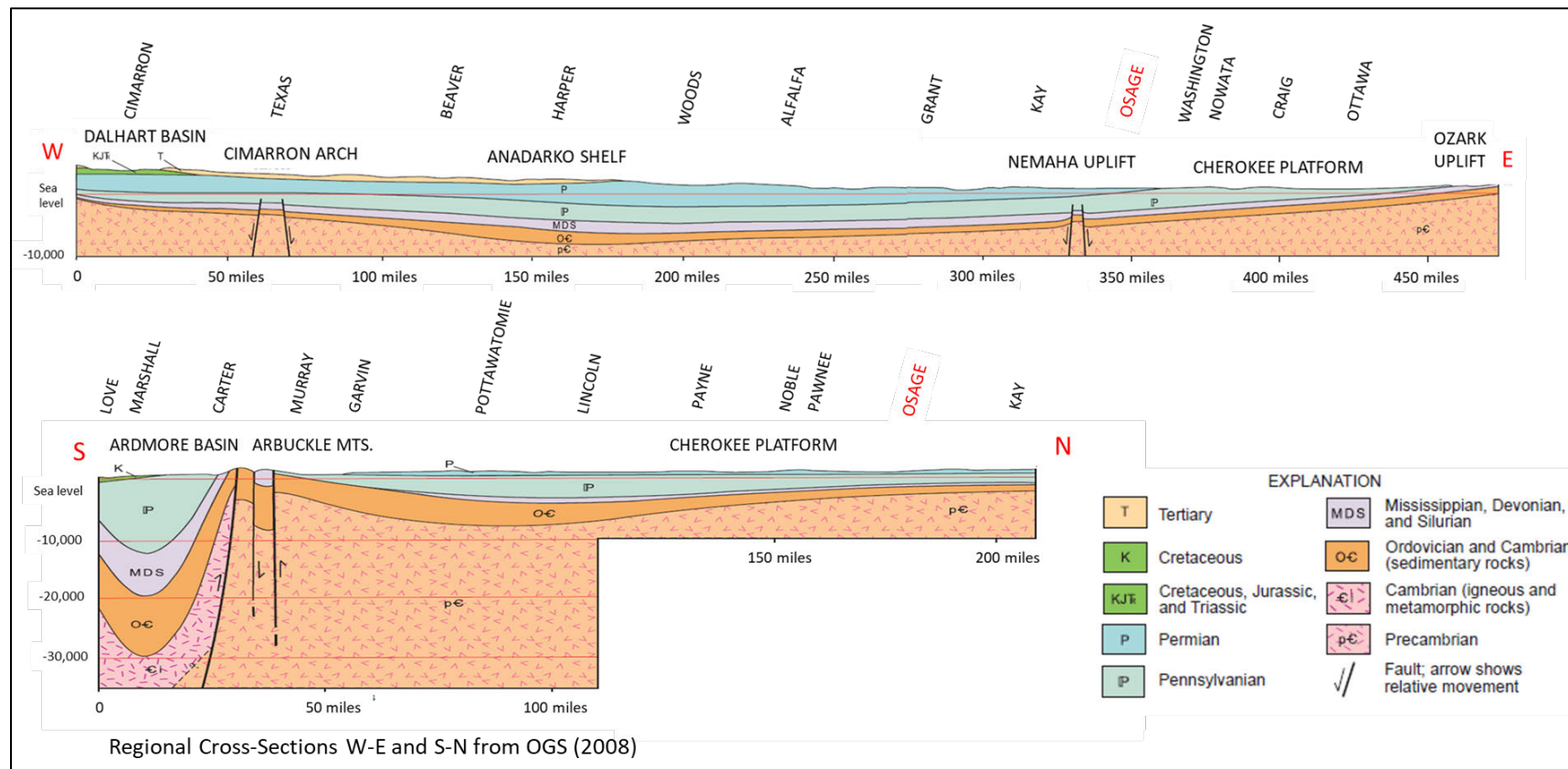


Figure 2.2—Regional cross-sections showing the position of Osage County on the Cherokee Platform, the lateral continuity of the Ordovician and Cambrian section, including the Arbuckle Group injection zone, and the gentle dip of the sedimentary strata to the southwest toward the Nemaha Uplift (cross-section W-E) and the Arbuckle Uplift (cross-section S-N).

Plan revision number: 0

Plan revision date: 6/24/2025

Structurally, the Site is located near the northwestern flank of the Osage High, a prominent Precambrian igneous feature (**Figure 2.3**). Tectonic activity in the region, such as the development of the Nemaha Ridge and Ozark Uplift, occurred during the Pennsylvanian period, driven by the Pennsylvanian Orogeny. This tectonic activity shaped the local fault systems, but the proposed site remains buffered from major basement-rooted faults associated with the Nemaha Uplift that offset Paleozoic strata, contributing to its suitability for geologic storage

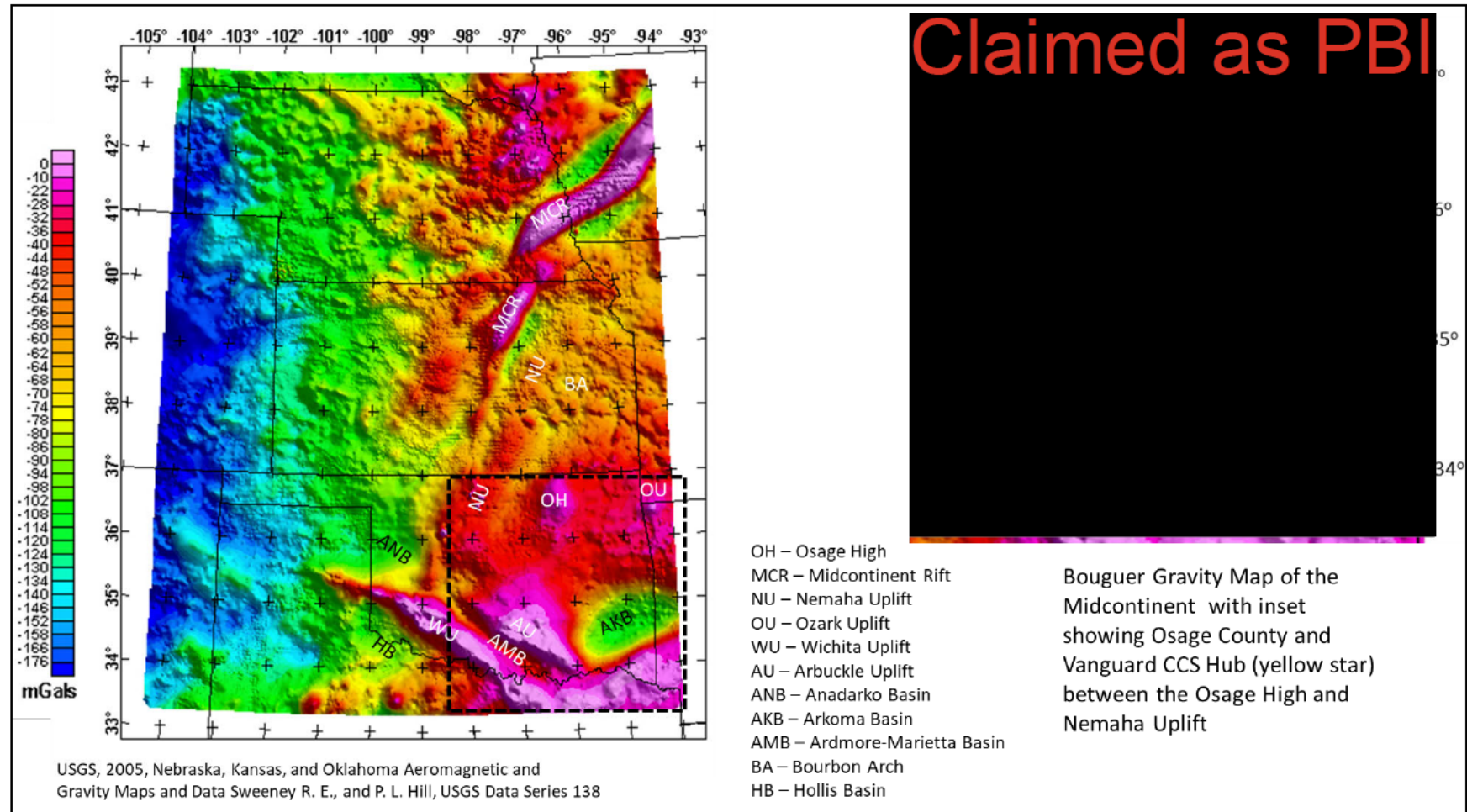


Figure 2.3—Gravity map of the Midcontinent Region showing prominent basement features. The NexGen Project Vanguard CCS site is in a tectonically quiescent area between the Osage High and the Nemaha Uplift.

The injection zone for CO₂ is within the upper and middle intervals of the Arbuckle Group (**Figure 2.4**), which exhibit enhanced dissolution porosity related to karst development, making them ideal for fluid injection. In central and western Osage County, the top of the Arbuckle Group is encountered at depths ranging from approximately 2,650 ft to >4,400 ft below ground surface (bgs). Confining units above the Arbuckle injection zone include shale intervals in the Ordovician Simpson Group and Devonian Woodford Shale that provide primary confinement to protect the shallow Vamoosa-Ada USDW, and the lower Mississippian Limestone (**Figure 2.4**) that provides secondary confinement. These confining zones provide effective containment of injected fluids due to their fine-grained, low-permeability characteristics and regional continuity that prevent the upward migration of injectate. Additional protection of the Vamoosa-Ada USDW is provided by the approximately 2,000 ft of shale-dominated Pennsylvanian section between the base of the aquifer and top of the Mississippian Limestone. Downward migration of CO₂ within the Arbuckle Group is prevented by a series of low-porosity, low-permeability baffling beds whose cumulative thickness forms an effective barrier to fluid migration (**Figure 2.4**).

The combination of geological stability, favorable injection zone characteristics, and effective confinement makes the site well-suited for carbon sequestration. The bedrock hydrology of the area features minor, discontinuous shallow aquifers within upper Pennsylvanian and lower Permian rocks, along with one major aquifer that is minimally used for local water supply. The primary aquifer, the Vamoosa-Ada aquifer (Osborn and Hardy, 1999), is an Underground Source of Drinking Water (USDW) in places, transitioning from freshwater (<10,000 mg/L) conditions in the east of the Project Area to brine-filled (>10,000 mg/L TDS) towards the west. In T.26N., R.6E., where the Elgin Sandstone is thick, it is a USDW to a depth of 1,100 ft.

Separation between the USDW and the proposed injection zone typically exceeds 2,500 ft, with approximately 2,000 ft of separation near the deepest areas with higher-quality water. This significant separation, combined with confining units, provides robust hydrologic isolation and ensures effective containment between the injection zone and overlying aquifers.

Plan revision number: 0

Plan revision date: 6/24/2025

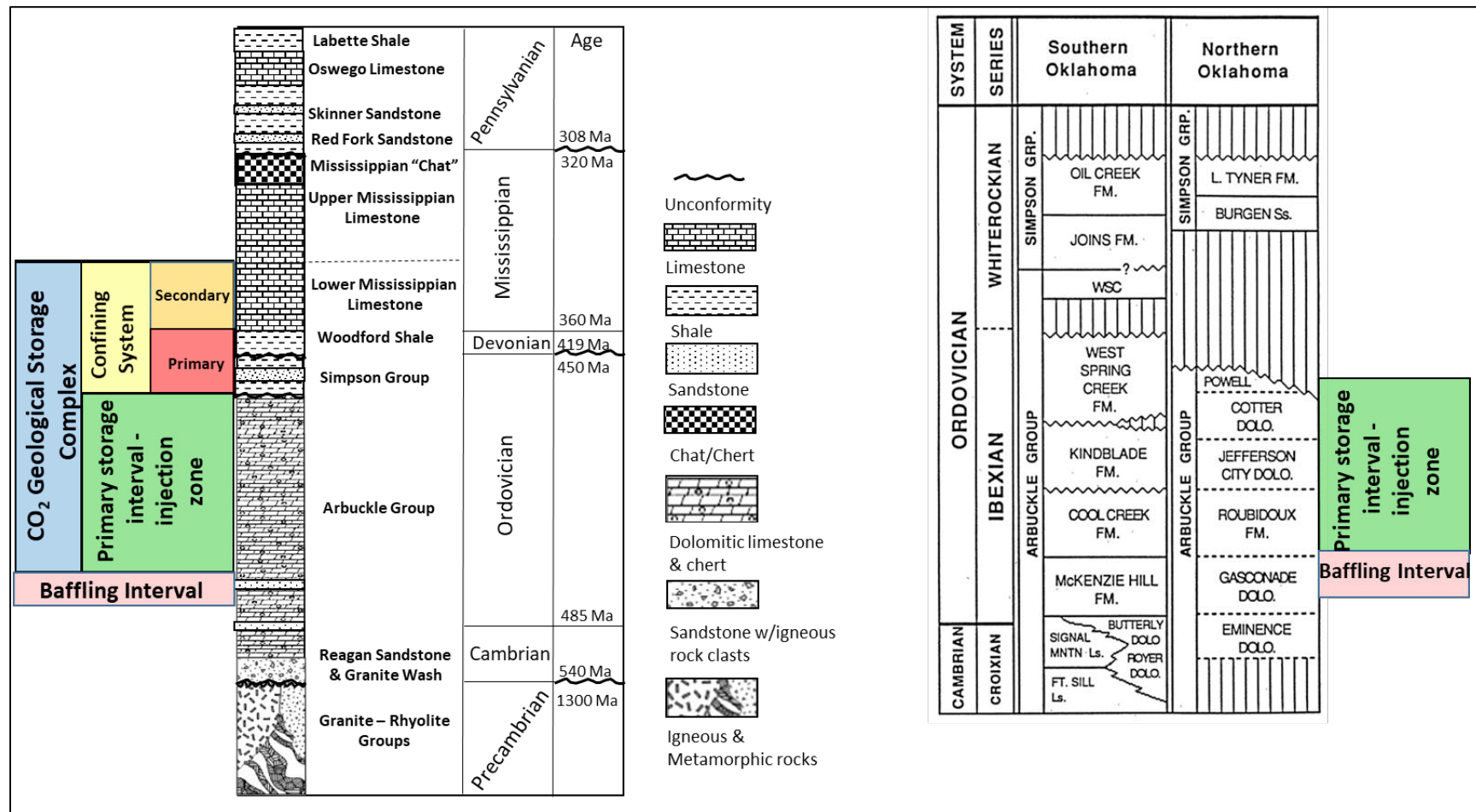


Figure 2.4—Detailed stratigraphy of the Cambrian through Middle Pennsylvanian in western Osage County, Oklahoma, with position the upper Arbuckle Injection and Storage zone, Simpson Shale-Woodford Shale-lower Mississippian Limestone Confining System and middle-lower Arbuckle baffling interval.

2.1.1 Tectonic and Structural History

The proposed geologic storage site is located on the southwestern flank of the Cherokee Basin within the Cherokee Platform, which spans northeastern Oklahoma and southeastern Kansas. The Ozark Uplift bounds the Cherokee Platform to the east, Nemaha Uplift to the west, Arbuckle Uplift and Arkoma Basin to the south, and Bourbon Arch to the north (**Figure 2.1** and **Figure 2.2**). The Cherokee Platform covers approximately 26,500 square miles and includes the Cherokee Basin, a Paleozoic sag that was influenced by the Bourbon Arch and the Osage High, with the sequestration site situated near the western flank of the Osage High (**Figure 2.3**). The basement rocks of the Osage High are of Precambrian age and their emplacement is attributed to processes related to the Grenville Orogeny and the Midcontinent Rift.

This igneous activity was initiated approximately 1.1 billion years ago, during the late Precambrian Grenville Orogeny that occurred due to the collision of the Yavapai-Mazatzal-Superior and Grenville Precambrian provinces. Extensional forces northwest of the Grenville collision were likely caused by a massive hotspot beneath the North American craton (Stein et al., 2015). The Midcontinent's triple junction, located beneath Lake Superior, includes the western and eastern arms of a failed rift system, each extending over 1,000 miles. The western arm (**Figure 2.5**) runs from Lake Superior southwest through Wisconsin, Minnesota, Iowa, Nebraska, and southern Kansas, leaving behind thick igneous layers dominated by basalt that generate the gravity anomaly evident in **Figure 2.3**. Precambrian basement provinces with varying ages, structures, and compositions were deformed by this rift, which is evident on gravity and magnetic maps (**Figure 2.3**; Sweeney and Hill, 2005).

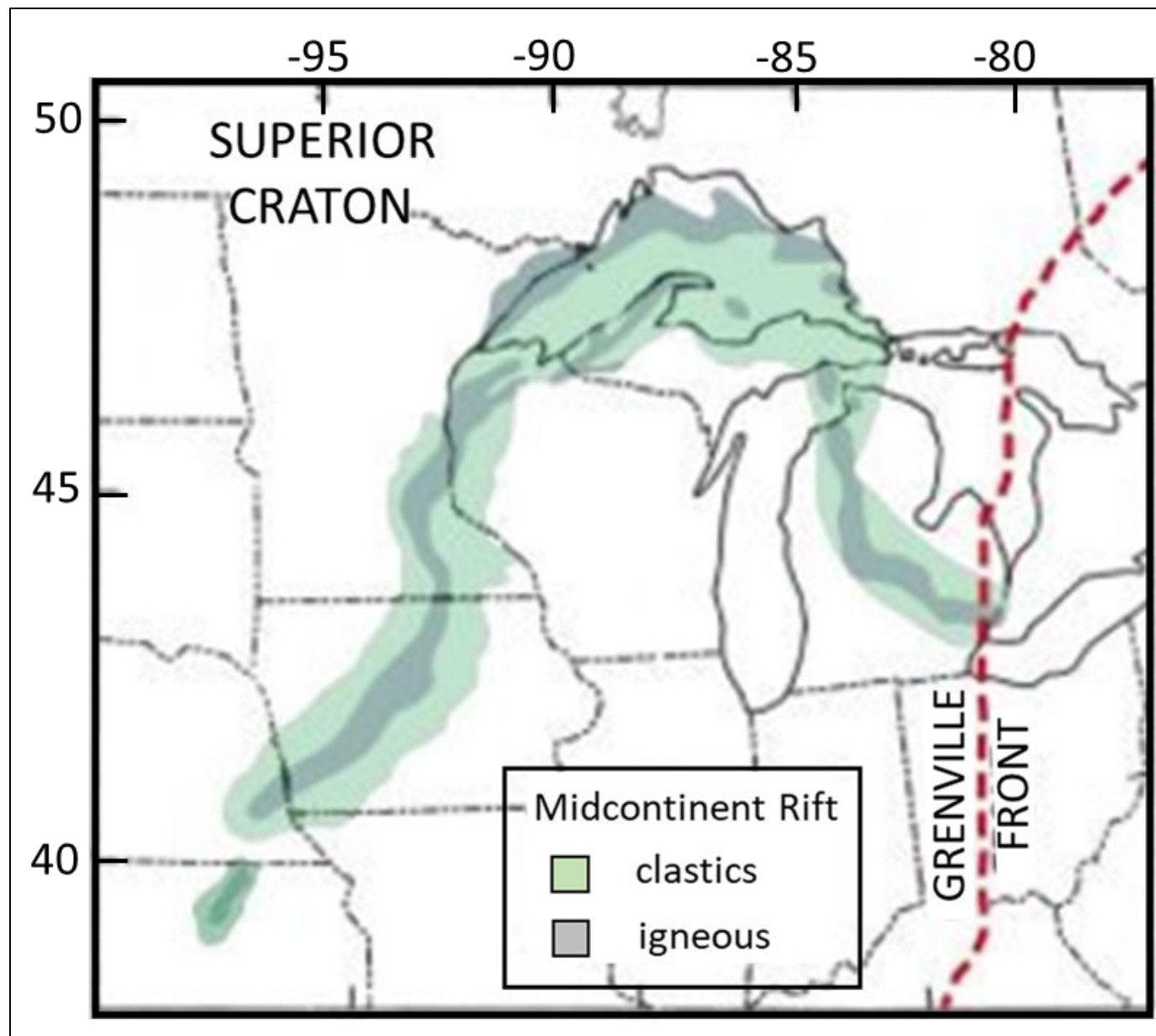


Figure 2.5—Map of Midcontinent Rift extending from Grenville Front to northeastern Kansas. Igneous rocks generate Bouguer gravity anomaly evident in Figure 2.3. After Stein et al. (2015).

The Nemaha Uplift, a series of uplifted fault blocks to the west of Osage County and the Vanguard CCS site, is attributed to isostatic uplift from the thick basalts beneath the Midcontinent ridge. The rhyolite and granite intrusions forming the Precambrian Hills in Osage County also occurred during the development of this rift. A Precambrian basement map of northeastern Oklahoma, including Osage County is shown in Figure 2.6.

Claimed as PBI

Figure 2.6—Precambrian basement map of northeastern Oklahoma. Vanguard CCS Hub AoR is on Washington Volcanic Group and Central Oklahoma Granite Group. After Campbell and Weber (2006). Basement rock interpretation from Denison (1981) and Denison et al. (1984).

The next major tectonic event to shape the Midcontinent was the formation of the Southern Oklahoma Aulacogen (**Figure 2.7**) that is an interpreted failed rift (Keller, 2014) or a transform fault associated with Iapetan rifted margin of Laurentia (Thomas, 2014) that began during the early to middle Cambrian. Rifting in this region, encompassing the present-day Wichita and southwestern Arbuckle mountains, produced large volumes of Early Cambrian gabbro, granite and rhyolite, the youngest dated at approximately 525 Ma (Gilbert, 2014). After rifting ceased, subsidence formed first the Oklahoma Basin (Johnson and Cardott, 1992) and its successor, the Anadarko Basin (Perry, 1989). The Pennsylvanian Orogeny (318–298 Ma), a major tectonic event, generated the Wichita, Arbuckle and Ouachita mountains. The Ouachita Mountain thrust and fold belt extends from central Arkansas into southeastern Oklahoma and includes intensely deformed rocks ranging in age from Lower Paleozoic to the Pennsylvanian (Lillie et al., 1983; Sellars, 1967; Roberts, 2005). Stress associated with the formation of the Ouachita mountains influenced basement rocks in the southern Midcontinent region and generated a major component to the present stress field in northern Oklahoma (Hurd and Zoback, 2012).

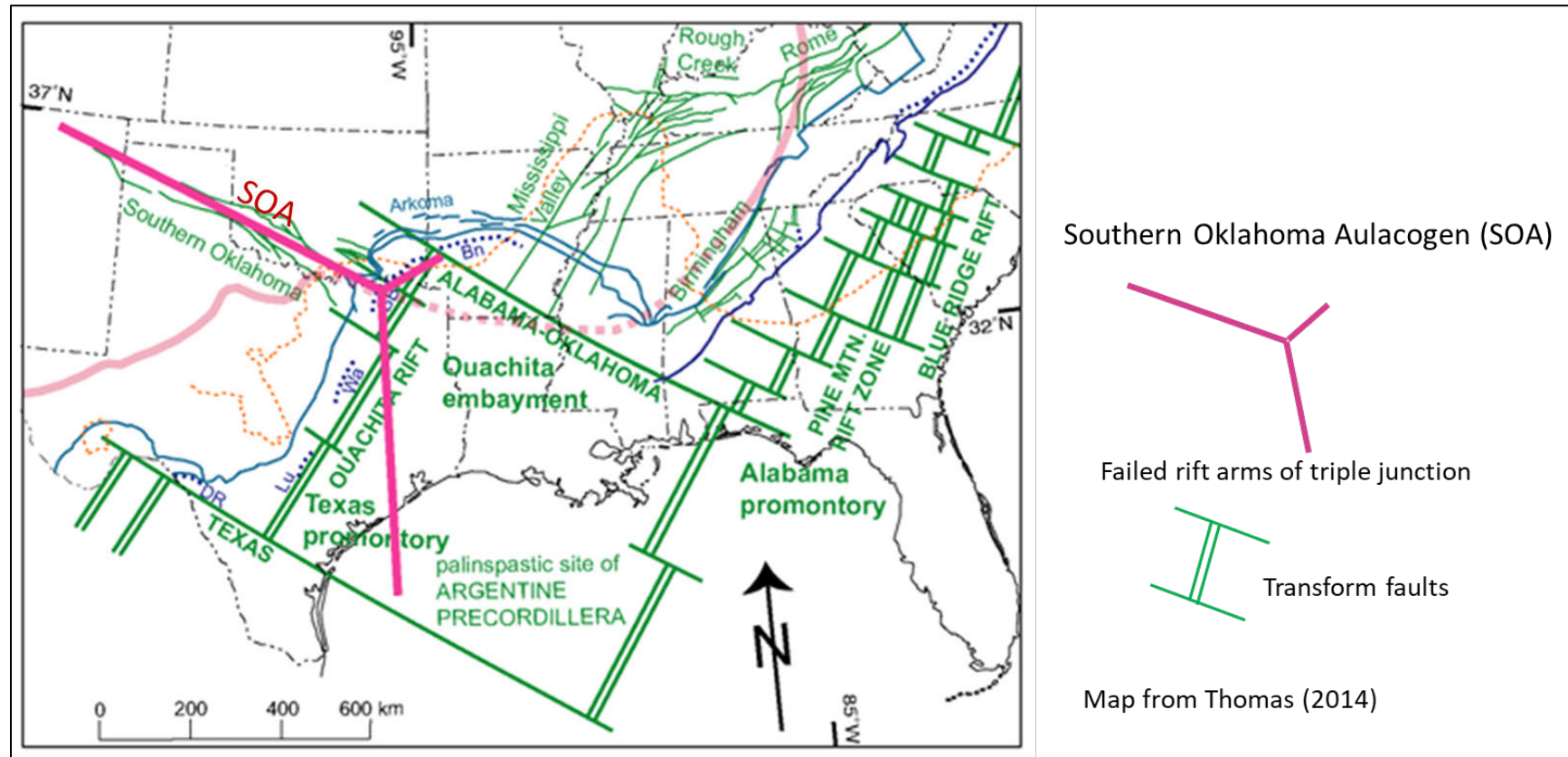


Figure 2.7—Southern Oklahoma Aulacogen interpreted as a failed rift associated with a triple junction and transform faults associated with lapetan rifting of Laurentia (after Thomas, 2014).

By the Middle Pennsylvanian, Oklahoma's geologic provinces were well-developed or actively forming (West, 2015). Cross-section W–E (**Figure 2.2**) shows the Arbuckle Uplift south of the gently dipping Cherokee Platform, where strata exhibit a west-southwest dip. Structural features in Osage County include localized domes, basins, folds, and surficial en echelon normal faults trending north-northwest, at high angle to the maximum horizontal stress orientation (Thorman and Hibpshman, 1979). Subsurface faults include the dominant SW–NE trending Labette and Wilzetta; smaller faults trending northwest are also present (Marsh and Holland, 2016; Hu, 2019). Compared to other regions of Oklahoma, Osage County has relatively minor structural deformation.

The Pennsylvanian marked a transition in the Midcontinent from a passive to an active margin. This shift began during the Late Mississippian and Early Pennsylvanian, driven by plate collision and the southward subduction of the Laurentian plate beneath Gondwana (Houseknecht, 1986). This collision initiated Appalachian Mountain building and influenced the development of geologic provinces throughout Oklahoma and Arkansas. In the late Pennsylvanian, uplifts and orogenies, including the Ozark Uplift (east), Ouachita Uplift (southeast), Arbuckle Uplift (south) and Wichita Uplift (southwest), further shaped the region. Early and middle Pennsylvanian tectonics divided the previously stable Oklahoma Basin, Ouachita Trough, and Southern Oklahoma Aulacogen into a series of basins and uplifts, creating the modern geologic provinces (**Figure 2.1**).

Fault zones trending southwest to northeast include the Nemaha, Labette, and Wilzetta (**Figure 2.8**). The Nemaha Fault Zone lies west of Osage County, while the Labette Fault Zone traverses Osage County and passes through the NexGen Carbon Oklahoma, LLC Project Vanguard CCS site. The inferred extension of the west branch of the Wilzetta Fault Zone passes southeast of the CCS site. Despite the proximity of these fault systems, no major mappable faults are evident in the Paleozoic section near the proposed NexGen CCS site. The Labette Fault, described by Denison (1981), exhibits no evidence of Paleozoic movement. A detailed map (**Figure 2.9**) shows the Labette Fault trend beneath the Vanguard CCS Hub's AoR without influencing the structural attitude of the overlying Mississippian section by generating faults or folds subparallel to the trend. The Labette Fault transects the northwest flank of the Osage High with no discernible offset as confirmed by 3-D seismic data.

Claimed as PBI

Figure 2.8—Known and inferred faults basement faults in northeastern Oklahoma from Marsh and Holland (2016) and Hu (2019). The Labette Fault and associated faults trending SE – NW across the Vanguard CCS Hub AoR, shown outlined in blue, are not expressed in the Paleozoic section; see **Figure 2.9**.

Plan revision number: 0

Plan revision date: 6/24/2025

Claimed as PBI

Figure 2.9—Contoured surface of Mississippian Limestone across the Labette Fault within the Vanguard CCS Hub AoR showing no apparent structural trends associated with the Labette and associated faults.

Fault distribution and variation in basement composition likely influence seismically active regions in central Oklahoma. However, the northwestern Osage County region surrounding the NexGen CCS site remains buffered from seismically active fault zones, making it a seismically stable portion of the Cherokee Platform. Seismic activity attributed to water injection is overwhelmingly basement generated (Hu, 2019) and isolation of the basement from CO₂ injection by intra-Arbuckle confining units or baffles is proposed. The cumulative effect of multiple low-permeability beds is an effective lower confining unit for the upper and middle Arbuckle injection zone. The basement rocks beneath the Arbuckle Group north of the Labette Fault are part of the Washington Volcanic Group rhyolite, and metarhyolite, whereas basement south of the Labette Fault is Central Oklahoma Granite Group, both aged between 1.4 and 1.2 billion years (Denison, 1981). Both rock types extend beyond Osage County into seismically active areas to the west and south, warranting their isolation from CO₂ injection.

The proposed injection zone is confined above by the Devonian-Mississippian Woodford Shale augmented by shale in the Ordovician Simpson Group in the southern part of the site, and lower Mississippian Limestone throughout the AoR. The Woodford Shale, a fine-grained organic and clay-rich marine deposit is complemented by the organic-lean shale of the Simpson Group. Together these shales act as the primary confining unit, while the Lower Mississippian Limestone provides secondary confinement. Both units exhibit regional continuity across most of the Cherokee Platform, ensuring effective containment of CO₂. Where present, Simpson Group shales are effective seals that would prevent injectate from reaching the Woodford Shale. The proposed injection zone is contained below by a series of low-permeability zones in the Arbuckle Group that isolate the upper part of the saline aquifer from the lower section (Watney and Holubnyak, 2017) and keep injectate and pressure from reaching the lower contact of the Arbuckle Group with the Reagan Sandstone or crystalline basement.

In addition to having a regionally continuous injection zone and multiple confining units, the Cherokee Platform has not experienced significant tectonic activity since the Pennsylvanian Subperiod, when the major faulting along the Nemaha Ridge and uplift of Ozark Dome, occurred in the latter stages of the Pennsylvanian orogeny. The Nemaha Ridge, a north-south trending positive feature, is linked to the Nemaha Fault Zone, which formed during isostatic uplift along the Mid-Continent Rift (Gerhard, 2004). While folding of shallow strata indicates vertical displacement across Nemaha faults in the Permian, no evidence shallow structure is associated with the Labette Fault to the east of the Nemaha Fault Zone. The Labette Fault, which extends northeasterly from Payne County, Oklahoma, to Labette County, Kansas, is an inferred basement structure showing no evidence of movement in Osage County during or after the Paleozoic. Historical saltwater disposal in the vicinity of the Labette fault trace in Osage County has not resulted in seismicity along the fault. This inactivity could be the result of several factors, including orientation of the fault approximately 40 to 45 degrees to principal horizontal stress, an optimal orientation to resist reactiveation (Morris et al., 1996).

The Osage High, or Precambrian Hills, to the southeast of the Vanguard CCS Hub AoR, is an igneous feature that influenced sedimentation during the Cambrian and Ordovician, especially thickness of the Arbuckle Group. Denison (1981) identified basement rocks in northeastern Oklahoma, including the Central Oklahoma Granite Group, Washington Volcanic Group, Spavinaw Group, and Osage Granite Group (**Figure 2.6**), with the Osage High associated primarily with the Osage Microgranite. These units, formed during the supercontinent Rodinia's assembly, appear to contribute to the area's tectonic stability. No recorded seismic events are associated with the Osage High's core or flanks (Hu, 2019; Luza, 2009; Walter et al., 2020).

Cross sections show the stratigraphic and structural relationships in northern Oklahoma. A west-to-east cross-section (**Figure 2.2**) illustrates the southwest dip of Paleozoic rocks, while a north-to-south section shows structural features, including the Arbuckle Mountains and compressional tectonics of the Ardmore Basin (**Figure 2.2**). A stratigraphic column (**Figure 2.10**) highlights regional lithologic units, their petrophysical log response, and their depths.

In summary, the proposed sequestration site is geologically well-suited for CO₂ storage, with consistent stratigraphy, structural stability, no historic seismicity, and effective confining and injection zones.

2.1.2 Stratigraphy

The general stratigraphy of the region is illustrated in the stratigraphic column (**Figure 2.10**). Northern Oklahoma's stratigraphy reflects a west-to-east progression of older geologic formations exposed at the surface. Regional bedrock geology is presented in (**Figure 2.12**), with a detailed geologic map of Osage County in (**Figure 2.13**). In addition to bedrock geology, these maps highlight sediment accumulation along modern streams shown as dendritic surface stream drainage patterns, including southerly drainage toward the Arkansas River and easterly drainage toward the Caney River.

Plan revision number:

Plan revision date: 6/24/2025

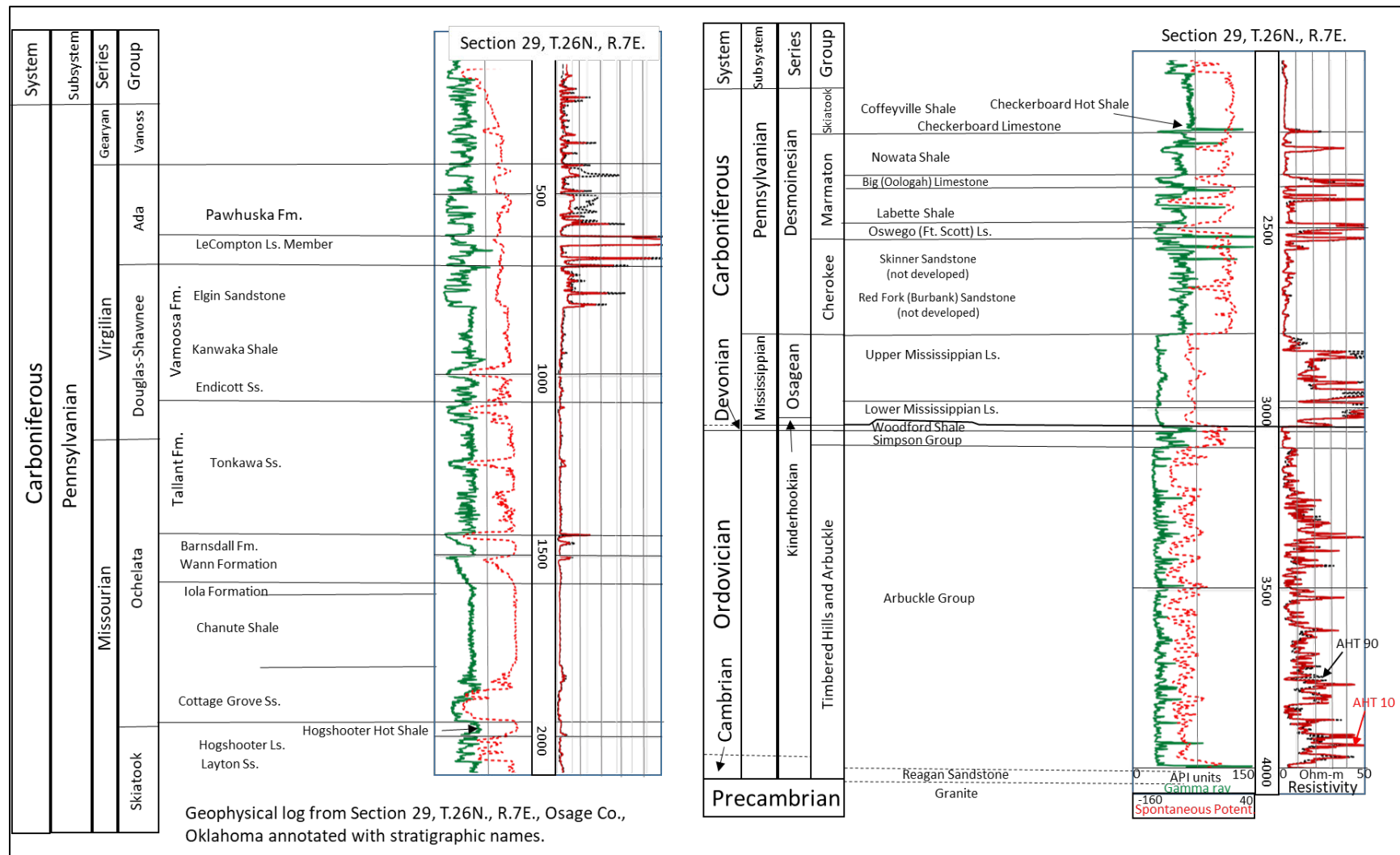


Figure 2.10—Stratigraphy and geophysical log response for the Paleozoic section and drilled portion of the Precambrian basement in T.26N., R.7E., Osage County, Oklahoma. Depths shown on log are ft below surface. A second geophysical log from T.27N., R.7E., Osage County, is Figure 2.11.

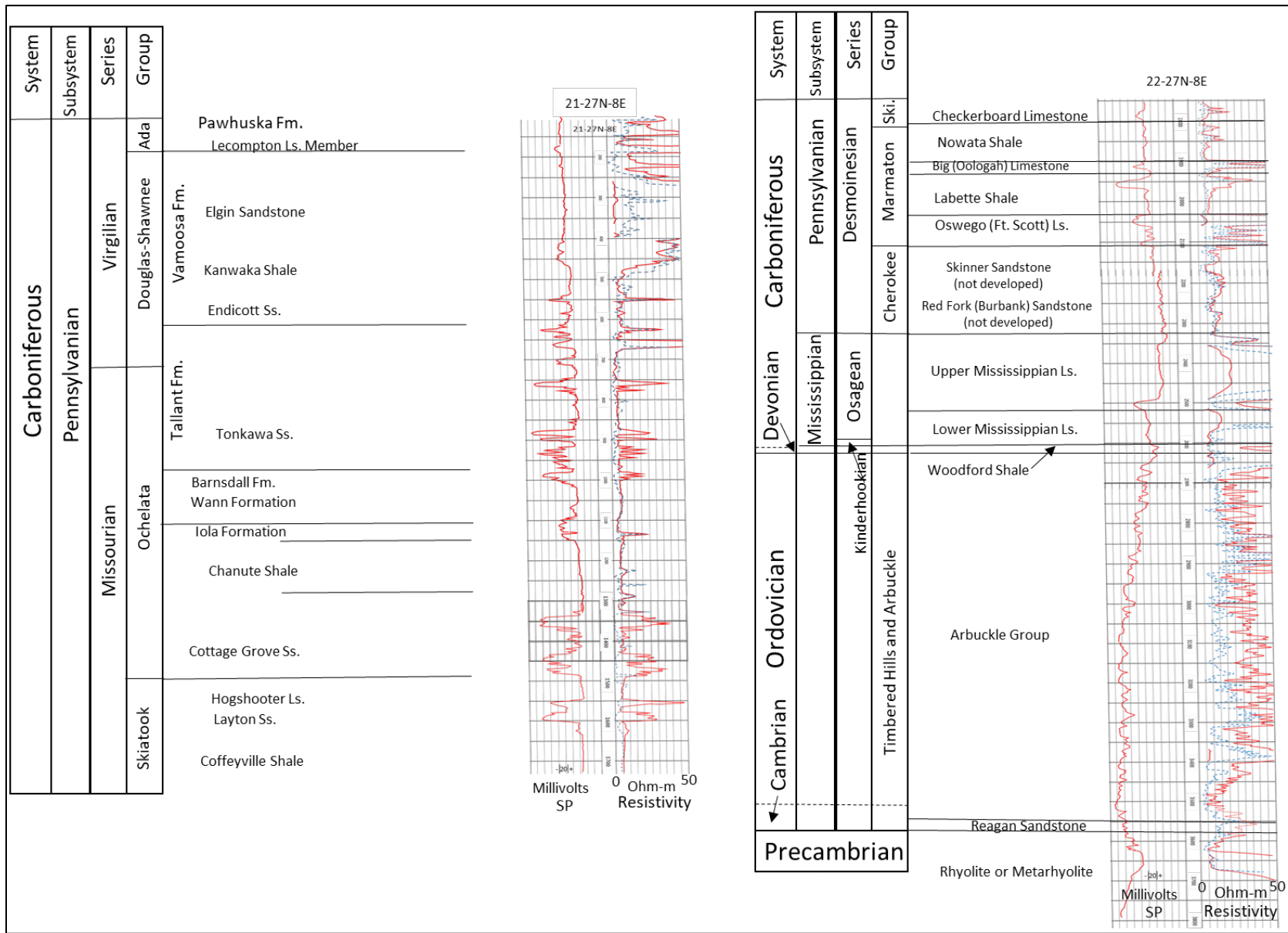


Figure 2.11—Representative vintage composite petrophysical log for the area of the Vanguard CCS Hub AoR (Sections 21 and 22, T.27N., R.7E., Osage County, Oklahoma) annotated with stratigraphy from Pennsylvanian at surface to Precambrian at total depth.

Plan revision number: 0

Plan revision date: 6/24/2025

Claimed as PBI

Figure 2.12—Geologic map of Oklahoma showing regional outcrop patterns, Osage County (black outline) and the Vanguard CCS Hub AoR (red). Map details available at <https://pubs.usgs.gov/publication/ofr03247>

Claimed as PBI

Figure 2.13—Detailed geologic map of Osage County showing the Vanguard CCS Hub AoR in red on the Pennsylvanian Ada Formation and Vanoss Group. Surface drainage pattern indicated by stream alluvium shown in light yellow. Faults indicated by the small black lines (arrows) are evident at the surface but die out with depth.

Paleozoic formations exhibit gentle dips of less than 1.5 degrees to the west and southwest in the central and eastern portions of Oklahoma. A location map (**Figure 2.1**) displays two regional cross-sections, W-E and S-N, and their relationship to Osage County and the proposed sequestration site. Cross-section W-E' (**Figure 2.2**) provides a west-to-east view of the generalized stratigraphy, emphasizing the relationship between sedimentary layers, crystalline basement, and tectonic features including the Anadarko Basin Shelf, Nemaha Ridge, and Ozark Uplift. Except where disrupted by structural features such as the Nemaha Fault and Uplift the sedimentary section dips between 0.25 and 0.5 degrees to the west-southwest over the Cherokee Platform.

Cross-section S-N (**Figure 2.2**) offers a north-to-south perspective, illustrating compressional tectonics associated with the Ardmore Basin and Arbuckle Mountains transitioning onto the Cherokee Platform. The proposed sequestration site is located approximately 25 miles east of this transect.

During the early Paleozoic era, shallow warm seas covered Osage County for over 100 million years, creating optimal conditions for carbonate sediment deposition. These carbonates formed the great American carbonate bank during the late Cambrian to early Ordovician (Derby et al., 2012). The Arbuckle Group, equivalent to the Ellenburger in Texas and New Mexico, represents these deposits. Periodic sea level fluctuations exposed carbonate banks to erosion, creating regional unconformities and karst features that enhanced porosity and permeability.

As sedimentation and burial progressed during the late Ordovician, local unconformities persisted, followed by Silurian and Devonian deposition. Regional uplift and erosion during Middle Devonian allowed meteoric flushing that promoted additional karsting within the Arbuckle Group. Rising sea level in the Late Devonian and Early Mississippian deposited sediments forming confining zones: Woodford Shale and Lower Mississippian argillaceous limestones, respectively. The primary confining unit is the Devonian Woodford Shale, with secondary confinement provided by the Lower Mississippian Limestone. Both units were deposited in marine environments mostly below normal wave base (Callner, 2014; Hill, 2017).

These regional confining units will be cored for petrophysical and geomechanical properties. Ordovician Simpson Group shale locally called Tyner will also be cored to evaluate its subregional confining characteristics near the proposed sequestration site.

In the project area, the thickness of the sedimentary section overlying the Precambrian basement ranges from approximately 3,600 ft in the east to 4,100 ft in the west. Strata relevant to the sequestration site are described in ascending order starting with the Precambrian.

2.1.2.1 Precambrian – Cambrian

Precambrian rocks form the basement beneath all local strata in Osage County. This basement, composed primarily of granite and other igneous and metamorphic rocks, is over 1 billion years old (Denison, 1981). **Figure 2.6** identifies the location of wells drilled into the basement as of 2006 and the distribution of Precambrian rock types.

The depth of the Precambrian basement varies across Osage County, ranging from less than 2,200 ft in the southeast and northeast to more than 5,000 ft along the western boundary (Rascoe and Hyne, 1988). These variations result from the regional structural dip to the southwest and thinning of the Paleozoic section over paleotopographic highs on the granite surface. **Figure 2.14** illustrates the structure of the Precambrian basement. Beneath the NexGen CCS Site, the crystalline basement

is the Washington Volcanic Group (WVG) north of the Labette fault and Central Oklahoma Granite Group to the south of the fault (**Figure 2.6**).

In some areas, the Cambrian Reagan Sandstone of the Timbered Hills Group overlies the Precambrian basement. This time-transgressive basal clastic unit fills topographic lows on the Precambrian erosional surface (Reeves et al., 1999). The Reagan is older in areas of low Precambrian relief and younger on basement highs. It is a fine-grained, well-sorted sandstone with an average thickness of 30 ft and a maximum thickness of 60 ft (Thorman and Hibbsman, 1979). Reagan deposition began during transgression associated with rising sea level, as basal sands were progressively deposited northward along with the overlying dolomitic carbonates (Dille, 1956). The Reagan Sandstone exhibits high porosity and permeability in parts of the south-central Midcontinent and was completed 28 times in Oklahoma oil and gas wells (Boyd, 2008). However, in Osage County the Reagan Sandstone is sporadically distributed and typically thin though occasional thicker sections are encountered (Reeves et al., 1999). With few wells drilled to basement, establishing the distribution of the Reagan Sandstone is difficult and only one well within the Vanguard CCS Hub AoR encountered a thin (6 ft thick) section of Reagan Sandstone. Stratigraphic testing at the NexGen Carbon Oklahoma, LLC-Project Vanguard CCS site will confirm its presence.

Claimed as PBI

Figure 2.14—Basement structure for northern Oklahoma and adjacent areas from Rascoe and Hyne (1988) digitized by the Oklahoma Geological Survey.

Plan revision number: 0

Plan revision date: 6/24/2025

2.1.2.2 Arbuckle Group

The Arbuckle Group is the primary injection zone for carbon sequestration at the NexGen CCS site. Deposited during the Mid-Cambrian to Middle Ordovician, it lies directly above the Reagan Sandstone where present, or directly atop the crystalline basement where the Reagan is absent. The Arbuckle Group or Arbuckle saline aquifer, formed as part of the “Great American Carbonate Bank” (Derby et al., 2012) and extends from the Arkoma Basin in Arkansas to the Anadarko Basin in Oklahoma, northward across Kansas to Nebraska, eastern Colorado, Iowa and Missouri (**Figure 2.15**).

Claimed as PBI

Figure 2.15—Distribution of the Arbuckle aquifer (Arbuckle and Timbered Hills groups) in the Midcontinent region, North America and the regional direction of groundwater flow in the aquifer relative to the proposed CCS site in Osage County (red star). After Jorgenson and Signor (1981).

Outside the Arbuckle Mountain Uplift, the Arbuckle Group is predominantly dolomitic limestone and dolomite with thin sandstone and shale beds. The combined Arbuckle/Timbered Hills group represents the thickest sequence of lower Paleozoic strata in Oklahoma ranging from >6,000 ft thick in southern Oklahoma to <500 ft in northern Oklahoma (Rascoe and Hyne, 1988). Thickness varies significantly in northern Oklahoma and Osage County, from being absent over basement hills on the Osage High to more than 1,400 ft in western Osage County. Thickness maps (**Figure 2.16 and Figure 2.17**) constructed from oil and gas exploration well data and seismic profiles (**Figure 2.18 and Figure 2.19**) confirm an Arbuckle thickness of approximately 900 ft at the Vanguard CCS site.

The Arbuckle Group carbonate sediments deposited in what is now northeastern Oklahoma, accumulated in a shallow shelf environment. Equivalent lithostratigraphic units include the El Paso Group (Texas), Ellenburger Group (north-central Texas), Knox Group (eastern United States), and Beekmantown Group (northeastern United States). The Arbuckle Group in northern Oklahoma is comparable to Arbuckle facies of the Ozarks and includes the Eminence Dolomite, Gasconade Dolomite, Roubidoux Formation, and Jefferson City, Cotter and Powell Dolomites (**Figure 2.4**). These dolomites, which vary in color from white to brown and texture from dense to coarsely crystalline, are significant reservoir rocks for hydrocarbons in Osage and Pawnee counties (Lynch, 1990; Rountree, 1980).

Claimed as PBI



Figure 2.16—Thickness of Arbuckle Group carbonate in Osage County and parts of Kay, Noble and Pawnee counties, Oklahoma, showing the thinning of the Arbuckle associated with elevated basement topography. Published seismic profiles and subsurface data from well logs provide detail that is not evident on regional-scale maps (Figure 2.17). Seismic profiles shown on map are Figure 2.18 and Figure 2.19.

Claimed as PBI

Figure 2.17—Thickness of Arbuckle Group in northern Oklahoma and adjacent areas from Rascoe and Hyne (1988). Outline of AoR in red.

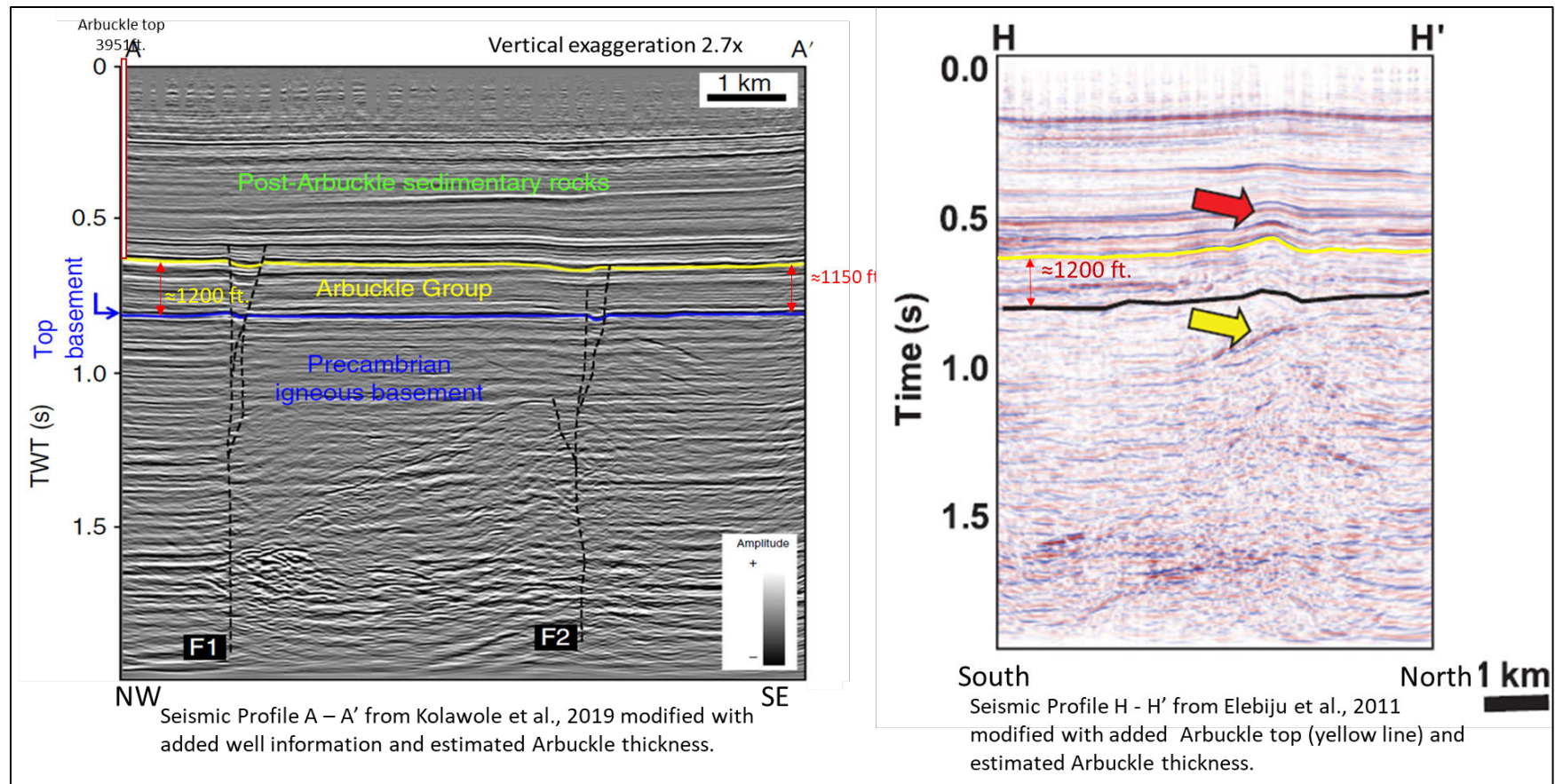


Figure 2.18—Seismic profile A -A' from Kolawale et al., 2019 and profile H – H' from Elebiju et al., 2011 showing normal thickness of Arbuckle carbonate. Location of profiles is shown on Figure 2.16.

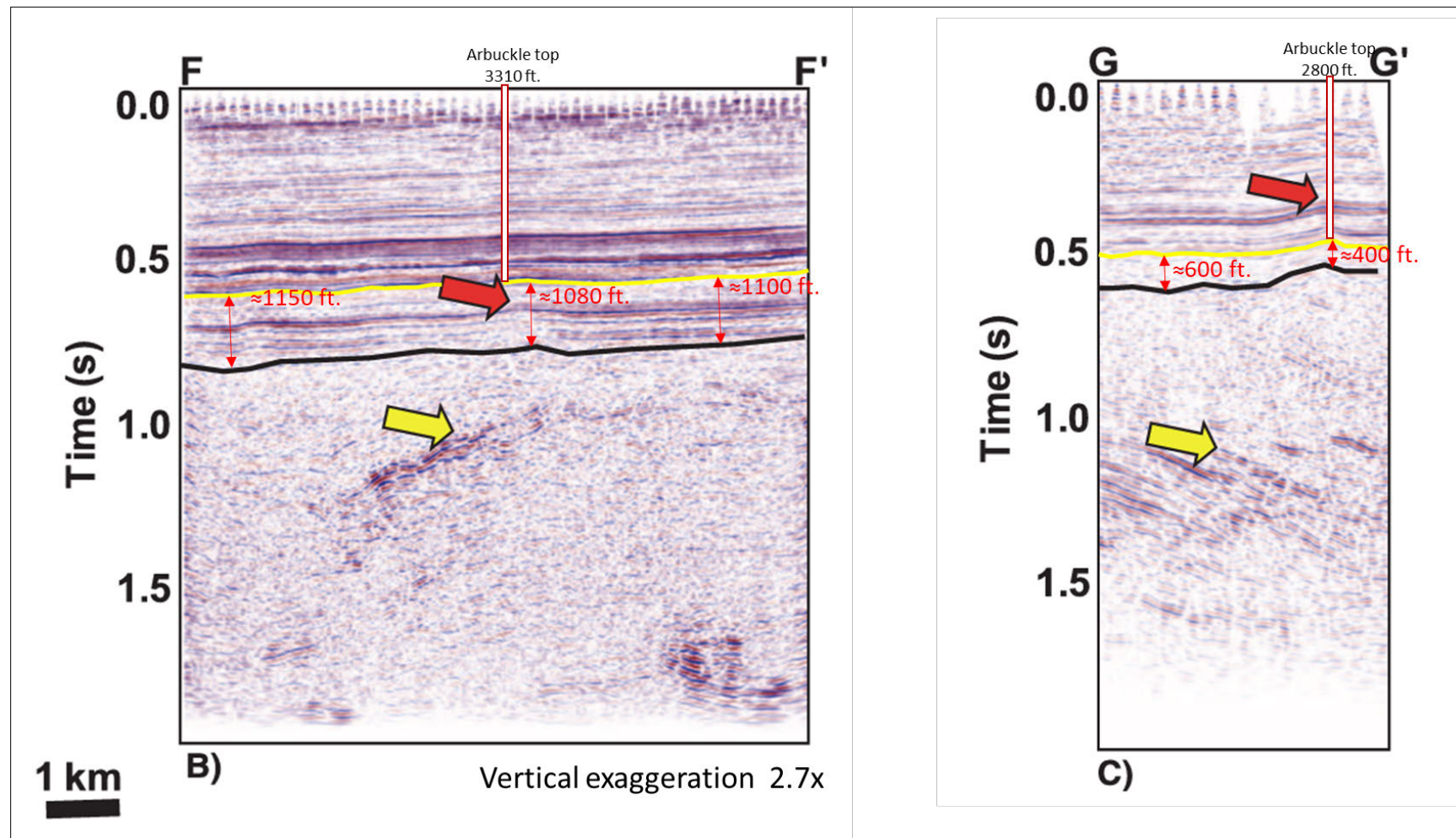


Figure 2.19—Seismic profiles F-F' and G-G' from Elebiju et al., 2011 modified with added well information, Arbuckle top (yellow) and estimated thickness showing normal thickness of Arbuckle and thinning of Arbuckle carbonate over granite basement monadnock, respectively. Location of profiles is shown on **Figure 2.16**.

The lowermost Arbuckle beds, as evidenced by thin radiogenic intervals within dolomite, contain granitic rock fragments eroded from nearby exposed Precambrian monadnocks or hills. The Arbuckle Group thins rapidly over these hills, is absent on several, and folded into anticlines that trapped oil and gas. The positions of the Arbuckle oil fields and their relationship to Arbuckle Group thickness are evident in **Figure 2.16**. The radiogenic beds are generated by potassium feldspar and identified by sharp but thin intervals of increased gamma-ray readings near the base (**Figure 2.20**). Major unconformities separate the Arbuckle Group from the Reagan Sandstone or Precambrian at the base, the Eminence Dolomite and the Reagan Sandstone, and the top of the Arbuckle Group from the overlying Simpson Group (Lynch, 1990) or the Woodford Shale if the Simpson Group is missing. The regional structural attitude of the top of the Arbuckle Group (**Figure 2.21**) is similar to the structure of the basement (**Figure 2.14**). Using average elevations for each area, the depth to the top of the Arbuckle is around 2200 ft along the Osage-Washington County line and around 4400 ft along the Osage-Noble County line.

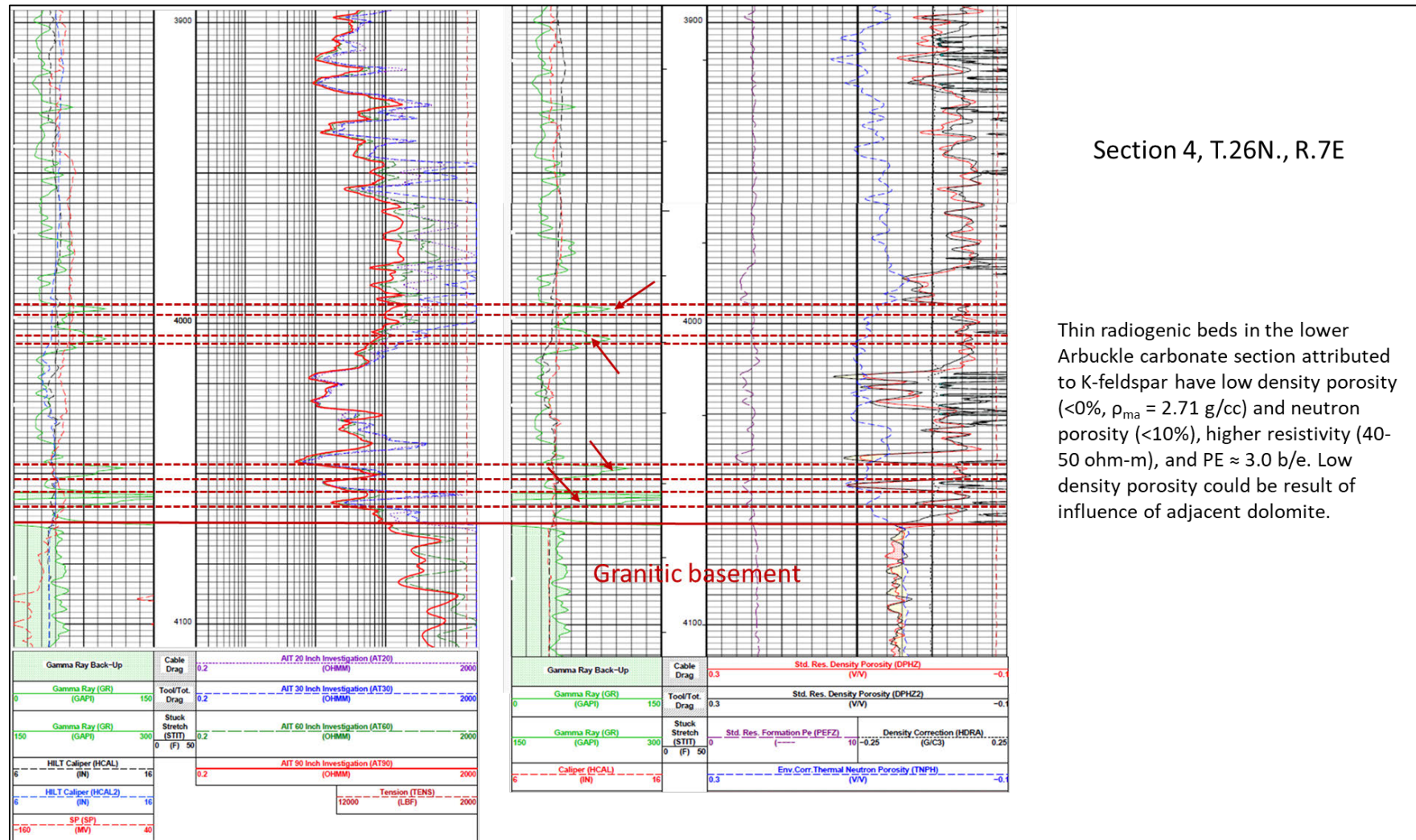


Figure 2.20—Petrophysical log showing radiogenic beds in dolomite toward the base of the Arbuckle Group .

Claimed as PBI

Figure 2.21—Structure of the Arbuckle Group in northern Oklahoma and adjacent areas from Rascoe and Hyne (1988) and digitized by the Oklahoma Geological Survey.

Reservoir development primarily occurs along sequence boundaries where diagenetic processes, such as dolomitization and dissolution during paleokarstic events, enhance porosity and permeability (Fritz et al., 2012). Studies, including DOE-funded research at Wellington Field in Kansas, and petroleum geology studies in Osage County, identified baffles or subregional confining zones within the Arbuckle (Rountree, 1980; Holubnyak et al., 2017). Overlying low-permeability Woodford Shale and Simpson Group shale where present, provide reliable barriers that prevent vertical fluid migration.

2.1.2.3 Simpson Group

The Simpson Group uncomfortably overlies the Arbuckle Group and consists of interbedded sandstones, shales, and thin limestones deposited during a regressive sequence. Thin sandstones within the Simpson in western Osage County have potential limited storability, and no perforations are planned for these units. More importantly, the “green shale” of the Tyner Formation occurs beneath part of the NexGen Carbon Oklahoma: Project Vanguard land position and where present, increases the thickness of the upper confining units. Regionally, the Simpson Group comprises three formations:

- **Lower Simpson (Burgen Sandstone):** A tight quartzose sandstone.
- **Middle Simpson (Tyner Formation):** Dominantly green shales interbedded with thin shallow marine limestone lenses and occasional thin sandstones, offering additional confinement to seal the underlying Arbuckle injection zone.
- **Upper Simpson (Hominy/Wilcox Sandstone):** A porous sandstone that subcrops west of the proposed CCS site and is productive in areas to the south and west (**Figure 2.22**).

The Simpson Group is thickest in southern Osage County, reaching approximately 200 ft, and thins rapidly to the north. Simpson Group formations reflect a large-scale shift of the shoreline (transgression and regression) in response to changes in sea level across the low-relief platform, resulting in clean quartz sands that are excellent oil and gas reservoirs and sources for glass sand in outcrop (Johnson, 2008).

2.1.2.4 Woodford Shale

The Woodford Shale, regionally referred to as the Chattanooga Shale in the Ozarks, was deposited during the late Devonian to early Mississippian on an unconformity surface. Conodont biostratigraphy of the closest outcrops in eastern Oklahoma confirms the Woodford in northeastern Oklahoma is Late Devonian (Boardman et al., 2009).

Figure 2.23 and Figure 2.24, are regional structure and thickness maps showing Woodford Shale distribution, with the shale absent along the northern margins of Osage County.

The Woodford Shale is typically highly radioactive compared to adjacent strata due to its significant uranium content, making it a distinct marker on gamma-ray logs. Also, the Woodford Shale is organic-rich, requiring petrophysical corrections when evaluated by density porosity logs. It is fissile, carbonaceous, calcareous, and dark gray to black in color, with thin beds rich in small pyrite concretions and grains (Foltz et al., 2016). In northern Oklahoma, the Woodford is more clay-rich and devoid of the chert that allows the Woodford to be naturally fractured in southern Oklahoma (Callner, 2014; Snider, 2014), where it is an important oil and gas reservoir.

Claimed as PBI

Figure 2.22—Thickness of the Simpson Group in northern Oklahoma and adjacent areas (Rascoe and Hyne, 1988) with locations of oil and gas fields producing from Simpson Group sandstones (Hu, 2019).

Claimed as PBI

Figure 2.23—Structure of the Woodford Shale in northern Oklahoma and adjacent areas from Rascoe and Hyne (1988) digitized by the Oklahoma Geological Survey.

Claimed as PBI

Figure 2.24—Thickness of the Woodford Shale in northern Oklahoma and adjacent areas (Rascoe and Hyne, 1988).

Deposition of the Woodford Shale began in the Late Devonian (Frasnian) and continued through the Early Mississippian (Kinderhookian) in southern Oklahoma (Over, 1992) where it typically overlies the Early Devonian Hunton Group. In the Anadarko Basin, the Woodford Shale exceeds 600 ft in thickness, while it thins onto the Cherokee Platform with an average thickness of 20 to 50 ft (Thorman and Hibshman, 1979). A regional isopach map illustrating the Woodford Shale's thickness is **Figure 2.23**.

2.1.2.5 Mississippian Age Sediments

The Mississippian Limestone, also referred to informally as the Mississippi Lime, disconformably overlies the Woodford Shale. Mississippian carbonates are widely distributed throughout the Midcontinent region and Oklahoma. In northern Oklahoma and Osage County, the Mississippian Limestone includes in ascending order, the St. Joe Group (Kinderhookian and Osagean), "Lower Mississippian," "Upper Mississippian," and Mississippi Chat (Osagean to Meramecian). The top of the Mississippian is marked by an unconformity that separates it from overlying Pennsylvanian shale. The Lower Mississippian has minimal permeability and serves as the secondary confining unit for the proposed Vanguard CCS site.

In northeastern Oklahoma, Mississippian rocks outcrop on the flanks of the Ozark Uplift. In Osage County the top of the Mississippian ranges from a subsurface depth of 1,400 ft (-800 ft TVDSS) along the Washington County line to 3,900 ft (-3,000 TVDSS) in northeastern Noble County. At the Project Site, the top of the Mississippian is encountered at 2,400 ft bgs in T.25N., R.8E. and more than 2,900 ft deep in T.27N., R.7E. The Mississippian Limestone encompasses the Kinderhookian, Osagean, Meramecian, and Chesterian series, with the Chesterian and most of the Meramecian sections subcropping southwest of Osage County (Hill, 2017; Hunt, 2017).

During Mississippian time, northeastern Oklahoma was covered by warm, shallow seas that facilitated the deposition of 200- to 350-foot-thick carbonate sediments. These sediments eventually lithified into clean calcareous limestone, cherty limestone, and argillaceous limestone with argillaceous (clay and silt) content increasing with the depth of water during deposition (Hill, 2017; Hunt, 2017). Because of the change in clay and silt content, the Mississippi limestone ranges in color from medium gray to dark brown depending on the percentages of carbonate grains versus clay. In addition to sourcing and storing oil and gas (Al Atwah et al., 2019; Hu, 2019), Mississippian carbonates host zinc and lead ores in the Tri-State mining district in the northeastern corner of Oklahoma, southeastern Kansas and southwestern Missouri (McKnight and Fisher, 1970).

The Mississippian Chat occurs along the Mississippian-Pennsylvanian unconformity and/or near the middle of the Mississippian interval above the lower Mississippian tight carbonates. The chat at the Pennsylvanian unconformity consists of in-situ upper Mississippian rocks or fragments of these rocks intermixed with sandstone and shale fragments from the lower Pennsylvanian section. These fragments include angular to subangular brecciated chert, tripolitic chert, unaltered limestone, sandstone, and shale embedded in a mud matrix (Jennings, 2014). The chat, likely formed due to weathering and meteoric groundwater interaction on paleotopographic highs (Manger, 2014), is characterized on well logs by low resistivity, low density, high porosity, and photoelectric (PE) values of approximately 2 b/e (Rogers, 2001).

2.1.2.6 *Pennsylvanian Age Sediments*

The Pennsylvanian Subsystem unconformably overlies the Mississippian and when complete spans from 323 to 298.9 million years ago (GSA, 2022). Pennsylvanian sedimentary packages consist of alternating sandstones (sometimes conglomeratic), marine and non-marine shales, limestones, and coal, collectively known as depositional cycles or cyclothems (Heckel, 1986). Depositional cycles, which characterize deposition on the shelf during the Pennsylvanian Subsystem and Early Permian system, resulted from cyclic changes in global sea level changes caused by glaciation in the southern hemisphere (Boardman et al., 1995). In North America, the Pennsylvanian is divided into six series: Morrowan, Atokan, Desmoinesian, Missourian, Virgilian and Gearyan. Uplift and erosion or non-deposition resulted in no preservation of Morrowan or Atokan rocks in Osage County (Rascoe and Hyne, 1988). The thickness of the Pennsylvanian section is up to 4,000 ft in western Osage County where Desmoinesian rocks unconformably overlie the Mississippian.

Desmoinesian Series

The Middle Pennsylvanian Desmoinesian Series (305–311 Ma), is composed of the Cherokee and Marmaton Groups. In western Osage County the Cherokee Group unconformably overlies the eroded Mississippian surface. The Cherokee and Marmaton groups were deposited during alternating periods of marine advance and retreat driven by cyclic changes in sea level. The Cherokee Platform acted as a depositional shelf, while the adjacent Arkoma Basin served as a sedimentary sink (Krumme, 1981).

- **Cherokee Group:** The Cherokee Group is present across Osage County and thickens to the east into the Cherokee Basin. The group includes important oil- and gas-producing reservoirs including the Bartlesville, Red Fork (Burbank), Skinner and Prue sandstones. Stratigraphy within the group is defined using coal, radiogenic black shales and limestones such as the Inola, Pink and Verdigris that represent transgression and widespread inundation of the depositional shelf during Cherokee time. Thicker sandstone reservoirs in the Cherokee Group fill channels that eroded the exposed shelf during sea level low stands generated by glacial maxima on the Gondwana continent in the southern hemisphere. The giant Burbank field to the west of the NexGen CCS site produces from the Burbank (Red Fork) Sandstone that filled a large valley. Red Fork, Bartlesville and Prue sandstones have not been observed on wireline logs of wells drilled on or around the CCS site. The Skinner Sandstone has not been observed in wells on the site but occurs within a few miles of the NexGen Carbon Oklahoma: Project Vanguard land position. In the CCS site area, the Cherokee Group is approximately 210 ft thick and more than 80 percent shale, contributing to the package of confining units within the proposed CCS site.
- **Marmaton Group:** The Marmaton Group is composed of carbonates separated by normal gray marine shale and radiogenic black marine shales associated with rapid flooding of the Pennsylvanian shelf. The Marmaton Group includes the Excello (black) Shale, Ft. Scott (Oswego) Limestone, Little Osage (black) Shale, Anna (black) Shale, Labette Shale, Oologah (Big) Limestone, and the thick shale (Nowata) that contains the Lake Neosho (black) Shale near the base and sandstones called Cleveland Sandstone toward the top (Cain, 2018). The Oswego and Big limestones are minor producers of oil and gas in northeastern Oklahoma, whereas the Cleveland Sandstone consists of thick channel filling

reservoirs that produce in Cleveland field in Pawnee County. In the Project Area the Marmaton Group is approximately 50 percent limestone, 45 percent shale and 5 percent sandstone.

Missourian Series

The Missourian Series (300–305 Ma) includes the Skiatook and Ochelata Groups. These units were deposited concurrently with Late Pennsylvanian tectonic events, including the Arbuckle and Wichita-Amarillo Uplifts and Ouachita deformation.

- **Skiatook Group:** The Skiatook Group includes the section between the Nuyaka Creek and Hogshooter radiogenic (black) shales (Cain, 2018) and contains well known lithostratigraphic units including Checkerboard Limestone, Coffeyville Shale, Layton Sandstone, and Hogshooter Limestone. The Checkerboard Limestone is regional and represents a widespread flooding event that culminates with deposition of the “Checkerboard black shale” immediately above the limestone (**Figure 2.10**). Overlying the Checkerboard is the deltaic Coffeyville Shale that contains the Layton Sandstone. A rise in sea level following Layton deposition resulted in shale and culminated with deposition of the Hogshooter Limestone where present, and Hogshooter radiogenic shale (**Figure 2.10**). The Skiatook Group in the area of the NexGen CCS site is about 260 to 270 ft thick and approximately 80 percent shale, 15 percent sandstone and 5 percent limestone.
- **Ochelata Group:** The Ochelata Group includes the Cottage Grove (Osage Layton) Sandstone, Chanute Shale, Avant Limestone, Perry Gas Sandstone, and Okesa/lower Tonkawa sandstone. In the area of the Vanguard CCS site, the Ochelata Group and the section extending to the Douglas and Shawnee Groups is approximately 800 ft thick of which shale is 60 percent, sandstone 37 percent and limestone 3 percent.

Virgilian Series

The Virgilian Series includes the Douglas, Shawnee, and Ada Groups. These units exhibit mixed marine and fluvial-deltaic facies resulting from high-frequency eustatic sea level changes related to Gondwanan glaciation (Boardman et al., 2009).

- **Douglas Group:** The Douglas Group includes the middle and upper Tonkawa sandstone, and Haskell and Lovell limestones. Cyclic shale, sandstones, and limestones continue in the Douglas Group and the Tonkawa Sandstone, a fluvial-deltaic deposit that is an important oil and gas reservoir in anticlinal fields along the Nemaha Uplift.
- **Shawnee Group:** This unit contains the Endicott Sandstone, Oread Limestone, Elgin Sandstone and Vamoosa Formation. The Vamoosa-Ada aquifer is the only major bedrock aquifer in Osage County (Osborn and Hardy, 1999) and as it dips deeper into the subsurface to the southwest, it becomes brine-bearing and known as the Hoover Sandstone. The Douglass and Shawnee Groups combined in the northern part of the NexGen Carbon Oklahoma: Project Vanguard CCS AoR are approximate 500 ft thick, consisting of 55 percent shale, 40 percent sandstone and 5 percent limestone. In the southern part of the AoR, sandstone decreases to 20 to 30 percent and shale increases to 65 to 75 percent.

- **Ada Group:** This youngest Virgilian unit consists of fluvial and deltaic sediments interbedded with fossiliferous shale and limestone. The Pawhuska Limestone near the base of the Ada Group is the most prominent stratigraphic unit and includes 3 limestones, including the Lecompton, which is mappable in outcrop and shown on the Miser (1954) State Geologic Map of Oklahoma (**Figure 2.25**).

Gearyan Series

The Gearyan Series is a name preferred by the Oklahoma Geological Survey and includes the Vanoss Group and Oscar Group, which include rocks formerly assigned to the Admire, Council Grove and Chase Groups of Permian age (Shelton et al., 1985).

Vanoss Group: The Vanoss Group consists of shale, thin limestones and lenticular sandstones. As a result, no important sandstone aquifers occur in the Vanoss Group. Most of the NexGen Carbon Oklahoma: Project Vanguard CCS site land position is on the Vanoss Group.

Oscar Group: The Oscar Group is mostly red claystone, lenticular sandstones and dolomites above the Neva Limestone that marks the base of the unit. The Oscar Group contains only minor aquifers in lenticular sandstones. It is located to the west of the Project Area.

2.1.2.7 Permian Rocks

Permian age rocks outcrop to the west of the NexGen CCS site land position. Former Permian units, including the Council Grove and Chase Groups are now assigned to the Pennsylvanian Gearyan Series (Shelton et al., 1985).

Claimed as PBI

Figure 2.25—Geologic map of Osage County and parts of adjacent counties (Miser, 1954). En echelon faults indicated by red arrows occur mostly to the east of the AoR. Important beds such as the Lecompton Limestone, a key stratigraphic marker on petrophysical logs in the lower part of the Ada Group, are marked.

2.1.3 General Hydrogeology

2.1.3.1 Precipitation

The annual precipitation for western Osage County is between 36 and 40 inches. Most precipitation occurs as rain between the months of March and October (Oklahoma Mesonet, 2024), with May being the wettest month (Oklahoma Climatological Survey, 2023). Rainfall in the summer is commonly short-duration and intense precipitation events. To utilize the stream flow generated by storms, impoundments ranging in size from small stock ponds to large reservoirs have been constructed to collect and store water for use during times of low precipitation. The NexGen Carbon Oklahoma, LLC, Project Vanguard CCS site is located on the OCWP Upper Arkansas Watershed Planning Region.¹ The OCWP defined region spans 13 counties features a moist, sub-humid climate with an average annual temperature of 60°F and precipitation ranging from 24 inches in the northwest to 42 inches in the east (OK Climatological Survey, 2023). Evaporation rates exceed precipitation in the western part of the region on an annual basis, leading to frequent droughts, whereas summer precipitation patterns result in occasional severe flooding from intense high-precipitation rate, short duration rainfall events. Watershed protection and flood prevention efforts are critical in this region and water storage/flood prevention, power generation and water supply reservoirs are constructed on the Arkansas and Caney rivers. Smaller reservoirs on Bird Creek and other streams provide flood control, recreation and municipal water supplies.

Freshwater resources in Osage County include the Arkansas River, other smaller streams, lakes, and aquifers. The region relies primarily on surface water supplies, with some dependence on bedrock and alluvial aquifers (OCWP, 2012). OCWP predicts that by 2060, groundwater withdrawals are expected to increase, necessitating conservation strategies, aquifer recharge, and surface water alternatives to address demand. Most increased demand on surface and groundwater is expected to be outside the area of the NexGen CCS site, as the area will continue to be dominated by ranching where water demand is not expected to change as compared to more populated areas in southeastern Osage County.

Historical and Environmental Considerations

Early oil industry practices, such as surface disposal of produced brine, raised environmental concerns in the mid-20th century. By the late 1940s or early 1950s, surface disposal practices were replaced by underground injection. The USGS, in collaboration with the Osage Tribal Council, the USDOE, and the Bureau of Indian Affairs, conducted a study in 1999 to characterize surface water quality in Osage County (Abbott and Tortorelli, 1999). The study focused on chloride concentrations, noting localized high levels in surface and groundwater during the mid-20th century. However, by 1999, elevated chloride levels were no longer prevalent regionally.

The NexGen CCS site is mostly within the Salt Creek Basin, which drains into the Arkansas River. Future water management practices will aim to mitigate risks such as groundwater storage depletion, increased pumping costs, and impacts on water quality, ensuring sustainable water use for the region.

¹ Oklahoma Comprehensive Water Plan (OCWP), is a strategic, statewide water management plan developed by the Oklahoma Water Resources Board (OWRB). The OCWP aims to ensure the sustainable use, allocation, and protection of Oklahoma's water resources to meet current and future demands for water across various sectors, including municipal, industrial, agricultural, and environmental needs.

2.1.3.2 Surface Water Resources

Surface water is the principal source of water to meet private, industrial, and public demand in the hydrologic region that includes Osage County. Major streams are the Caney, Verdigris and Arkansas Rivers. All streams generally have sufficiently abundant flow, but as a result of the climate in the region, experience a range in discharge from flooding to low flow, particularly in late summer and fall. The Arkansas River flows along and forms the southwestern and much of the western boundary of Osage County. The Verdigris River originates in Kansas and flows some 140 miles in eastern Oklahoma. Major tributaries of the Verdigris River include the Caney River and Bird Creek. The Caney River is the major tributary that joins the Verdigris River immediately upstream from its confluence with Bird Creek. Major tributaries of the Caney include Buck, Pond and Sand Creeks that drain northeastern Osage County. The Bird Creek and Hominy Creek watershed drains much of southeastern Osage County before joining the Verdigris River. Southwestern Osage County is drained by Doga, Bug and Salt Creeks that flow directly into the Arkansas River. The part of northwestern Osage County not drained by the Salt Creek watershed is drained by Beaver Creek, a stream that joins the Arkansas River in Kay County (**Figure 2.26**).

Claimed as PBI

Figure 2.26—The location of the proposed Project Vanguard CCS Hub AoR in relation to regional surface drainage. Osage County is outlined in black and the AoR in red. The AoR is located on the drainage divide between the Bird Creek/Hominy Creek and Salt Creek watersheds.

The dependability of surface water supply for many public water systems and other users is achieved by the construction of reservoirs. The larger two lakes to the east are Oologah on the Verdigris River and Skiatook on Hominy Creek, constructed in 1963 and 1984, respectively, by the U.S. Army Corps of Engineers. Skiatook Lake is closest to the proposed CCS project but is still more than 25 miles to the east and has no effect on local surface water. Surface drainage to the east-southeast of the proposed site is to the Hominy-Bird Creek watershed, whereas drainage to the west is to Salt Creek. Major streams to the south and west of Osage County include the Arkansas River, Salt Fork of the Arkansas River, Cimarron River and the Chikaskia River. The Arkansas River mainstem originates in Kansas and flows into Oklahoma where it is a major surface stream. Tributaries to the west of the Arkansas River include the Salt Fork, Black Bear Creek and Red Rock Creek (OCWP, 2012).

Reservoirs on the Arkansas River increase the dependability of surface water for public water systems and provide electrical power and flood control. The largest lakes are Kaw and Keystone, constructed by the U.S. Army Corps of engineers in 1976 and 1964, respectively (OCWP, 2012). Keystone Lake is to the southeast of the proposed CCS project, forms part of the southern boundary of Osage County, and has no impact on the proposed CCS site. Kaw Lake is to the west of the proposed CCS site, but surface drainage in the site area is to tributaries of Salt Creek that joins the Arkansas River to the south (**Figure 2.26**).

2.1.3.3 Regional Hydrogeology

According to information from the Oklahoma Water Resource Board, the proposed Vanguard CCS Hub AoR is located in part in an area without a recognized freshwater aquifer and in part in an area overlying the Vamoosa-Ada aquifer (**Figure 2.28**). The nearest recognized major alluvial aquifer is to the west of the proposed CCS site is along the Arkansas River. The Vamoosa-Ada aquifer is a major bedrock aquifer (Osborn and Hardy, 1999) that underlies part of the proposed CCS site and outcrops to the east. Though the Vamoosa-Ada aquifer occurs in the subsurface below the proposed CCS site, the lack of water in the immediate area is illustrated by the scarceness of water supply wells (OWRB, 2024). According to the OWRB Groundwater Well Record Search, six domestic water wells, three deep (402 ft) groundwater test wells, and 1 cathode protection well occur within the Vanguard CCS Hub AoR or the 1-mile-wide buffer around the AoR. Monitoring wells in the Burbank Oil Field are 1.2 to 3 miles west of the AoR. (**Figure 2.27**).

Claimed as PBI

Figure 2.27—Map from Oklahoma Water Resources Board (OWRB) showing the classification of shallow wells in Osage County. Within the AoR and the 1-mile buffer, OWRB identifies 6 domestic water wells, 3 groundwater test wells, and 1 cathodic protection well. The groundwater monitoring wells to the west of the AoR are associated with the Burbank oil field. Details for the wells associated with the AoR are provided in Table 2.1b

Plan revision number: 0

Plan revision date: 6/24/2025

Table 2.1b—Shallow Wells from Oklahoma Water Resources Board within the AoR or 1-mile buffer, including water wells, groundwater test wells and cathodic protection wells.

Num ber	Location: Section, Township and Range	Location: Latitude and Longitude	Dept h (ft)	1 st Water (ft)	Aquifer and Yield	OWRB ID No. Type and date
1	NW SE SE 19, T.27N., R.08E., Osage Co., OK Address: not reported	36.79, -96.48	220	Not reported	Not reported	30094 Domestic Groundwater Well 09/03/1993
2	SW NE NE 17, T.26N., R.08E., Osage Co., OK Address: not reported	36.74, -96.46	254	200	Vamoosa-Ada USDW 12 gpm	14801 Domestic Groundwater Well 08/18/1986
3	NW SE NE 17, T.26N., R.08E., Osage Co., OK Address: not reported	36.74, -96.46	100	Not reported	Vamoosa-Ada USDW Not reported	23706 Domestic Groundwater Well 10/16/1986
4	NE NW NE 10, T.25N., R.08E., Osage Co., OK Address: 211 Braden School Rd., Ponca City, OK	36.67, -96.43	55	37	Vamoosa-Ada USDW 2.8 gpm	228429 Domestic Groundwater Well 06/19/2024
5	SW NE SW 15, T.25N., R.08E., Osage Co., OK Address: 1815 Co. Road 5902, Pawhuska, OK	36.63, -96.43	134	120	Vamoosa-Ada USDW 18 gpm	230495 Domestic Groundwater Well 10/11/2024
6	SE NW NW 31, T.25N., R.08E. Osage Co., OK Address: not reported	36.61, -96.49	100	10	Vamoosa-Ada USDW 2 gpm	14738 Domestic Groundwater Well 09/26/1987
GWT- 1	SE NW SW 17, T.25N., R.07E., Osage County, OK Address: P.O. Box 1599, Pawhuska, OK	36.64, -96.57	402	none	none	139160 Groundwater Test Hole 10/28/2011
GWT- 2	NE SW NE 29, T.25N., R.8E., Osage Co., OK Address: P.O. Box 208, Pawhuska, OK	36.62, -96.46	402	none	none	141513 Groundwater Test Hole 01/02/2012
GWT- 3	NE SE NE 14, T.28N., R.6E., Osage Co., OK Address: 6916 County Rd 4650, Shidler, OK	36.91, -96.62	402	none	none	139315 Groundwater Test Hole 10/17/2011
CP-1	SE 17, T.27N., R.7E., Osage County, OK Address: not reported	36.81, -96.56	250	none	none	149870 Cathodic Protection or Anode Well 01/17/2013

Claimed as PBI

Figure 2.28—Position of the Vanguard CCS Hub AoR (red) in relationship to the Vamoosa-Ada aquifer (VA) that trends south to north across Osage County (outlined in black) and underlies the proposed CCS site. Major Aquifer Map downloaded from the Oklahoma Water Resources Board website.

2.1.3.4 Regional Aquifers and Confining Units/Aquitards

2.1.3.4.1 Alluvial Aquifers

The Arkansas River Alluvial Aquifer is the only alluvial aquifer pertinent to Osage County and the regional hydrogeology of the proposed CCS project site (**Figure 2.28**). The two other important alluvial aquifers, Cimarron and Salt Fork, both join the Arkansas River from the west and, therefore, have no bearing on the hydrogeology of Osage County. At its closest point, the Arkansas River alluvial aquifer is approximately 7 miles west of the proposed project. The Arkansas River Alluvial Aquifer and the adjacent terrace aquifer are important resources for the Osage Nation and have been characterized via an extensive coring program (Cope, 2003; Mashburn et al., 2003). Based on the coring, the sediments that make up the aquifer are silt and fine sand at the surface with grain size increasing with depth. Much of the alluvium is stacked coarse to medium-grained sands with a layer of gravel at the base that is composed of locally derived sedimentary rock and distance-transported igneous clasts (Mashburn et al., 2003). Windblown sand and silt sourced from the floodplain form terrace deposits mostly on the northern or downwind (leeward) side of the Arkansas River valley. Windblown terrace deposits border the alluvial aquifer but generally have low yields in Osage County (Mashburn et al., 2003). In contrast, coarse sand and gravel sections of the Arkansas Alluvial Aquifer have high yields that can reach hundreds of gallons per minute with a municipal/industrial well near Ponca City reporting a yield of 900 gallons per minute (OWRB, 2024). The thickness of the windblown terrace deposits is highly variable but generally less than 30 ft. The alluvium along the Arkansas River is typically less than 50 ft thick with an average saturated thickness of 20 to 30 ft.

Recharge of the alluvial and terrace aquifer is from precipitation. Precipitation falling on the terrace deposits may move into the neighboring alluvium. Natural groundwater discharge occurs as seepage into tributaries cutting the floodplain or directly into the Arkansas River. Water quality in the Arkansas Alluvial Aquifer is adequate for irrigation and domestic, stock, and limited industrial purposes without treatment. It is important to note that this aquifer and any recharge to this aquifer is not present in the area of the NexGen Carbon Oklahoma: Project Vanguard CCS project site.

2.1.3.4.2 Bedrock Aquifers

Bedrock groundwater (groundwater) pumped from the Vamoosa-Ada major aquifer and other minor aquifers is underutilized in Osage County (OCWP, 2012; OWRB, 2024). The low use of groundwater is the result of low population density and the distribution of available surface water to populated areas via rural water districts. Currently, permitted and projected withdrawals are primarily from the Vamoosa-Ada aquifer, and because of the low utilization, bedrock aquifer storage depletion is not expected to occur in the region. According to OCWP (2012), the availability of permits for new groundwater wells is not expected to limit the use of groundwater to meet future local demand. The North-Central Oklahoma aquifer, which borders Osage County on the west and has no bearing on the proposed NexGen Carbon Oklahoma: Project Vanguard CCS site, has low well yields and storage that limit withdrawals.

The Vamoosa-Ada aquifer is a major bedrock aquifer in Oklahoma (**Figure 2.28**) and the most important bedrock aquifer in Osage County and the central part of the state (Osborn and Hardy, 1999). The aquifer outcrops immediately to the east and dips westward beneath the proposed CCS

site. The Vamoosa-Ada aquifer underlies approximately 2,320 sq miles in parts of Osage, Pawnee, Payne, Creek, Lincoln, Okfuskee, and Seminole counties (D'Lugosz et al., 1986).

The aquifer consists principally of the Late Pennsylvanian age Vamoosa Formation and the overlying Ada Group, which is in hydrologic connection with the Vamoosa Formation. The western boundary of the confined Vamoosa-Ada aquifer, as defined by the occurrence of 1,500 mg/L dissolved solids (D'Lugosz et al., 1986), is three times the secondary drinking-water standard (U.S. Environmental Protection Agency 40 CFR 143 Subpart A). The highest yields are in Creek County, where coarser-grained sandstone occurs.

Rocks comprising the aquifer formed in nearshore and fluvial environments, transitioning from marine in the west to fluvial in the east (D'Lugosz et al., 1986). Because of changes in depositional environments over time and across the sediment dispersal system, the aquifer consists of a complex sequence of fine- to very fine-grained sandstone, siltstone, conglomerate, and shale. Thin limestones are interbedded throughout the sequence. The sediments that formed the Vamoosa-Ada aquifer were primarily sourced from the Arbuckle and Ouachita Uplifts. As sediment was transported and dispersed in a northerly system, overall depositional energy and grain size decreased northward. The basal sandstone of the Vamoosa Formation is conglomeratic with clasts of Arkansas Novaculite in Okfuskee County, whereas the stratigraphically equivalent Gypsy Sandstone in Pawnee County is fine-grained sandstone.

Terrell (1972) differentiated sub-environments in the Vamoosa-Ada aquifer on the basis of geometry, distribution, and lithology of the sandstone units. The more significant sub-environments, hydrologically include: (1) stream channel and near channel, (2) distributary channel, (3) deltaic, and (4) delta fringe and shallow marine. Individual sandstone units are either thin bedded or lenticular. Although both types are fine grained and well sorted, thin-bedded units generally are finer grained and less well sorted. Thin-bedded sandstones are 1 to 5 ft thick and are laterally extensive. These sands probably were deposited in the delta-fringe to marginal shallow-marine environment (D'Lugosz et al., 1986).

Lenticular sandstones are 5 to 30 ft thick and are 10 to 600 ft wide with well-defined upper, lower, and lateral contacts. These sandstones probably represent distributary, channel, or near-channel deposits. The aggregate thickness of water-bearing sandstones is greatest south of the Cimarron River, where it reaches a maximum of 550 ft in the vicinity of Seminole. North of the Cimarron River, the average aggregate thickness of the sandstones is about 100 ft, but locally it may be as much as 200 ft. Well yields generally increase toward the south where thicker sections of coarser grained sandstone occur (D'Lugosz et al., 1986). Groundwater supplies in Pawnee County are not extensively studied, but in Payne County, well yields from the Vamoosa-Ada aquifer are larger south of the Cimarron River and decrease to the north (Shelton et al., 1985).

The water-yielding capabilities of the aquifer are generally controlled by lateral and vertical distribution of the sandstone beds and their physical characteristics, which are in turn related to the environments of deposition. Studies by Terrell (1972) show that lenticular sandstones have a preferred direction of grain orientation. Measurements of these sandstones show that maximum horizontal permeability is parallel to the preferred direction of grain orientation and that horizontal permeability is 18 percent greater than vertical permeability. Thin bedded sandstones do not display this preferred direction of permeability. According to D'Lugosz et al. (1986), flow of groundwater is also controlled by variations in permeability related to changes in lithology, sandstone thickness, and faulting, and that transmissivity values derived from seven aquifer tests

ranged from 70 to 490 ft²/D, with values decreasing from south to north with decreasing sandstone thickness, whereas hydraulic-conductivity values range from 2 to 4 ft/D. According to D'Lugosz et al. (1986) an approximate hydrologic budget for the aquifer for 1975 gives values, in acre-ft/yr, of 93,000 for recharge, 233,000 for runoff, and 2,003,000 for evapotranspiration. The total of these values is almost equal to the average annual precipitation of 2,330,000 acre-ft/yr. An estimated 60 million acre-ft of water containing a maximum of 1,500 mg/L of dissolved solids is stored in the aquifer, of which an estimated 36 million acre-ft or 60% of the total stored is available for use (D'Lugosz et al., 1986).

Water in the Vamoosa-Ada aquifer is generally suitable for municipal, domestic, and stock use (D'Lugosz et al., 1986). Geochemically, the water is dominantly sodium bicarbonate or sodium calcium bicarbonate type, with the remainder classifying as sodium sulfate, calcium sulfate, sodium chloride, or indeterminate types. Laboratory and on-site chemical-quality data indicate that mineralization of both ground and surface waters is greater than normal in some areas. Bromine exceeding 1 mg/L was detected in water samples from seven wells and 12 stream sites, indicating probable contact with oilfield brine (D'Lugosz et al., 1986).

Most recharge to the Vamoosa-Ada aquifer is derived from precipitation falling directly on the outcrop area. Water flow in the Vamoosa-Ada aquifer is from east to west following the structural dip of Pennsylvanian strata on the Cherokee Platform. The aquifer is recharged directly and meteoric freshwater saturates the aquifer at the surface and in the shallow subsurface. With increasing depth and reaction of groundwater with minerals that make up the aquifer and subsurface fluids, the groundwater becomes increasingly solute-rich and eventually saline. The transition from freshwater to more solute-rich brackish water is shown in **Figure 2.29**, a cross-section extending from the outcrop of the Vamoosa-Ada Aquifer in T.27N., R.9E. to the AoR. Beneath the AoR, the depth of the base of the Vamoosa-Ada aquifer and USDW is around 500 ft to the north, increasing toward the south to 800 to 1,100 ft. In the area to the west, where the Vamoosa-Ada aquifer is brine-bearing, the base of known treatable water decreases to less than 100 ft.

Claimed as PBI

AoR to very saline and briny beneath the AoR. The inset map shows the location of featured wells in Cross-section W-E relative to the Vanguard CCS Hub AoR. Water resistivity (R_w) was calculated using the SP method (Asquith and Krygowski, 2004) and the resistivity (R_t) method (Schlumberger, 1972). Wireline log characteristics of shallow freshwater-bearing sandstones are shown in **Figure 2.33** and additional cross-sections **Figure 2.30** and **Figure 2.31**.



Figure 2.30—Cross section A–A' in T.25N., R.6E. to R.8E. showing the transition from freshwater to brine in the Vamoosa-Ada aquifer in the southern part of the AoR. The green line is vertically exaggerated surface topography.

Plan revision number: 0

Plan revision date: 6/24/2025

Claimed as PBI

Figure 2.31—Cross section B–B' in T.26N., R.6E. to R.8E. showing the transition from freshwater to treatable saline water in the Vamoosa-Ada aquifer in the central part of the AoR. The green line represents vertically exaggerated surface topography.

2.1.3.5 Regional Flow

The Cambrian-Ordovician Arbuckle Group is identified as the proposed injection zone for the NexGen Carbon Oklahoma, LLC-Project Vanguard CCS site. Groundwater flow within the Arbuckle is directed west-southwest, as illustrated on the potentiometric surface map (**Figure 2.15**).

The structural dip of the Arbuckle Group in western Osage County is less than 1 degree to the west-southwest (**Figure 2.32**) consistent with the regional dip of formations within the AoR, which ranges between 0.5 and 1.5°.

Claimed as PBI

Figure 2.32—Location of the proposed Vanguard CCS Hub AoR (red) between the Osage High to the southeast and the Nemaha Fault Zone to the west. The AoR is located in a tectonically stable area almost entirely north of the basement hills and overlying anticlinal folds of the Osage High, and east of the basement-faulted structures of the Nemaha Fault Zone. The regional dip across the AoR away from the influence of the buried hills is approximately 50 ft/mile or 0.54° west. Red circles identify wells that cored the upper Arbuckle.

Studies on flow rates in deep saline aquifers, such as the Arbuckle Group in southern Oklahoma, show that circulation rates vary widely from meters/day for shallow circulation paths to around one meter/year for deeper paths such as Vendome Well in the Chickasaw National Recreation Area (National Park Service, 2015). In aquifers such as the Arbuckle Group in northern Oklahoma where structural dip is less and fracturing less-frequent, flow rates are estimated to be centimeters per year. Site-specific data on regional fluid flow in the injection zones will be gathered through injection wells and in-zone monitoring wells once operational.

2.1.3.6 Non-USDW Aquifers

Section 2.1.3.7 Hydrologic and Hydrogeologic Information [40 CFR 146.82(a)(3)(vi), 146.82(a)(5)] provides a detailed discussion of the hydrologic properties of each USDW and non-USDW within the AoR. **Figure 2.33** provides a depiction of aquifers above the Arbuckle that are USDWs within part of the AoR, but not the entire AoR. All sources of potential freshwater were evaluated by examining wireline logs of wells drilled for oil and gas. These logs include recent or modern surveys with the full suite of porosity and resistivity curves as well as photoelectric curves that estimate lithology, and vintage logs, many of which set 100 ft or less of surface casing. The modern logs allow the better estimation of R_w and total dissolved solids (TDS), whereas the vintage

logs allow the mapping and assessment of potential freshwater zones that were cased off in wells drilled later when the guidelines for surface casing to protect shallow water were more stringent.

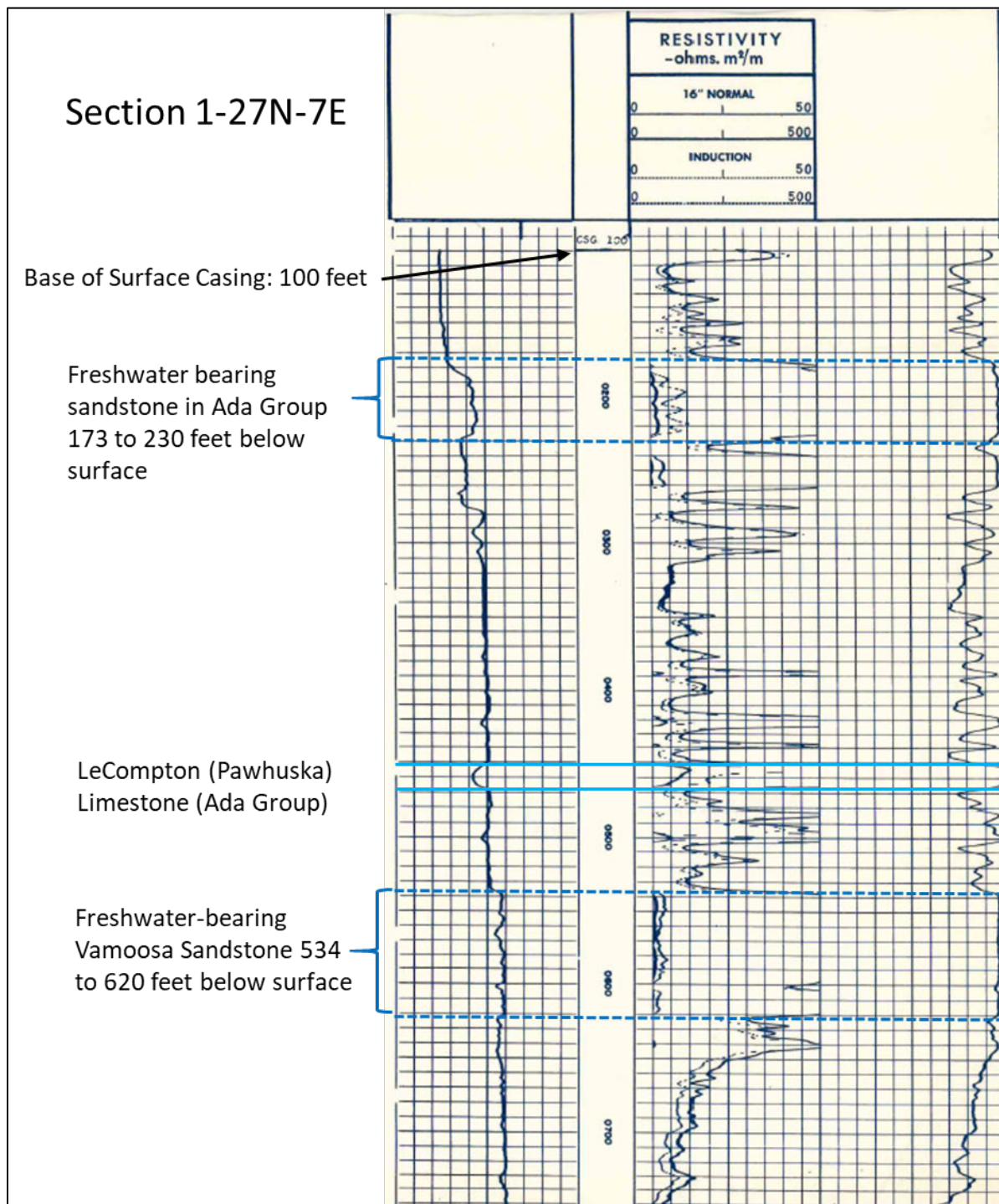


Figure 2.33—Image of vintage wireline log showing resistivity (Rt) and spontaneous potential (SP) characteristics of the Vamoosa-Ada aquifer (Vamoosa Sandstone USDW) and an unnamed sandstone aquifer in the upper Ada Group near the contact with the overlying Vanoss Group. Both intervals are characterized by positive SP deflection toward the depth track and resistivity exceeding 50 ohm-m. Cross sections showing the depth of the base of treatable water are **Figure 2.30** and **Figure 2.31**.

2.2 Maps and Cross Sections of the AoR [40 CFR 146.82(a)(2), 146.82(a)(3)(i)]

[EPA recommends that the maps and cross sections required by 40 CFR 146.82(a)(2) and (3)(i) be accompanied by a brief narrative description interpreting the figures and providing an overview of key features important to the project.

2.2.1 Map of the Area of Review

2.21a_NexGen_Vanguard_AoR_Map_60x72.pdf is a map of the AoR with all required information per 14 CFR §146.82 at a scale of 1 in. to 2,000 ft (1:24,000). A smaller scale (1:130,000) version is also included in **Figure 2.34**. A version at 1:24,000 scale with a recent satellite imagery basemap is provided in **2.21b_NexGen_Vanguard_AoR_Map_SatImage_60x72.pdf**

All data that informs the map is provided in an ESRI file geodatabase (**NexGen_Carbon_OK_DR.gdb**). Data sources of artificial penetrations, clean-up sites, hydrologic data, mines and quarries, faults, and structures are summarized as follows:

Artificial Penetrations

Oil and Gas Wells

Well locations, including production wells, abandoned wells, plugged wells, dry holes, service wells, unknown wells, and injection wells are sourced from the DrillingInfo well database^{2*}. 224 wells penetrate the two confining zones, the Woodford and the lower Mississippian Limestone. A list of all 926 oil and gas wells that have been drilled within the AoR is provided in **x_AoR_Oil_and_Gas_Well_List_DI.xlsx**.

Water Wells

Water Well locations were obtained from the Oklahoma Water Resources Board (OWRB)^{3*}. The OWRB supervises the licensing of water well drillers and pump installers and was guided by the comprehensive standards developed in cooperation with the Well Drillers Advisory Committee.

There are five water wells identified that are located within the AoR. All five of these wells are designated as domestic, though their current operational status is unknown. The deepest water well within the AoR is drilled to 254 ft below ground surface. A list of water wells within the AoR is provided in **x_AoR_Water_Well_List_OWRB.xlsx**. Well files for all water wells within the AoR are provided in **x_Water_Well_Files_OWRB.zip**.

Clean-Up Sites

EPA clean-up site data is from the United States Environmental Protection Agency (EPA) Geospatial Data of Regulated Facilities or Cleanup Locations database^{4*}. No EPA cleanup sites are identified within the mapped area.

² Retrieved from Drillinginfo – Accessed 8/5/2024

³ <https://oklahoma.gov/owrb.htm> - Accessed 1/15/2025

⁴ <https://www.epa.gov/frs/epa-frs-facilities-state-single-file-csv-download> - Accessed 1/20/2025

Plan revision number: 0

Plan revision date: 6/24/2025

State cleanup sites are sourced from the Oklahoma Department of Environmental Quality (ODEQ)^{5*}. No cleanup sites are present within the AoR or mapped area.

Hydrologic Data (Surface Waters and Springs)

Hydrologic data was obtained from the Oklahoma Water Resources Board (OWRB)^{6 x}. The OWRB digitized lakes, rivers, and creeks based on USGS 1:100,000 topographic maps to generate the hydrologic dataset. 28 seasonal/intermittent streams, 11 perennial streams, one medium sized lake, and 268 ponds are within or intersect the AoR.

Mines and Quarries

The locations of mines and quarries were sourced from the USGS Mineral Resources Program (MRP)^{7*}. There are no mines or quarries located in the AoR.

Faults

Surface fault locations were obtained from the Oklahoma Geological Survey (OGS)⁸, which incorporates geological mapping data from Heran et al. (2003) and Miser (1954). 10 surface faults with an unknown slip sense intersect the AoR with their representation quality ranging from excellent to good.

Structures Intended for Human Occupancy

There are 40 residential structures intended for human occupancy identified within the AoR. Potential structures were sourced from the FEMA Geospatial Resource Center's USA Structures database.⁹ Points within the AoR were reviewed in conjunction with satellite imagery to confirm if a structure is present. The nearest potential structure for human occupancy in relation to all the injection wells is located approximately 0.45 miles from Vanguard I-5.

⁵ <https://gisdata-deq.opendata.arcgis.com/> - Accessed 1/20/2025

⁶ <https://oklahoma.gov/owrb.htm> - Accessed 1/15/2025

⁷ <https://mrdata.usgs.gov/usmin/> - Accessed 1/15/2025

⁸ <https://www.ou.edu/ogs/data/fault> - Accessed 1/16/2025

⁹ https://disasters.geoplatform.gov/USA_Structures/ - Accessed 1/25/2025

Plan revision number: 0

Plan revision date: 6/24/2025

Claimed as PBI

Figure 2.34—Area of Review basemap showing the location of the project wells: Vanguard I-1, Vanguard I-2, Vanguard I-3, Vanguard I-4, Vanguard I-5, Vanguard I-6, Vanguard I-8, Vanguard I-9, Vanguard I-10, Vanguard I-12, residential structures, and existing artificial penetrations in the mapped area: including oil and gas wells, water wells, and mines.

2.2.2 Maps of the Injection and Confining Zones

2.2.2.1 Arbuckle Group (Injection Zone)

The Arbuckle Group injection zone is distributed across the Midcontinent region of North America and evidence from wells drilled for oil and gas exploration confirms its thickness in northern Oklahoma and Osage County. Published regional-scale thickness maps such **Figure 2.17** lack the detail necessary to capture thinning of the Arbuckle Group over granitic basement hills to the southeast of the AoR. A more detailed thickness map (**Figure 2.16**) and inset in **Figure 2.34**) shows thinning of the Arbuckle injection zone as the carbonate onlaps basement hills and complete absence of the Arbuckle Group over several higher relief basement hills.

Claimed as PBI

Figure 2.35—Cross-section T – T' showing the thickness of subunits in the Arbuckle Group and their continuity across the AoR. Inset map (Figure 2.16) shows location of Cross-section T – T' relative to Arbuckle thickness, seismic surveys, and outline of the AoR. The Arbuckle Group includes all carbonate between the base of the Woodford Shale-Simpson Shale confining zone and top of the Reagan Sandstone or granitic basement. The Arbuckle Group is uniform thickness away from the area of buried basement hills and expected to be 800 to 1000 ft thick within the AoR. The regional Arbuckle Group thickness from Rascoe and Hyne (1988) is Figure 2.17.

2.2.2.2 Lower Mississippian Limestone and Woodford Shale (Confining Zones)

The upper confining zone for the upper Arbuckle injection interval is composed of the Simpson Group shale, Woodford Shale and lower Mississippian Limestone. The thickness of these confining beds changes across the AoR but their combined thickness provides low permeability intervals required to confine injectate to the underlying upper Arbuckle Group injection zone. The thickness of the combined Simpson shale and Woodford Shale is shown in **Figure 2.35**, and the thickness of the lower Mississippian Limestone in **Figure 2.37**.

Vintage wireline logs provide most of the petrophysical log data in Osage County. To correlate the resistivity properties of modern wireline surveys to the large set of vintage logs, cross-section R–R' was constructed. The location of cross-section R–R' is shown in **Figure 2.37**, whereas the cross-section is **Figure 2.39**. The corresponding gamma-ray curve and porosity log responses of the upper confining zone are shown in (**Figure 2.36**) a cross-section showing the petrophysical properties of Woodford-Simpson shale and lower Mississippian Limestone, including density and neutron porosity, gamma-ray response, and photoelectric absorption (PE). The lower Mississippian confining zone and Mississippian stratigraphy are highlighted in this figure to demonstrate lateral and vertical changes in the Mississippian Limestone. The Mississippian section in western Osage County is unconformably overlain by the Pennsylvanian Cherokee Group. Within the AoR the Cherokee Group is dominantly shale, which provides another low-permeability barrier between the upper Arbuckle injection zone and the closest USDW in the Vamoosa-Ada aquifer.

Claimed as PBI

Figure 2.36—Cross-section NE-SW showing gamma-ray and density-neutron porosity log profiles and petrophysical properties of Simpson Group shale, Woodford Shale and lower Mississippian Limestone confining zones. The lower Mississippian Limestone confining zone (shaded brown) is the first significant prograding carbonate wedge in the Mississippian interval.

Claimed as PBI

Figure 2.37—Thickness of the combined Simpson shale and Woodford Shale to form the Simpson-Woodford confining zone. The approximate position of the AoR is outlined in red and Arbuckle Group oil and gas fields are shaded red.

Claimed as PBI

Figure 2.38—Thickness of the lower Mississippian Limestone confining unit relative to the AoR. Cross-Section R-R' is **Figure 2.39** that shows the resistivity characteristics of the upper confining zone. Figure 2.36 is Cross-Section NE-SW that uses porosity curves from modern logs to highlight the petrophysical properties and lateral changes in thickness of the lower Mississippian Limestone confining zone. Red colored areas are Arbuckle oil and gas fields.

Claimed as PBI

Figure 2.39—Cross-section R-R' showing resistivity characteristics of the Woodford Shale-Simpson Group shale and lower Mississippian Limestone confining zones on a vintage and modern wireline well logs. Inset maps show location of Cross-section R-R' relative to the thickness of the two confining zones.

2.2.3 Cross Sections Through the AoR

Table 2.2 lists the maps and cross-sections used in this evaluation. Regional maps illustrate the distribution and structure of stratigraphic units, including the dip and structural relationships of key formations. Cross-sections provide visual interpretations of the sedimentary sequences and the crystalline basement, emphasizing features such as faults, uplifts, and confining zones.

Each map and cross-section has been reviewed to ensure alignment with the project goals, including the identification of confining units, injection zones, USDWs and other aquifer beds, and structural stability.

Table 2.1—Maps, Cross Sections and Other Figures Through the AoR

Figure Number	Description
Fig. 2.30	Petrophysical log cross section A-A' in the southern part of the AoR showing the Vamoosa-Ada USDW and the transition from freshwater to brine in the aquifer with increasing depth.
Fig. 2.31	Petrophysical log cross section B-B' in the central part of the AoR showing thicker sections of the Vamoosa-Ada USDW and the transition from freshwater to treatable saline water with depth.
Fig. 2.32	Structural contour map on the top of the Arbuckle Dolomite showing the AoR in a tectonically stable area between the Osage High and the Nemaha Fault zone
Fig. 2.35	Cross-section T – T' showing the thickness of subunits in the Arbuckle Group and their continuity across the AoR.
Fig. 2.36	Cross-section NE-SW showing petrophysical properties of the lower Mississippian Limestone, Woodford Shale, and Simpson Group shale Confining zones.
Fig. 2.37	Thickness map of the combined Simpson Group shale and Woodford Shale confining zone.
Fig. 2.38	Thickness of the lower Mississippian Limestone confining zone.
Fig. 2.39	Cross-section R-R' correlating resistivity responses of modern and vintage Petrophysical logs across the Woodford-Simpson and lower Mississippian Limestone confining zones.
Fig. 2.51	Cross section and enlarged sections of petrophysical logs showing porosity and microresistivity permeability in the Arbuckle injection zone.
Fig. 2.58	Thickness of shale in the Simpson Group that helps form the Simpson Group shale-Woodford Shale confining zone.
Fig. 2.59	Thickness of the Woodford Shale part of the Simpson Group shale-Woodford Shale confining zone.
Fig. 2.60	Stratigraphic cross section S-N showing lithostratigraphy and petrophysical properties of the interval between the upper Arbuckle and the Pennsylvanian Oswego Limestone including low-porosity confining zones (purple) in the Woodford-Simpson and lower Mississippian Limestone, high porosity Mississippian Chat reservoir and the shale-dominated low-permeability Cherokee Group.
Fig. 2.67	Lower baffling zone in the Arbuckle Group consisting of a series of low-porosity, low-permeability strata.
Fig. 2.72	Geophysical log sections across the upper Arbuckle Group, Simpson Group and lower Mississippian Limestone showing petrophysical properties of the logged interval.

2.3 Faults and Fractures [40 CFR 146.82(a)(3)(ii)]

2.3.1 *Faults and Fractures in the Area of Review*

2.3.2 *Literature Review*

The available recent literature on faults and fractures in western Osage County includes seismic and well-log-based interpretations. Seismic interpretations are primarily associated with the 3D surveys distributed across the area (**Figure 2.18**) and include Elibiju et al. (2011), Keeling (2016) and Kolawole et al. (2019). Petrophysical well-log based subsurface analysis of western Osage County, including structural maps of key stratigraphic units is found in Milad et al. (2024). More regional analyses of stress, faults and fractures include Lund Snee and Zoback (2022), Hu (2019, and Marsh and Holland (2016).

2.3.3 *Seismic Data*

The existing 3D surveys in western Osage County provide most information regarding potential faults and fractures impacting the injection/storage and confining intervals. Of the six 3D surveys in western Osage County, only two, Pearsonia and Antelope, included parts of the northern end of the AoR with the Pearsonia survey providing the most coverage. The remainder of the AoR is not surveyed by 3D seismic but scheduled to be surveyed by an extensive 2D grid as part of this application. To investigate faults and their impact on fluid flow in the injection zone and confining bed integrity, the Pearsonia 3D survey was analyzed by two independent geophysicists who identified both tectonic faults and karst/carbonate-collapse driven faults. Tectonic faults appear to offset the basement but have little impact on the confinement interval compared to carbonate collapse-driven faults. In contrast, karst/collapse-driven faults do not appear to impact the basement but influence overlying strata that appear to sag into low areas on the surface of the Arbuckle Group. Karst collapse-driven faults appear to flatten or sole out in the middle Arbuckle and are detached from the lower Arbuckle and basement. Clear northeast-southwest lineaments are observed on the top of the Arbuckle that appear to line up with faults associated with carbonate-collapse but could relate to subseismic tectonic faults that triggered later karst collapse features. While the top of the Arbuckle and the Woodford Shale confining layer appear to have noticeable fault offset, interpretation and mapping of the Mississippian secondary confinement horizon demonstrates little to no fault offset, suggesting potential fault leakage risks above the secondary confining zone could be considered minimal. The known seismic surveys and published seismic profiles detailing geology in western Osage County are listed in **Table 2.3**.

Table 2.2—Seismic surveys and published seismic profiles, Osage County, Oklahoma.

Survey Name	Location	Relation to AoR
Antelope	T.28 & 29N., R.6, 7 & 8E.	Includes northern end of AoR
Pearsonia	T.27 & 28N., R.6, 7 & 8E.	Includes northern one-fourth of AoR
Wild Creek	T.25N., R.4 & 5E.	West of AoR
Gray Horse	T.24 & 25N., R.5 & 6E.	Southwest of AoR
Big Heart	T.22 & 23N., R.9 & 10E.	Southeast of AoR
Radcliff	T.28N., R.5 & 6E.	West of AoR
Profile Source	Survey	Relevance to Project
Elebiju et al. (2011)	Wild Creek	Arbuckle thickness
Elebiju et al. (2011)	Gray Horse	Arbuckle thickness; faulting
Elebiju et al. (2011)	Not provided T.25N., R7 & 8E.	Arbuckle thickness; basement highs southeast of AoR
Kolawole et al. (2011)	Wild Creek	Arbuckle thickness & faulting
Elebiju et al. (2011)	Pearsonia	Arbuckle thickness
Elebiju et al. (2011)	Antelope (2)	Arbuckle thickness
Keeling (2016)	Wild Creek	Arbuckle thickness and paleokarst
Firkins (2021)	Wild Creek, Gray Horse, Antelope, Pearsonia and Big Heart	Arbuckle thickness; faulting types

The transmissivity of faults and capability of enhancing flow or impeding flow via mechanical smearing of phyllosilicate clay minerals along the fault plane or cataclasis and cementation is important to forming flow boundaries in the injection and storage zone. Likewise, the sealing of faults by clay-mineral rich gouge or cemented debris resulting from cataclasis is essential to the integrity of fault-transsected confining beds. The role of shale/clay-mineral smears along faults in siliciclastic dominated intervals is well studied and straight-forward (Yielding, 2002; Yielding et al., 1997). Because of the high solubility of carbonates and in particular, limestone, the estimation of the sealing capabilities of phyllosilicate mineral smears in fault planes in carbonates is more difficult (Sapiie et al., 2002).

The two more important variables governing formation of fault smears are the abundance of shale or clay-mineral rich beds in the faulted interval and amount of displacement along the fault. Both factors are used to compute a shale gouge ratio (Yielding, 2002) that reflects the amount of clay volume in the slipped interval. In the upper Arbuckle Group, faults evident on seismic and microimaging logs have low values of offset and juxtapose dolomite with minimal clay content and dissolution-enhanced porosity against similar porous rock. Furthermore, with carbonate-collapse-driven faulting, the downdropped block is moving downward into a void and at the same time likely rotating away from the stationary block, thereby reducing the probability of generating

smear or cataclastic debris along the fault plane that would reduce transmissivity. If the collapse-driven faulting generated a depression on the surface of the Arbuckle Group that initiated failure in the overlying Simpson Group, Woodford Shale and/or lower Mississippian Limestone, the high volume of phyllosilicate-rich shale in these strata is expected to generate clay-mineral gouge that would inhibit fluid flow across or along the fault. If the collapse-driven faults, as interpreted from 3D seismic, sole out in the shalier zone at the base of the middle Arbuckle Group, the potential for clay smear gouge could be greater, thereby sealing faults that might transect the low-porosity, low-permeability dolomite beds that form baffles to fluid flow.

2.3.4 Well Data

Faults and fractures in the area of review were evaluated at regional and local scales using published maps, maps constructed specifically for this application and subsurface data including seismic borehole imaging. Based on the published fault maps of northern Oklahoma (Marsh and Holland, 2016; Hu, 2019) (**Figure 2.8** and **Figure 2.9**) the CCS site overlies the Labette fault that trends southwest to northeast across Osage County. Extensive mapping of the area finds no expression of the Labette fault in the Paleozoic section. The location of the Labette fault is primarily based on the change in basement rocks from rhyolite and metamorphosed rhyolite (metarhyolite) north of the fault and granite to the south.

Neither the Labette fault nor major faults at high oblique angle to the Labette fault are evident on structure contour maps constructed on the top of the Mississippian Limestone (**Figure 2.9**). This mapping does not preclude the strike-slip movement along these faults, but the evidence for vertical displacement is lacking. Structural contour maps constructed on the top of the Mississippian Limestone are **Figure 2.9** and **Figure 2.38**. A regional structural contour map constructed on the top of the Arbuckle Group using a contour interval of 100 ft shows no apparent vertical offset within the AoR (**Figure 2.32**).

This map confirms that the proposed CCS site is located in a structurally quiescent area on the northwestern flank of the Osage High between the high and the Nemaha Fault zone to the west (**Figure 2.32**) where uplift continued into the Permian (Davis, 1984). Since there is no evidence of major deformation occurring in the Midcontinent region after Woodford deposition and before the pre-Pennsylvanian unconformity, mapping of the Arbuckle Group below the Woodford Shale confining unit and the top of the Mississippian Limestone above the lower Mississippian confining unit should identify any faults that offset the Woodford Shale and lower Mississippian Limestone and impact seal integrity.

The dataset of values for the top of the Mississippian Limestone (including Mississippian “Chat”) is much larger than the dataset for Woodford Shale tops or Arbuckle Group tops. For this reason, within the projected Area of Review (AoR), the structural attitude of the top of the Mississippian Limestone provides the best subsurface mapping horizon for detecting faults using changes in contour gradient and trend.

Mapping and a published seismic section from Elebiju et al. (2011) that is similar to **Figure 2.40** confirm that the confining and injection zones within the AoR are laterally continuous and free of transecting, transmissive faults that could facilitate fluid migration upward into the USDW.

Claimed as PBI

Figure 2.1—Portion of the central part of the Vanguard CCS Hub AoR contoured on the top of the Mississippian Limestone (C.I. = 50 ft). Only two faults were identified within the 72 sq mile mapped area, indicating the sedimentary section, including the Woodford Shale and lower Mississippian limestone confining units, is not disrupted by basement-rooted faults.

Plan revision number: 0

Plan revision date: 6/24/2025

Claimed as PBI

Figure 2.2—Seismic line that transects the Vanguard CCS Hub AoR close to the boundary between T.27N. and T.28N. and illustrates the continuity of the Arbuckle Group injection zone and the overlying Woodford Shale confining unit. The amber line represents top of basement and light green arrow indicates the base of Woodford Shale/top of Arbuckle Group reflector. The pink line marks the Pennsylvanian Mississippian contact. The inset map shows the location of the line within the Pearsonia 3D seismic survey.

A bedrock geologic map of the region (**Figure 2.12**) illustrates shallow faults within Osage County. However, no known faults indicated on the composite digital surface geology (**Figure 2.12**) or the Oklahoma Geology Map (Miser, 1954) (**Figure 2.25**) extend to depth and impact the integrity of the Woodford Shale-Simpson Group confining unit or the lower Mississippian Limestone that provides secondary confinement. These faults, which are identified in offset of surface beds have been shown to die out with depth in thick Pennsylvanian shale intervals. The presence of sealing beds above the Arbuckle Group is further supported by pressure measurements from drill stem tests and static fluid levels that indicate the Arbuckle Group is underpressured across Oklahoma with respect to a normal brine gradient (Puckette, 1996). Additionally, the production of significant amounts of oil and natural gas from shallower reservoirs including the Mississippi chat as well as different salinities for Mississippian Chat and Arbuckle formation waters, confirm the presence of high-quality seals above the Arbuckle injection zone.

In the Burbank field to the west of the AoR, fluid flow from injection wells to producing wells identified east-west permeability enhancement that is estimated at five times north-south and interpreted as a fracture network (Kleinschmidt, 1976; Perdue Petroleum, 2020). Years of injection of natural gas, water, polymer and carbon dioxide confirm the east-west preferential flow pattern and without direct evidence to the contrary it is inferred a similar pattern should exist in brittle rocks under the Site. Fracture orientation in the Arbuckle Group in the northern part of the NexGen Carbon Oklahoma, LLC-Project Vanguard CCS site determined by Elejibu et al. (2011) using seismic attributes is dominantly west northwest-east southeast (azimuth 300°/120°).

Evaluation of fractures and faults within the AoR relied on petrophysical logs and more specifically resistivity profiles and formation microimaging surveys. Two microresistivity image logs that surveyed approximately 90 ft in the Arbuckle injection zone, the Woodford Shale-Simpson shale primary confining zone and lower Mississippian Limestone secondary confining zone were used to establish the abundance, distribution and attitude of faults and fractures. The interpretation of these features was provided by Schlumberger. The location of the surveyed boreholes is shown in the inset map in **Figure 2.40** and **Figure 2.41**. The Shaw 5A-8 well in T.27N., R.7E. is within the AoR and the Hickory Creek Dome 2A-22 in T.27N., R.8E. is three miles to the east of the AoR. The distribution of strikes of fractures and faults provided by Schlumberger are shown in **Figure 2.41** and **Figure 2.42**.

Claimed as PBI

Figure 2.3—Strike plots of conductive natural fractures. **(A)** The upper Arbuckle injection zone, Woodford Shale and lower Mississippian Limestone confining zones, upper Mississippian and lower part of the Cherokee Group in the Shaw 5A-8, and **(B)** Mississippian interval in the Hickory Creek Dome 2A-22. Fractures in the Shaw 5A-8 exhibit a singular dominant strike of NNW-SSE, whereas conductive fractures in the Mississippian section of the Hickory Creek Dome 2A-22 form three distinctive strikes: NNW-SSE, NW-SE, and NE-SW.

Claimed as PBI

Figure 2.4—Strike plot of faults interpreted for the Shaw 5A-8 and Hickory Creek Dome 2A-22 in the lower Cherokee Group, Mississippian, Woodford Shale and upper part of the Arbuckle Group. Fractures in the Shaw 5A-8 have dominant NE–SW strike, whereas the Hickory Creek Dome 2A-22 has a NW–SE dominant strike trend.

Plan revision number: 0

Plan revision date: 6/24/2025

The vertical distribution of fractures across the lower Mississippian Limestone confining zone is shown in **Figure 2.43**, an interpretation of faults fractures by Schlumberger personnel. No faults are evident on the formation microimaging survey and fractures evident in the lower Mississippian confining zone and the carbonate interval above have small fracture heights (approximately 2 ft) and are separated by intervals of unfractured rock. Drilling induced fractures (**Figure 2.44**) common on both microimaging surveys strike WSW–ENE and confirm the regional maximum horizontal stress direction proposed by Lund Snee and Zoback (2022) shown in **Figure 2.45**.

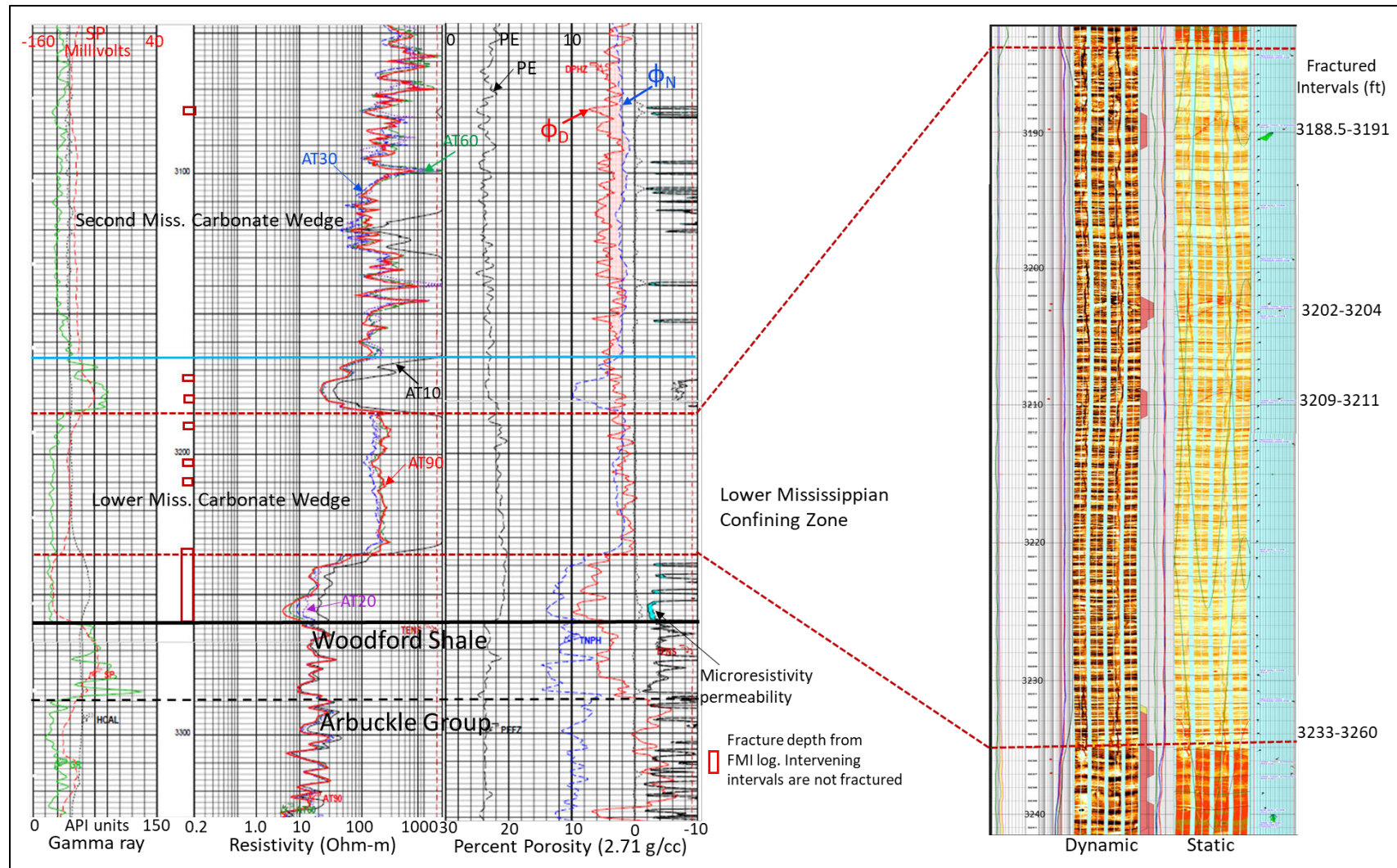


Figure 2.5—Vertical distribution of fractures across the lower Mississippian Limestone confining zone as determined by interpretation of formation microimaging survey by Schlumberger. Thin (2 to 3 ft thick) fractured intervals are separated by intervals of unfractured rock in the Shaw 5A-8 borehole. Tracking in the resistivity profile of the AT10, AT20, AT30, AT60 and AT90 curves also suggests the absence of major fractures.

Claimed as PBI

Figure 2.6—(A) Dip direction and magnitude showing near-vertical induced fractures, and (B) Strike plot of drilling-induced fractures in the Shaw 5A-8 interpreted from the formation imaging survey. WSW-ENE strike of induced fractures aligns with principal horizontal stress (σ_H) as reported by Lund Snee and Zoback (2022).

Claimed as PBI

Figure 2.7—State of stress in Oklahoma and southern Kansas from Lund Snee and Zoback, (2022). Color shading indicates strike-slip movement is expected for faults in the vicinity of the Vanguard CCS Hub AoR shown in red. Stress orientation established by Birdie et al. (2017) in southern Kansas is east-west. Fine dark lines are faults from various sources cited in Lund Snee and Zoback (2022).

2.4 Injection and Confining Zone Details [40 CFR 146.82(a)(3)(iii)]

The injection zone encompasses the geologic formation, group of formations, or a segment of a formation with sufficient areal extent, thickness, porosity, and permeability to accept carbon dioxide injection via wells associated with a CCS project. The Ordovician-aged dolomites of the upper Arbuckle Group exhibit the necessary attributes to serve as an effective injection interval at the NexGen Carbon Oklahoma, LLC- Project Vanguard CCS site. The dolomites and thin sandstones of the Arbuckle Group, located between depths of 2,650 ft and 3,350 ft, possess the necessary characteristics to serve as an effective injection interval within the Vanguard CCS Hub AoR. The injection zone is at least 2,000 ft below the lowermost freshwater zone, which for permitting purposes is treated as a USDW (less than 10,000 mg/L total dissolved solids). A schematic cross-section illustrating the stratigraphy and well placement is provided in Section 1.0 (**Figure 1.3**).

Demonstrating confining isolation for a Class VI injection site requires an impermeable containment layer and the absence of vertically transmissive faults or fractures that could compromise the containment system. The Confining Zone is defined as a geologic formation, group of formations, or part of a formation overlying the injection zone that acts as a barrier to vertical fluid movement. At the proposed site, the Woodford Shale-Simpson Group shale, and lower Mississippi Limestone serve as the primary confining zones. Above the Mississippian Limestone are several Pennsylvanian-age shale-dominated intervals that add hundreds of ft of low-permeability rocks. The only issue with Pennsylvanian shale units is that they were penetrated by many more petroleum exploration wells than the deeper Lower Mississippian and Woodford confining units. Injection targets are defined as formations below a depth of 2,500 ft, marking the top of the supercritical CO₂ window.

The geologic characteristics of the proposed site summarized in **Table 2.4**, are based on regional core data and offset analog information. Site-specific data will be collected during the drilling of a stratigraphic test well.

Plan revision number: 0

Plan revision date: 6/24/2025

Table 2.3—Geologic characteristics of the proposed Vanguard CCS Hub Site.

Zone of Interest to Vanguard CCS Hub AoR		Depth	Areal Extent	Thickness	Lithology	Porosity and Permeability	Mineralogy	Potential for Geochemical Reactions	Capillary Pressure and Integrity of Confining Zone	Additional Data Collection
Upper and Middle Arbuckle Group Injection and Storage Zone	2,650 to 3,300 ft	Present throughout AoR	500 to 700 ft	Dolomite and minor amounts of chert and sandstone	Matrix 8-10% Vugs and channels >20% porosity. 0.0001 md to 1000 md, average 40 md based on injection rates	Dolomite, minor quartz and minor calcite in fractures	Dolomite-low, calcite-high near injection site, and quartz-low			Conventional core for porosity and permeability, mineralogy and rock-injectate reactions
Woodford Shale/ Simpson Shale Primary Confining Zone	2,600 to 2,950 ft	Present throughout AoR	Combined 4 to 60 ft	Organic-rich Woodford Shale, calcareous shale, and silty/sandy shale. Thin ss. in Simpson Group	Woodford: core 2.9% porosity; 0.005 md perm. Sidewall core 0.1% porosity; 0.231 md perm. Porosity 0.6 to 1.8% from log. Simpson: 1.2 to 5% porosity from log.	Illite clay and quartz, calcite in fractures in Woodford	Illite clay and quartz-low, Calcite high	Capillary pressure not available, expected to be high similar to other non-cherty shale	Conventional core for porosity and permeability, capillary pressure, mineralogy, rock-injectate reactions, and mechanical properties	
Lower Mississippian Secondary Confining Zone	2,550 to 3,200 ft	Present throughout AoR	20 to 110 ft	Limestone, argillaceous limestone, and dolomitic limestone with chert	<1% to 4% porosity from core, sidewall core and logs, 0.001 to 0.144 md core and sidewall core	Calcite, dolomite, silt, chert/quartz and clay minerals	Calcite- high, all others-low	Capillary pressure not available, expected to be high	Conventional core for porosity, permeability, capillary pressure, rock-injectate reactions and mechanical properties	
Middle and Lower Arbuckle Baffle Zone	3,800 to 4,200 ft	Present throughout AoR	40 to 80 cumulative ft	Dolomite	≤4% from density log ($\rho_{ma} = 2.86 \text{ g/cm}^3$)	Dolomite from log	Dolomite	Capillary pressure not available, expected to be high	Conventional core for porosity, permeability, capillary pressure, rock-injectate reactions and mechanical properties	

2.4.1 Data on the Injection Zone

The primary injection targets for carbon sequestration at the NexGen CCS site are intervals of higher porosity and permeability in the upper and middle sections of the Arbuckle Group (**Figure 2.52**), adapted from Derby et al. (2012), illustrates the Great American Carbonate Bank that surrounded the North American craton during the early Ordovician. Regionally, the Arbuckle Group extends across the South-Central Plains states and was deposited during the late Cambrian to middle Ordovician. The Arbuckle lies directly above the Reagan Sandstone or “granite wash”, if present, or otherwise directly atop the basement rocks. It consists predominantly of dolomite in northern Oklahoma, subdivided into formations based on insoluble residue zonation (Ireland, 1944; McCracken, 1955), whereas limestones outcropping in the Arbuckle Mountains are subdivided with some success using depositional facies stacking patterns (Swinea et al., 2011) and biostratigraphy (Ethington and Dresbach, 1990). The Arbuckle is the thickest lower Paleozoic sequence in Oklahoma, though thickness varies within Osage County. It is absent over basement highs (Rountree, 1980) but exceeds 1,400 ft in thickness in western Osage County.

The Arbuckle was deposited in a shallow shelf environment. Equivalent lithostratigraphic units include the El Paso Group in southwestern Texas, the Ellenburger Group in central and north Texas, the Knox Group in the eastern U.S., and the Beekmantown Group in the northeastern U.S. In southern Oklahoma, member formations of the Arbuckle Group include the Fort Sill Limestone, Signal Mountain Limestone, their hydrothermal dolomite equivalents the Royer Dolomite and Butterly, respectively, McKenzie Hill Formation, Cool Creek Formation, Kindblade Formation and West Spring Creek Formation (Ham, 1973; Lynch, 1990). However, investigations (Fritz et al., 2012; Lynch, 1990) of the highly dolomitized Arbuckle Group in northern Oklahoma infer that the Arbuckle in Osage County aligns more closely with the Ozark stratigraphy and that nomenclature is used in this application (**Figure 2.47**, adapted from Fritz, et al., 2012).

Dolomite units within the Arbuckle Group are important oil and gas reservoirs in Oklahoma and Osage County (Akin, 1964; Rountree, 1980). The textures, fabric, pore types and color for Arbuckle cuttings from wells drilled in Osage County are described by Rountree (1980), and karst features in cores from Osage County are described by Lynch (1990). Regional depositional settings, illustrated in **Figure 2.48**, suggest permeability is better developed in shallow subtidal facies. Cyclic changes in sea level, coupled with subsidence produced stacked facies as more proximal supratidal and upper intertidal faces prograded over more distal lower intertidal and subtidal facies. Facies stacking generated sections where less porous and permeable upper intertidal and supratidal facies separate cleaner lower intertidal shallow subtidal facies. Porosity enhancement associated with drops in sea level, subaerial exposure, and meteoric dissolution generated karst features described in Lynch (1990) and Lynch and Al-Shaieb (1991). Regional unconformities generated by declines in sea level have associated karst features that enhance reservoir properties (**Figure 2.49** and **Figure 2.50**, adapted from Fritz, 2012). Permeability measurements for small scale features in core including matrix pores and fractures by Morgan and Murray (2015) demonstrate the wide range of values and orders of magnitude differences in magnitude between matrix and fracture permeability.

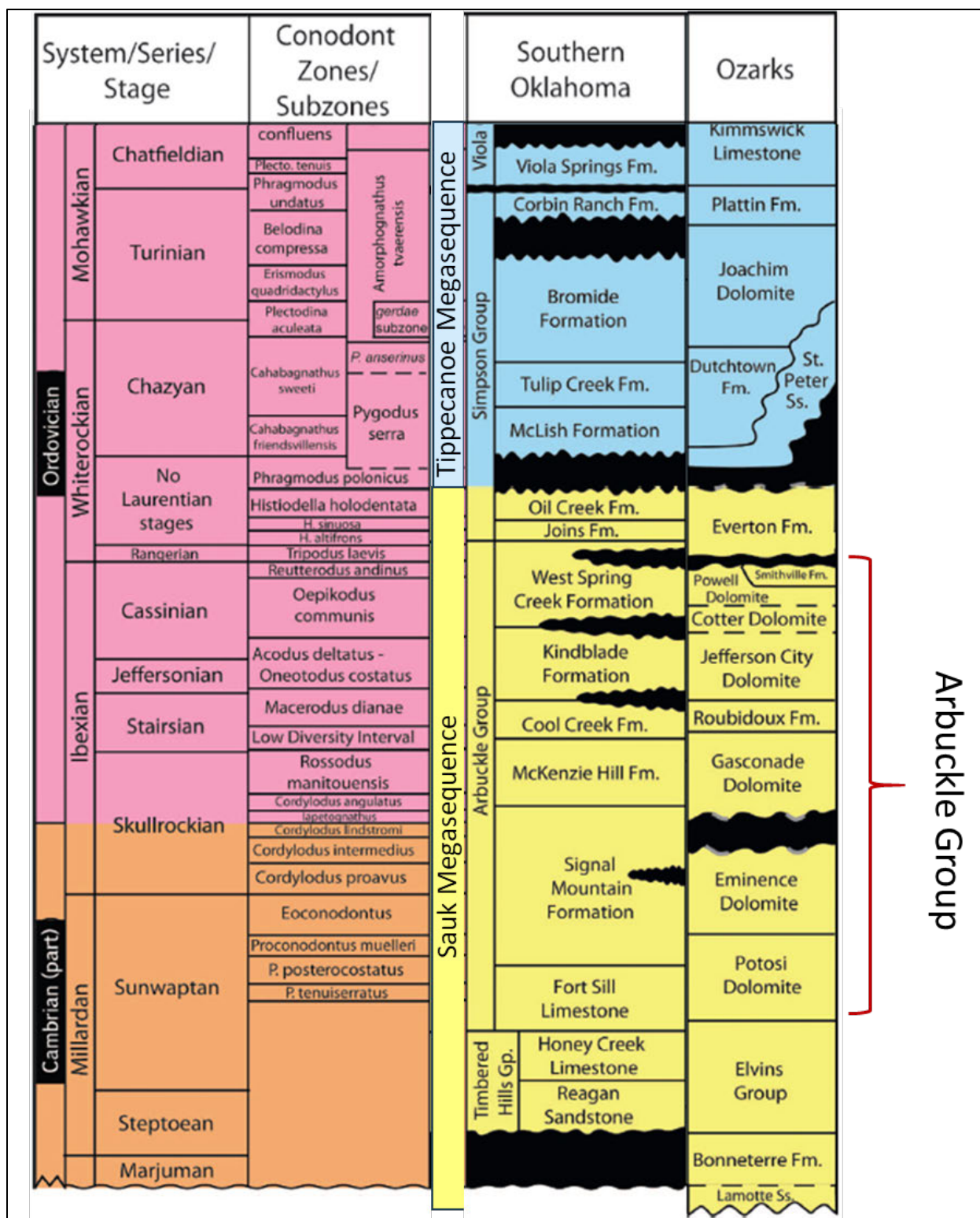


Figure 2.8—Stratigraphic nomenclature and biostratigraphy for the Arbuckle Group and adjacent strata that make up the Sauk and Tippecanoe Megasequences. After Fritz et al., 2012 and Ethington et al., 2012.

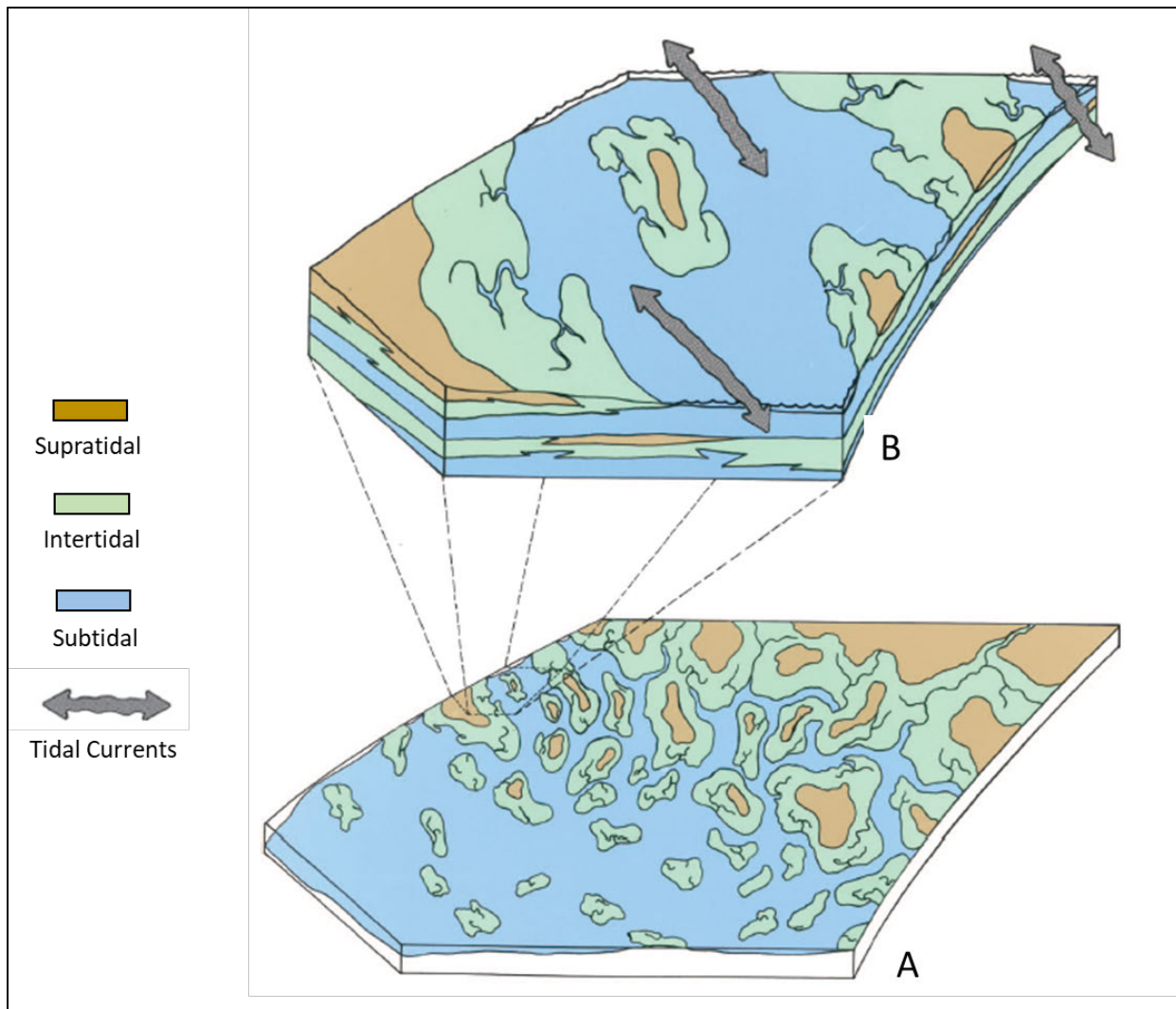


Figure 2.9—Block diagrams showing (A) the regional depositional setting for Arbuckle carbonates and (B) the hypothetical depositional model showing tidal currents from Fritz et al., 2012.

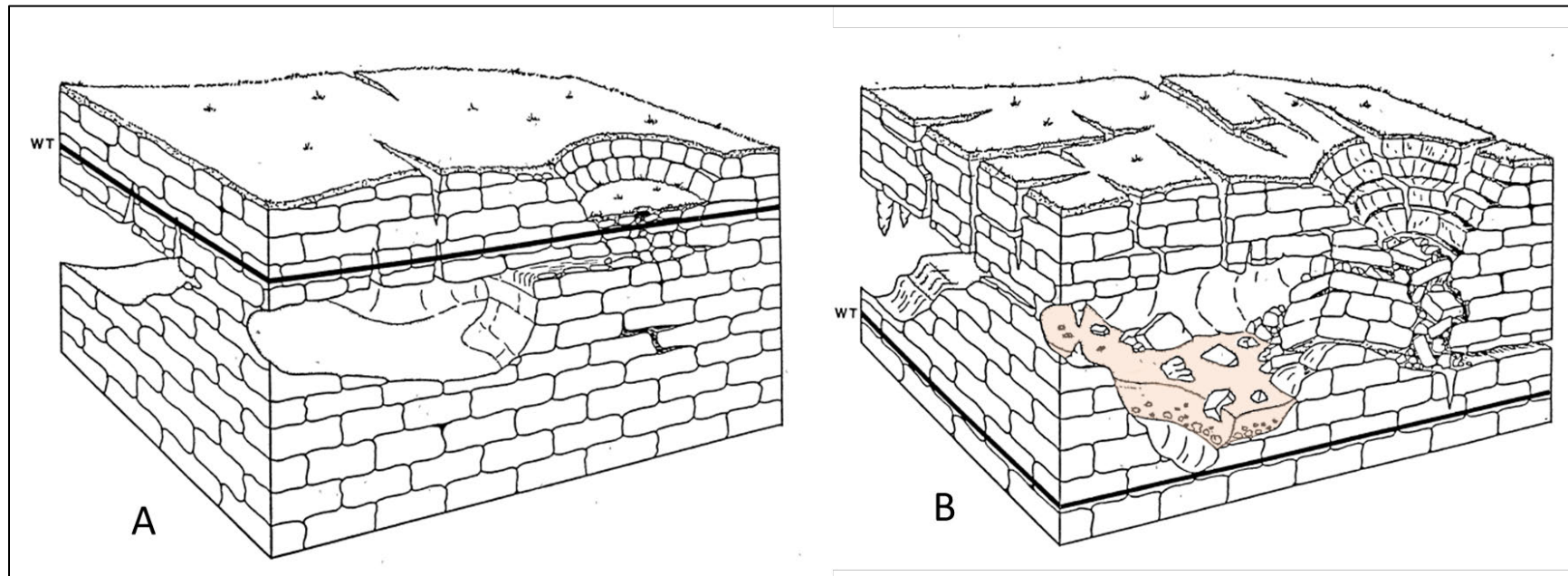


Figure 2.10—Initial (A) and main (B) stages of karst development from Lynch (1990). Brown shading represents sediment infill; heavy black line is the water table.

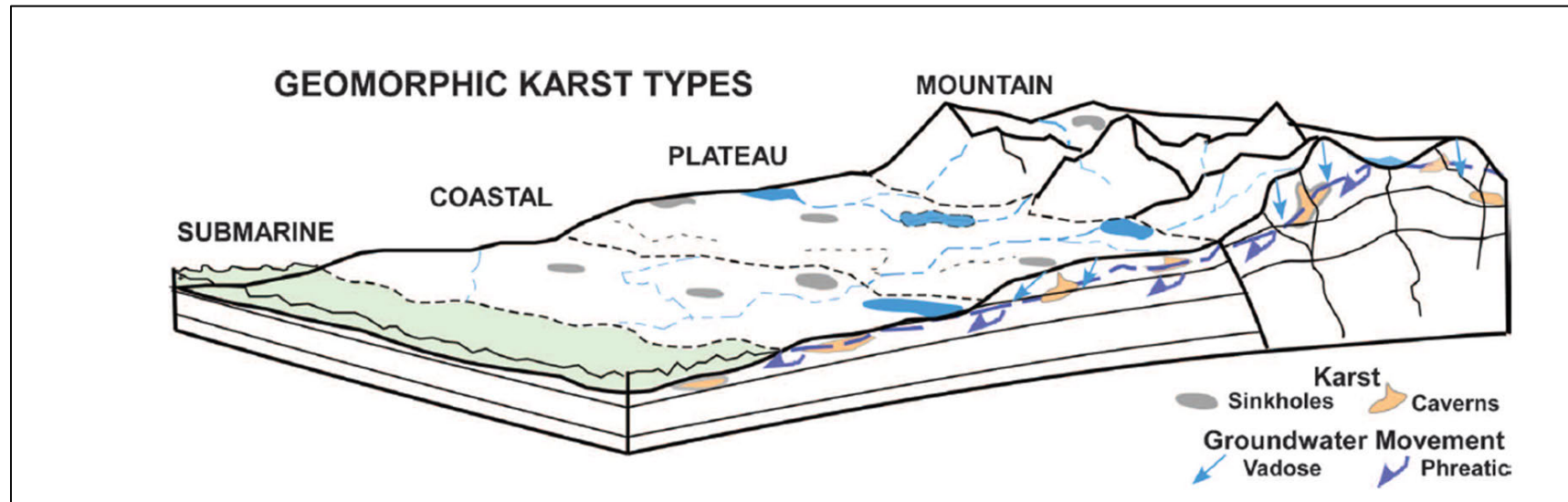
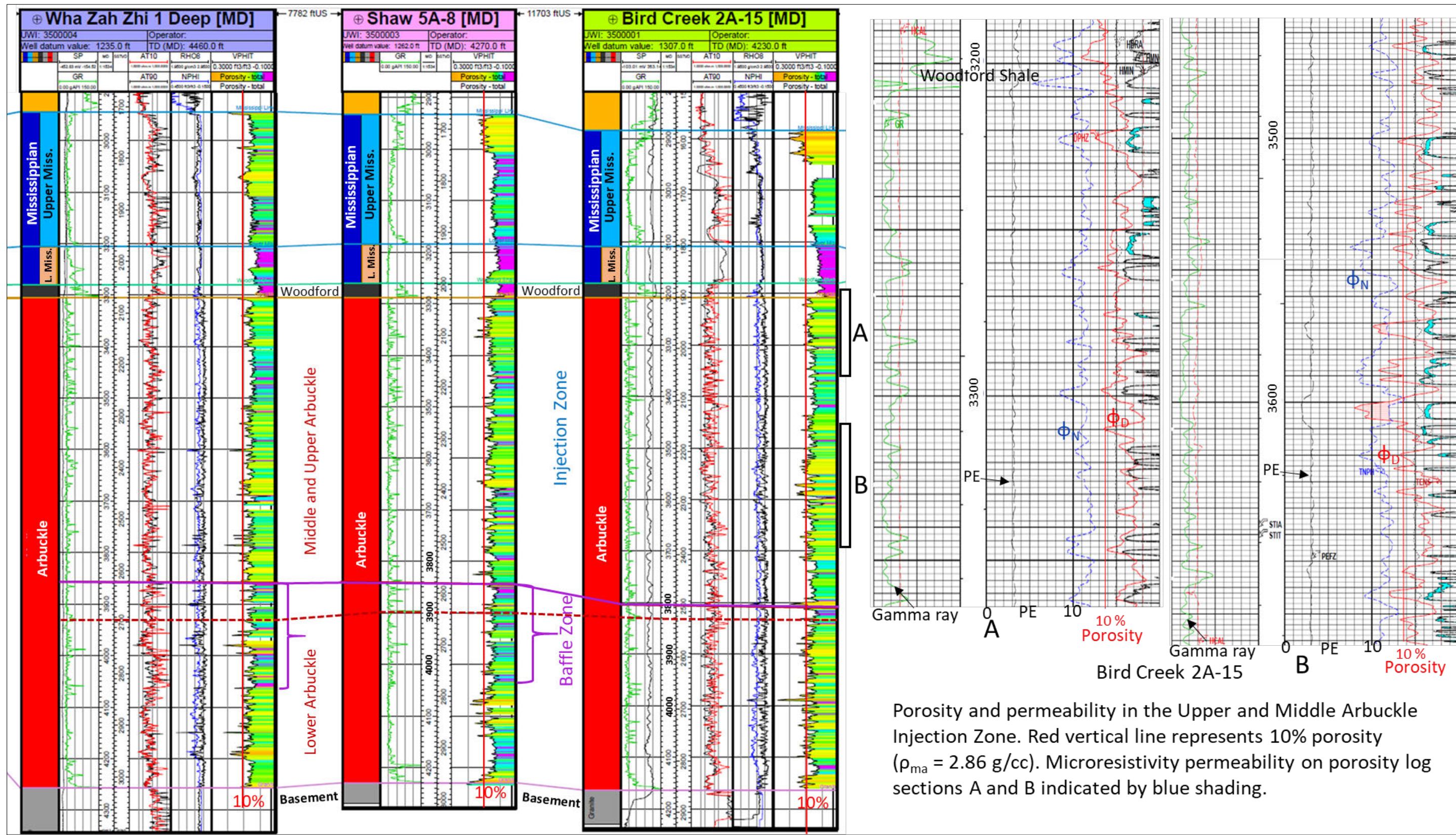


Figure 2.11—Regional karst environments from Fritz et al. (2012) after Jakucs (1977). Arbuckle karst likely developed in coastal and plateau settings depending on magnitude of sea-level decline.



Claimed as PBI

Figure 2.13—Lateral extent of Arbuckle and equivalent Cambro-Ordovician carbonates across North America.

In eastern Kay, Noble, Pawnee and western Osage Counties, the Arbuckle saline aquifer is known to accept large volumes of disposal fluids with no detectable increase in pressure (Murray and Holland, 2014). As a result of its regional distribution, the Arbuckle aquifer remains hydrostatically connected to areas of recharge on the Ozark Uplift. The hydraulic continuity of Arbuckle aquifer is manifested in several ways. Across the Midcontinent region, including the deep Anadarko basin, the Arbuckle Group remains near normal pressure, despite being more deeply buried than overlying overpressured strata in the Pennsylvanian (Al-Shaieb et al., 1995). Though pressure differences on the Cherokee Platform are not as striking as those in the deep Anadarko Basin, the original reservoir pressure in the Burbank sandstone reservoir of 1,350 psi (Perdue Petroleum, 2020) gives a minimum pressure gradient of 0.465 psi/ft compared to a 0.38 to 0.41 for most of the Arbuckle Group in western Osage County (**Figure 2.53**), further illustrating the isolation of the Arbuckle regional aquifer from Pennsylvanian reservoirs. Regionally, the Arbuckle Group remains underpressured despite the disposal of billions of barrels of water in the Arbuckle in southern Kansas (Newell et al., 2024) and northern Oklahoma (OCC, 2024). Another manifestation of the regional distribution of the Arbuckle aquifer is water chemistry that differs from the pore-water chemistries of shallower reservoirs. As an aquifer, the water chemistry in the Arbuckle Group slowly transitions from freshwater to brine with depth, in contrast to compartmentalized reservoirs that lack the hydraulic connectivity to freshwater recharge. As an example, Arbuckle water is chemically different from water in the closest shallower conventional reservoir in the upper Mississippian section, the Mississippian Chat. These differences are illustrated in **Table 2.8b** - Comparative water chemistry of the Arbuckle and Mississippi Chat reservoirs.

Claimed as PBI

patterns in Arbuckle saline and freshwater aquifer confirm the regional pattern from Jorgenson and Signor (1981), whereas subnormal pressures in the Arbuckle Group confirm vertical isolation of the injection zone from shallower normally pressured reservoirs and the integrity of the upper confining units for the Arbuckle Group injection zone. Vanguard CCS Hub AoR is outlined in red.

Geophysical surveys in northern Oklahoma, including Osage County, illustrate the thickness, lateral extent, and tectonic modification of the Arbuckle Group. Interpretations of the Antelope, Wild Creek, Pearsonia, and Grey Horse 3-D seismic datasets in western Osage County have been published. For example, Keeling (2016) identified significant karst features including sinkholes using negative amplitude data from the Wild Creek Survey approximately 6 miles west of the AoR. Elebiju et al. (2011) published seismic lines from the Pearsonia survey showing continuous Arbuckle section in an area including the northern part of the AoR. Jennings (2014) contributed geomechanical information on the Mississippian Limestone, which confirmed fracture orientation and provided Youngs modulus values and other geomechanical data to predict the competence of the lower Mississippian confining unit.

Karst and other dissolution features within the Arbuckle Group injection zone were interpreted using formation microimaging surveys for the Shaw 5A-8 well in Section 8, T.27N., R.7E. and the Hickory Creek Dome 2A-22 well in Section 22, T.27N., R.8E. Those results are discussed further in the section on porosity and the relationship dissolution features density porosity is demonstrated.

2.4.1.1 Depth, Areal Extent and Thickness

The depth to the Arbuckle Group top varies across the AoR from 2650 ft below surface along the southeastern edge of the AoR to more than 3350 ft along the western boundary of the AoR. The Arbuckle aquifer is widespread across the Midcontinent of North America and Oklahoma (**Figure 2.52** and **Figure 2.15**). The thickness of the Arbuckle Group in the vicinity of the Vanguard CCS Hub AoR is shown in **Figure 2.16**. Based on this map, the total Arbuckle Group is between 800 and 1000 ft thick under the AoR, a result of the AoR being to the north of the Osage High where the Arbuckle thins over buried granite hills. Wireline-logs were available for eighteen (18) wells drilled to basement in western Osage County and eastern Kay County in T.25N., to T.29N., R.3E. to R.8E., The average thickness of the Arbuckle Group in these wells, including the thinner sections of 175 and 150 ft, respectively, immediately to the south the AoR, is 911 ft. Away from the buried hills, the average thickness for Arbuckle Group in the remaining 16 wells is 1070 ft. The upper and middle sections of the Arbuckle Group are approximately two-thirds of the total Arbuckle carbonate thickness. Based on this ratio, the thickness of the combined upper and middle Arbuckle injection zone averages approximately 600 ft under the AoR. Average measured thickness of the combined upper and middle Arbuckle sections in the five modern wells within the AoR is 640 ft,

A comprehensive study by Milad et al. (2022) with the Oklahoma Geological Survey analyzed data from 988 wells distributed throughout Osage County, including raster images, and core from one well. Wireline logs for 168 wells were digitized, with some featuring complete log suites with gamma-ray, resistivity, bulk density, neutron porosity, density porosity, and sonic porosity. The thickness of the Arbuckle Group in these digitized well logs ranges from a minimum of 35 ft to a maximum of 1,100 ft, with an average thickness of 303 ft. The 35-ft interval represents the thinnest mapped Arbuckle thickness for the Milad et al. (2024) study, which did not include zero (0) thicknesses of the Arbuckle Group over prominent basement highs such as the Wildhorse field in T.22N., R.10E. and Osage-Hominy field in T.23N., R.8E. (Rountree, 1980)

According to Milad et al. (2024), 41 of the digitized wells penetrated the Precambrian basement and contain the entire Arbuckle Group. Based on this dataset, the average porosity of the Arbuckle Group is 10 percent. Since the Arbuckle Group is characterized by significant karst features and solution-collapse brecciation, localized porosity can be highly variable and range from near zero

to near 20%. These karstic features are attributed to meteoric dissolution associated with repeated subaerial exposure events driven by fluctuations in relative sea level (Fritz et al., 2012).

2.4.1.2 Porosity

Milad et al. (2024) attribute enhanced porosity and permeability in the Arbuckle Group to karst features that increase its suitability as a storage reservoir. On average, the combined upper and middle Arbuckle Group under the AoR is 640 ft, whereas the total Arbuckle Group is approximately 900 ft thick. Average dolomite density porosity (matrix = 2.86 g/cm³) in the combined upper and middle sections is 8%, with a range between <1% and 18%. Higher values are observed in sandstone, but they were excluded from the average. Cumulative ft of porosity calculated for wells with modern log suites ranged from 175 ft of 8% or greater porosity in Section 15, T.27N., R.7E to >200 ft of >8% porosity Section 29, T.26N. R.7E. The two example wells both had an additional approximately 100 ft of 6 to 7.9% porosity. Lithological analysis, derived from both core samples and photoelectric (PE) log interpretations, indicates that dolomite is the dominant lithology. Porosity types in the Arbuckle cores from Osage County examined by Lynch and Al-Shaieb (1991) are dominantly vuggy, solution-enlarged fracture, intergranular, intraparticle, and fracture (**Figure 2.32**). Karst features such as solution enlarged vugs and fractures described by Lynch (1990) and shown in significantly improve the storage potential of the Arbuckle aquifer.

Interpretation of formation microresistivity imaging surveys in the approximately upper 90 ft of the Arbuckle injection zone confirms the importance of dissolution porosity and in particular, small vugs to the total porosity. Data from logs in the Milad et al. (2024) study show an average porosity of 11.4 percent, while core measurements yield a mean value of 7.5 percent. The nature of vuggy and fracture pores makes conventional porosity measurements difficult to obtain in rock with heterogeneity in reservoir properties that extends beyond the diameter of the conventional core or core plug. Therefore, porosity and permeability measurements for the Arbuckle and many other carbonates tend to be biased toward less-permeable, more competent rock that can be sampled for conventional porosity and permeability measurements.

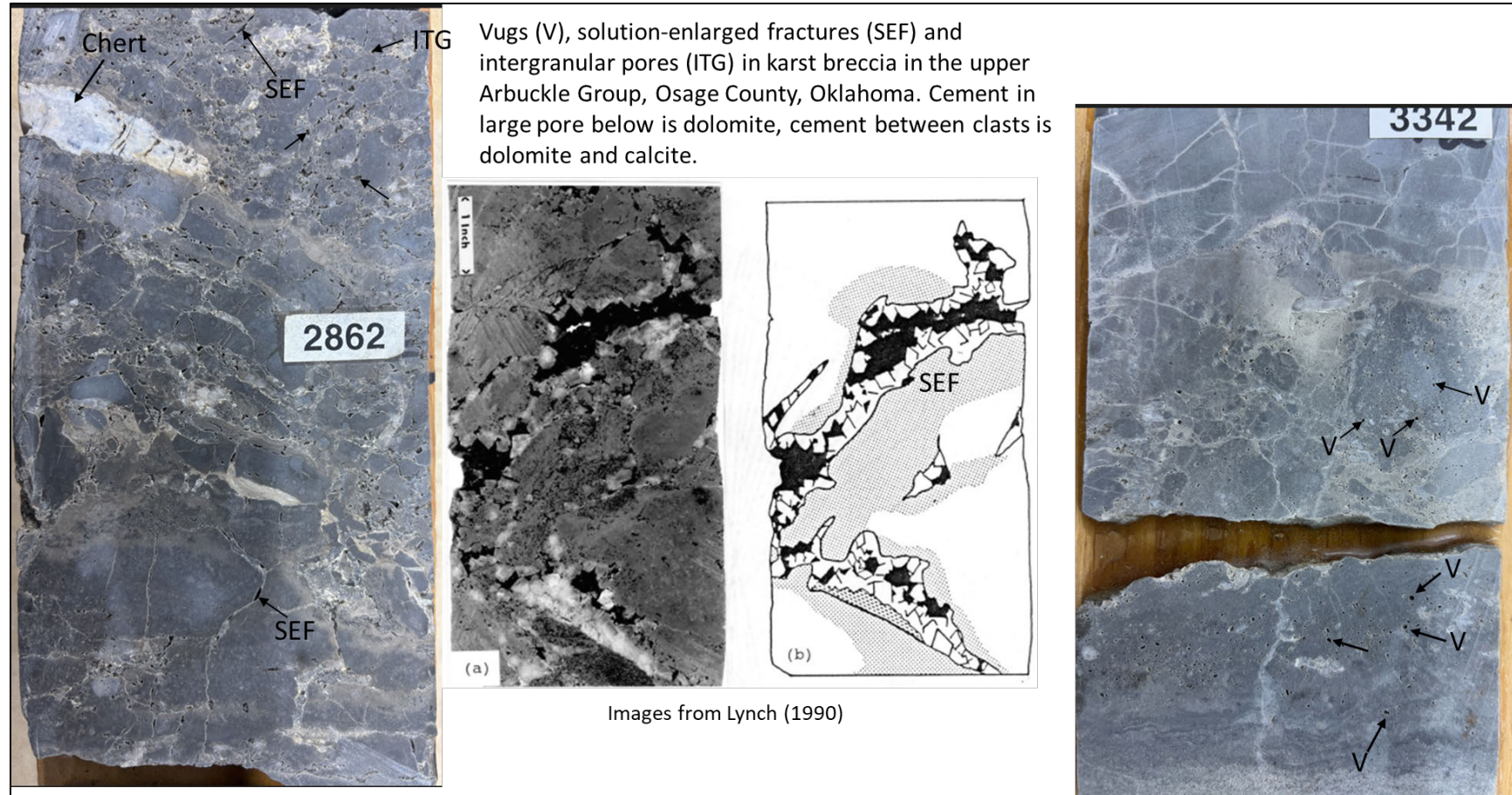


Figure 2.15—Core photographs of the Cotter Dolomite in the upper Arbuckle from wells closest to the AoR. Pore network is dominantly intraparticle and interparticle vugs and solution-enlarged fractures. Permeability of large pores shown in middle photograph and sketch from Lynch (1990), is difficult to quantify using conventional methods.

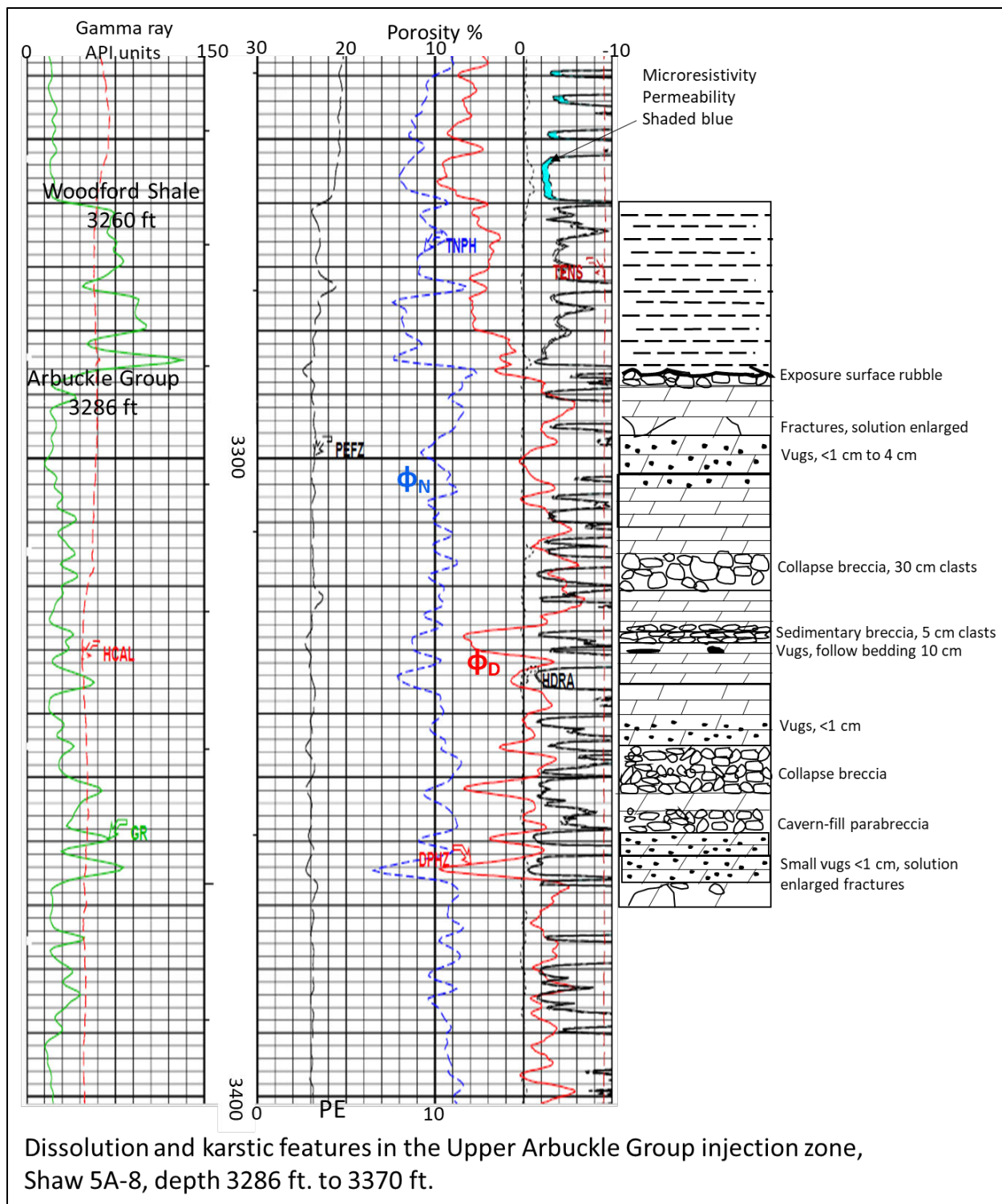


Figure 2.16—Comparison of dissolution and karst features to density and neutron porosity in the upper 84 ft of the Arbuckle Group, Shaw 5A-8 well. Interpreted collapse and cavern-filling breccia are lower porosity compared to zones of small vugs like those shown in Microresistivity formation images for the Shaw 5A-8 and the Hickory Creek Dome 2A-22 wells are shown in and, respectively.

Plan revision number: 0

Plan revision date: 6/24/2025

Claimed as PBI

neutron porosity, and gamma-ray curves. Woodford Shale from 3260 ft to 3284.5 overlies rubble zone (3284.5 to 3286 ft) along Woodford – Arbuckle contact. Top eight (8) ft of Arbuckle dolomite lacks vuggy pores and is low porosity (<-2-4%, 2.71 g/cc matrix density (ρ_{ma}) as logged and 4%, 2.86 g/cc ρ_{ma}) corrected for dolomite. Location of well shown on inset map.

Claimed as PBI

Figure 2.56 continued—Dissolution and karst features in the Upper Arbuckle Group injection zone as interpreted using formation imaging logs, density and neutron porosity, and gamma-ray curves. Apparent collapse breccia around 3324 ft has relatively low porosity (<4%, 2.71 g/cc pma; 4%, 2.86 g/cc pma), whereas interval with vuggy porosity at 3298 to 3304 has higher porosity (0%, 2.71 g/cc pma and 8%, 2.86 g/cc pma). High porosity (6%, 2.71 g/cc pma and 14%, 2.86 g/cc pma) from 3326 ft to 3330 ft is vuggy porosity in sedimentary breccia. Shaw 5A-8, Section 8, T.27N., R.7E, depth 3294 ft to 3320 ft. Location of well shown on inset map.

Plan revision number: 0

Plan revision date: 6/24/2025

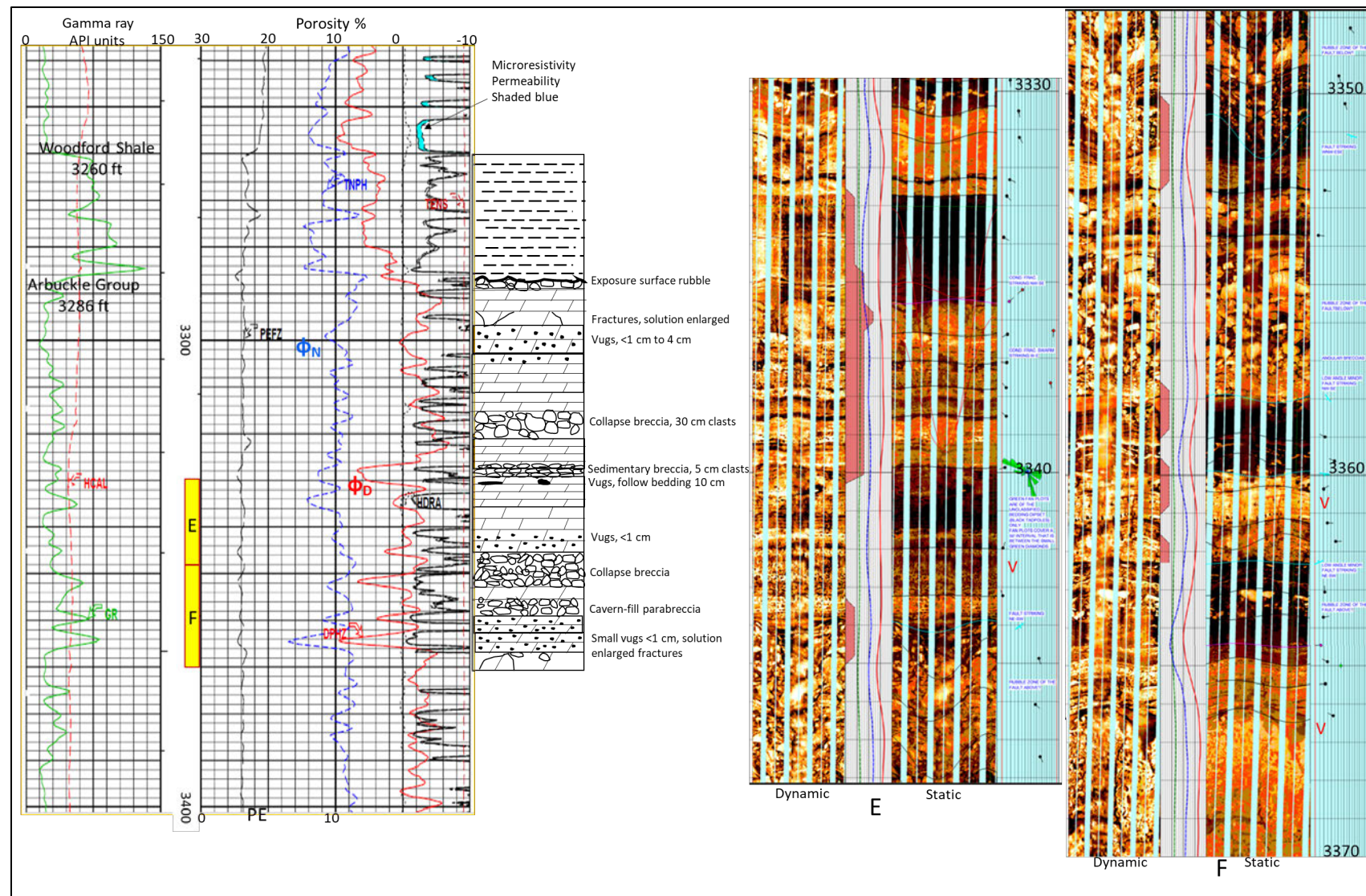


Figure 2.56 continued—Higher porosity (>0%, 2.71 g/cc pma and 8%, 2.86 g/cc, pma) corresponds to intervals with small vugs as dominant type of pores. Shaw 5A-8, Depth 3330 ft to 3370 ft.

Claimed as PBI

Figure 2.18—Dissolution and karstic features in the Upper Arbuckle Group injection zone as interpreted using formation imaging logs, density and neutron porosity, and gamma-ray curves. Hickory Creek Dome 2A-22, depth 3260 ft. to 3294 ft. Higher density porosity at 2710 ft to 2714 ft (6%, 2.71 g/cc ρ_{ma} , 12.6%, 2.86 g/cc ρ_{ma}) and 2741 ft to 2746 ft (0%, 2.71 g/cc ρ_{ma} and 8%, 2.86 g/cc ρ_{ma}) correlate to intervals with vuggy porosity

Claimed as PBI

Figure 2.57 continued—Dissolution and karstic features in the Upper Arbuckle Group injection zone, as interpreted from formation imaging logs, density and neutron porosity, and gamma-ray curves. Porosity >1% (2.71 g/cc ρ_{ma}), 9% (2.86 g/cc ρ_{ma}) at 2770 ft and 2790 ft associated with vugs. Hickory Creek Dome 2A-22, T.27N., R.8E., depth 2753 ft to 2800 ft. Location of the well is shown on the inset map.

2.4.1.3 Permeability

As with most karsted carbonate reservoirs, permeability values vary widely, from 0.0001 millidarcies (mD) to as high as 1,000 mD, reflecting notable heterogeneity in reservoir properties as a result of vuggy, solution enlarged and fracture pores. Morgan and Murray (2015) analyzed permeability at a finer scale in four Upper Arbuckle cores, supplementing these findings with data from middle and Lower Arbuckle outcrops in the Slick Hills and Arbuckle Mountains. Their work suggests that high injection rates observed in the Arbuckle are likely associated with sections with solution-enlarged vugs or fractures that exhibit significantly higher permeability than the surrounding matrix.

Permeability within the injection zone in the upper and middle Arbuckle Group is evident on microresistivity logs as shown in the example in **Figure 2.51**. Microresistivity indicates intervals permeable to mud filtrate but permeability cannot be accurately quantified. Permeability measurements must come from other sources such as core analyses, drill stem tests or pumping tests.

2.4.1.4 Mineralogy

The Arbuckle Group in Osage County is overwhelmingly dolomite, with minor amounts of quartz as detrital grains in dolomite, chert in dolomite, or detrital grains in thin sandstone, siltstone and shale beds, calcite as cement in fractures, and clay minerals found mostly in thin argillaceous beds or infill sediment in karst features. Lynch (1990) analyzed Arbuckle core samples from two wells close to the AoR, the Oliphant Lafortune in Section 8, T.25N., R.6E. approximately 3 miles to the west of the AoR, and the Oliphant Nate in Section 15, T.24N., R.7E., approximately 4 miles south of the AoR. X-ray diffraction of these samples showed the Arbuckle was more than 95% to 100% dolomite in carbonate samples. Additional x-ray diffraction of clasts and matrix from the Lafortune and Nate cores found only dolomite with minor amounts of quartz, confirming the mineralogy reported by Lynch (1990). A representative spectrum from a discrete sample of the Cotter Dolomite is shown in **Figure 2.74**. Photoelectric adsorption (PE) measurements of around 3 barns/electron (b/e) from petrophysical logs indicate dolomite (**Figure 2.51** and **Figure 2.55**).

2.4.1.5 Potential for Geochemical Interactions

Injection of CO₂ into brine-filled carbonate aquifers is expected to generate carbonic acid that will dissolve the rock matrix. As calcite is more reactive than dolomite, dissolution of calcite in limestone will enlarge the current pore network and improve permeability (Seyeddi et al., 2020). This dissolution enhances porosity and permeability near the injector to the point of generating wormholes, but reaction of the carbonated water with the rock buffers fluid acidity resulting in a decrease in dissolution with distance from the point of injection. Seyeddi et al. (2020) also indicated that precipitation of carbonate minerals could reduce total porosity and permeability through occlusion of micropores, but since millimeter-scale pores in carbonate rocks account for most of the pore volume, reduction in microporosity is insignificant when compared to the total pore volume. In contrast to injection into pure limestone, injection of CO₂ into less-soluble dolomite, found little impact on rock matrix or porosity (Mathis and Sears, 1984). In addition to reactions between CO₂ injectate and rock, injectate will also contact tubulars and cement. Therefore, these interactions will be expected and mitigated using specialty steel and cement that

is less reactive to CO₂ and or carbonic acid. Details of the type of material to be used are provided in the section on well design.

2.4.1.6 Additional Data Collection Plans

During the drilling of the stratigraphic test well the injection zone will be cored to collect samples for a variety of characterization studies. These could include confirming mineralogy of the injection zone, testing rock-injectate reactions under reservoir conditions, determining rock matrix density and geomechanical properties, and measuring porosity and permeability.

2.4.2 Data on the Confining Zones

The security of injection relies on demonstrating geologic containment and confirming the absence of vertically transmissive faults that could compromise the containment system. Per the EPA standard outlined in 40 CFR §148.21(b), the confining zone must be laterally extensive with sufficiently low permeability and porosity to restrict the vertical flow of CO₂ or formation fluids. At the proposed injection site, two upper confining zones have been identified: the primary confining zone is the Simpson Group-Woodford Shale, and the secondary is the lower Mississippi Limestone. Both zones meet EPA standards and will effectively restrict the upward vertical migration of fluids out of the designated injection zone. Isolation of injectate from the lower Arbuckle and basement at the proposed site is provided by low-porosity, low-permeability intervals within the Arbuckle Group that will prevent downward migration of fluids out of the designated injection zone. The effectiveness of the lower confining zone is evidenced by the reduction of seismicity in northern Oklahoma when deep brine disposal wells were plugged back to depths several hundreds of ft above the Arbuckle Group contact with the basement (Skoumal et al., 2024).

2.4.2.1 Depth Areal Extent and Thickness

The depth, areal extent, and thickness of the confining and injection zones are based primarily on modern and vintage log data including five (5) newer wells with full geophysical log suites within the Vanguard CCS Hub AoR and twelve (12) additional wells (3 newer and 9 vintage) in surrounding townships that drilled to basement. Well information, along with regional subsurface data were used to construct cross sections and thickness maps of the Arbuckle Group (**Figure 2.16** and **Figure 2.34**), Simpson Group shale (**Figure 2.22**), Woodford Shale (**Figure 2.24**, combined Woodford and Simpson Group shale (**Figure 2.35** and **Figure 2.60**), and lower Mississippian Limestone (**Figure 2.37** and **Figure 2.61**).

Plan revision number: 0

Plan revision date: 6/24/2025

Claimed as PBI

Figure 2.19—Thickness of shale in the Simpson Group. Simpson Group shale thins in T.26N., R.8E., where the Woodford Shale thickens, suggesting Woodford sediment filled a valley eroded in the Simpson surface. Vanguard CCS Hub is outlined in red (approximate). Arbuckle oil and gas field shown in red.

Claimed as PBI

Figure 2.20—Thickness of the Woodford Shale confining unit around the Vanguard CCS Hub AoR. Thickness values are from modern logs and vintage logs that were calibrated to modern logs with gamma-ray and neutron porosity curves. Thickness trends are indicative of Woodford channel filling observed in other areas of Oklahoma (McCullough and Slatt, 2015). The location of the core used to characterize the Woodford Shale confining zone is indicated.

Claimed as PBI

Figure 2.21—Stratigraphic Cross-section S-N showing the relationship between the Arbuckle injection zone, Woodford Shale-Simpson Shale confining zone, lower Mississippian confining zone. Location of cross section and Vanguard CCS Hub AoR shown in inset map. In addition to the primary and secondary confining zones, shale-dominated intervals in the Pennsylvanian such as the Cherokee Group offer tertiary confining capabilities.

Claimed as PBI

Figure 2.22—Thickness of the lower Mississippian Limestone confining unit based on gamma-ray, density-neutron porosity and microresistivity curves. East to west trend reflects carbonate buildup subparallel to paleoshoreline. Locations of wells on the west and east sides of the CCS site that cored the Mississippian are shown. Information from these non-public cores was essential for the characterization of the lower Mississippian Limestone confining unit. Thickness changes in the Mississippian are not influenced by basement hills associated with Arbuckle oil and gas fields.

2.4.2.1.1 Upper Confining Zone

The upper confining zone is the combined net shale in the Simpson Group, Woodford Shale and lower Mississippian Limestone. The base of the confining zone is shale in the Simpson Group, where the Simpson Group is present, the base of the Woodford Shale where the Simpson Group is absent, and base of the low-porosity, low-permeability lower Mississippian Limestone if both Simpson and Woodford are absent. Where the Simpson Group is absent, the Woodford Shale is located immediately above the Arbuckle injection zone and with a thickness of <1 to 60 ft (5). In the southern part of the AoR, the Simpson Group is shale, shale with thin sandstone beds, or shale overlying thicker Hominy/Wilcox Sandstone (**Figure 2.58**).

The AoR is located on the truncation edge of the Simpson Group (**Figure 2.58; Figure 2.22**) that was eroded during uplift associated with the Middle Devonian Acadian orogeny. When the Woodford Sea transgressed this eroded surface, it filled valleys with thicker accumulations of mud compared to the interfluves. As a result, the Woodford Shale is thicker in areas where the underlying Simpson Group was eroded, and thinner in areas where the Simpson is thicker (**Figure 2.60 and Figure 2.59**). As shown in **Figure 2.62**, the Woodford Shale is close to 60 ft thick in valleys formed on the eroded Simpson surface and thins to <1 foot in areas where the Simpson Group shale is thicker. In some areas, within the AoR, the Woodford Shale is difficult to separate from Simpson Group shale on vintage logs without gamma-ray curves. To address the uncertainty in allocating shale to the Woodford Shale or Simpson Group, a combined thickness map of Simpson Group net shale and Woodford Shale was constructed (**Figure 2.61**). Immediately overlying the Woodford Shale is the dense limestone of the lower Mississippian Limestone. The lower Mississippian Limestone is distributed across the AoR, thins around 20 ft thick along the northern boundary of the AoR and is thickest in T.26N., R.7E. where it reaches 110 ft in thickness (**Figure 2.62**). The depth to the stacked Simpson Group, Woodford Shale and lower Mississippian Limestone confining zone is approximately 2500 ft below surface along the southeastern edge of the AoR and 3200 ft along the western boundary.

Claimed as PBI

Figure 2.23—Cross section R-R' showing characteristic resistivity of the Woodford-Simpson Group confining zone and the lower Mississippian Limestone confining zone on both modern and vintage geophysical logs. Low-permeability, low-porosity carbonate has >50 ohm-m resistivity for all resistivity curves. This figure is Figure 2.39.

2.4.2.1.1a Woodford Shale-Simpson Group Shale Confining Zone

The Woodford Shale rests unconformably on Devonian Hunton Group in more basinal settings where more complete stratigraphic sections are preserved, and on progressively older units on the shelf and Cherokee Platform. In the northern part of the proposed CCS site area, Woodford Shale rests directly on Arbuckle Group carbonate if no unconformity detritus accumulated prior to Woodford deposition. Simpson Group shale and sandstone occur in the southern part of the CCS site area and Woodford Shale unconformably overlies the Simpson Group. The Woodford Shale consists of alternating shale and thin (centimeter-scale) calcareous facies and occurs at depths of approximately 2,750 to 3,440 ft below ground level. Regional structure and thickness of the Woodford Shale are shown in Figures A-7a and A-7b, respectively. Detailed thickness of the Woodford Shale within and adjacent to the AoR is shown in **Figure 2.59**.

A detailed evaluation of the Woodford Shale and other confining units will be conducted using samples and data collected from a stratigraphic test well. Until that dataset is available, characterization of the Woodford Shale is based on the cored Woodford to the east of the NexGen CCS site and results from other studies of the subsurface Woodford Shale in northern Oklahoma and outcrops on the western flank of the Ozark Uplift.

The Woodford Shale is a tight, petrolierous shale found extensively across the Anadarko and Arkoma basins and the Cherokee Platform. It thins to the northeast and outcrops on the flank of the Ozark Uplift where it is locally called the Chattanooga Shale after the partially age equivalent Chattanooga Shale in Tennessee. Regionally, the thickness of the Woodford Shale varies significantly, ranging from 900 ft thick in the basin depocenter to 0 ft where truncated or not deposited in northern Oklahoma (**Figure 2.24**). Chert in the Woodford Shale increases toward the Ouachita Trough and axis of the Oklahoma Basin where upwelling of nutrient-rich water promoted growth of algae and radiolarians in the upper oxygenated layers of the Woodford Sea and water stratification due to density generated anoxic bottom water conditions favorable to the preservation of organic matter and uranium that gives the Woodford its characteristic highly radiogenic gamma-ray signature. Chert beds formed by the transformation of opal radiolarian tests to microquartz decrease in frequency and thickness northward away from the southern Oklahoma upwelling zone and are absent in cores from northern Oklahoma and not observed in outcrops on the flanks of the Ozark Uplift. As a result, the Woodford Shale in northern Oklahoma has far fewer natural fractures than its chert-rich coeval equivalents in southern Oklahoma. Locally, the thickness of the Woodford also changes because Woodford sediment infilled an eroded pre-Woodford topography. Under the Vanguard CCS Hub AoR, Woodford Shale thickness varies from <1 to 60 ft thick in response to the paleotopography of the underlying Simpson Group to the south and Arbuckle Group where the Simpson Group is absent. The higher clay and detrital silt content and absence of bedded chert in the Woodford Shale in northern Oklahoma contribute to its nearly impermeable nature that effectively prevents vertical fluid migration. In the cored well east of the CCS site, the Woodford is thin bedded (centimeter scale) alternating more clay-rich, carbonate, and quartz-rich layers. More brittle beds contain thin fractures that are healed with carbonate cement. These small fractures terminate against adjacent more clay-rich beds and are crosscut by separation of the core along bedding planes, indicating the resistance of cemented fractures to reopening during coring (**Figure 2.54**). Fractures are scarce in the lower section of the Woodford and become more prevalent in the more calcareous upper section close to the contact with the Mississippian Limestone.

Organic carbon content in the Woodford varies significantly and decreases northward on the shelf because of more oxygenated water during deposition and influx of terrestrial silt and clay. The shale contains enough organic carbon to retain dark gray to black color, but the decrease in uranium results in a dark shale with a much less radiogenic gamma-ray curve. The primary organic matter is oil-prone Type II kerogen, predominantly derived from planktonic material (Comer and Hinch, 1987; McCarthy et al., 2011).

The thermal maturity of the Woodford Shale varies greatly across Oklahoma from around 0.5 vitrinite reflectance (%VR_o) in shelf and platform areas to >6.0 %VR_o in the Arkoma Basin (Cardott and Comer, 2021). On the Cherokee Platform vitrinite reflectance for the Woodford Shale varies from around 0.5 to 1.7 %VR_o, (Cardott and Comer, 2021) indicating strong oil generation potential. Core analysis confirms that as-received wireline logs overestimate porosity and require correction for matrix density, clay-mineral and organic matter content and in some cases drilling fluid. Neutron porosity is a reliable indicator of clay mineral content and increasing seal ductility and competence.

The Simpson Group shale is an efficient confining zone that effectively isolates sandstone reservoirs, when present, from fluids in the underlying Arbuckle Group. The thickness and percentage of sandstone in the Simpson Group increases to the south as evidenced by the distribution of oil accumulations in the Simpson Group shown in **Figure 2.22**. The Simpson Group is a shallow marine deposit in which eolian sand deposits were reworked by shallow marine processes. As a result of the marine reworking, Simpson Group sandstones are nearly 100% quartz and prone to porosity reduction from carbonate and silica cement.

Shale beds in the Simpson Group are illite rich giving them the ductility necessary to be an effective seal. The characteristic light gray to green color of shale in the Simpson Group indicates low organic matter content and consequently lower porosity than dark shale. Simpson Group shale is not a source rock or reservoir and thus it has not been studied other than to map its distribution as a seal that separates reservoir sandstones.

2.4.2.1.1b Lower Mississippian Confining Zone

Based on position of the proposed CCS site between two cores of the Mississippian Limestone and general east-west depositional facies trends in this area, inferences regarding the mineralogy and petrophysics beneath the site based on these cores have merit. In both cored wells, core porosity and matrix-corrected density porosity were similar, allowing for the use of petrophysical logs to predict rock properties where core is not available. In the case of the lower Mississippian confining zone, core measurements corroborated the low porosity measured by density logs and confirmed permeable and nonpermeable beds inferred from microresistivity and caliper measurements. The lower Mississippian confining unit at NexGen CCS site is dominantly dense argillaceous dolomitic limestone interspersed with occasional chert nodules and shale layers.

During Mississippian time, northeastern Oklahoma was covered by shallow seas with warm, oxygenated conditions, leading to the deposition on a low declivity carbonate ramp that resulted in sediment packages or wedges that prograded southward toward the subsiding Oklahoma Basin, the lower Paleozoic basin that existed prior to the Pennsylvanian orogeny and formation of the Anadarko and Arkoma basins (Childress and Grammer, 2019; Mazzullo et al., 2019). As a result of erosion of the younger Meramecian and Chesterian sections prior to Pennsylvanian deposition, the Mississippian section in northern Oklahoma is almost all Osagean (Hunt 2017; Hill 2017). Within western Osage County and the proposed CCS site, the lower Mississippian is argillaceous,

interbedded dark to medium gray nodular and sometimes dolomitic limestone and dark gray shale with scattered chert nodules. It represents deposition at a position on the carbonate ramp below normal wave base that received an influx of carbonate grains from an upslope position during storms. Cleaner carbonate intervals are fine-grained packstones composed of abraded grains and transported from a northerly shallower water source. Much of the low-porosity, low permeability carbonate is mudstone to wackestone (Vanden Berg et al., 2019). Depositional facies belts in the Mississippian Limestone run subparallel to the paleoshoreline and thin both landward and basinward. Similar depositional facies in the lower Mississippian are observed in both cores whose locations are shown in **Figure 2.38 and Figure 2.61**, the thickness map of the lower Mississippian confining zone. In the area containing the proposed CCS site, lower Mississippian is separated from the upper Mississippian by an argillaceous interval (**Figure 2.62; Figure 2.30**). Also shown in **Figure 2.30**, the overall thickness of the Mississippian limestone is 250- to 350-ft and can change over short distances between wells as the upper surface was weathered and eroded prior to Pennsylvanian deposition. Weathered cherty limestone called “chat” often occurs immediately beneath the pre-Pennsylvanian unconformity. A second occurrence of Mississippian Chat often occurs toward the base of the upper Mississippian cherty section.

The lower Mississippian confining unit develops a southeast to northwest thickness trend that is consistent with the distribution patterns deposition on a gently inclined carbonate ramp. The lower Mississippian is approximately 40 to 70 ft thick across most of the Vanguard CCS Hub AoR as shown in the thickness map of the clean carbonate in the lower Mississippian limestone. The lower Mississippian becomes more clay-and silt-rich along the northern margin of the AoR, causing the thickness of clean carbonate to decline (**Figure 2.62**, and **Figure 2.36**). The low-porosity, low-permeability limestone remains thick along the southern boundary of the AoR where the Woodford Shale is thinner (**Figure 2.59**).

Within the AoR the top of the lower Mississippian confining zone is approximately 2,500 to 3,200 ft below land surface, with over 1,000 ft of vertical separation from the deepest treatable slightly to moderately saline water in the upper Pennsylvanian Vamoosa-Ada USDW (**Figure 2.29**). The lower Mississippian limestone consists of dense, argillaceous carbonate rock (**Figure 2.63**) that provides a robust secondary seal above the Woodford Shale-Simpson Group shale primary confining zone for the proposed Arbuckle injection zone.

Plan revision number: 0

Plan revision date: 6/24/2025

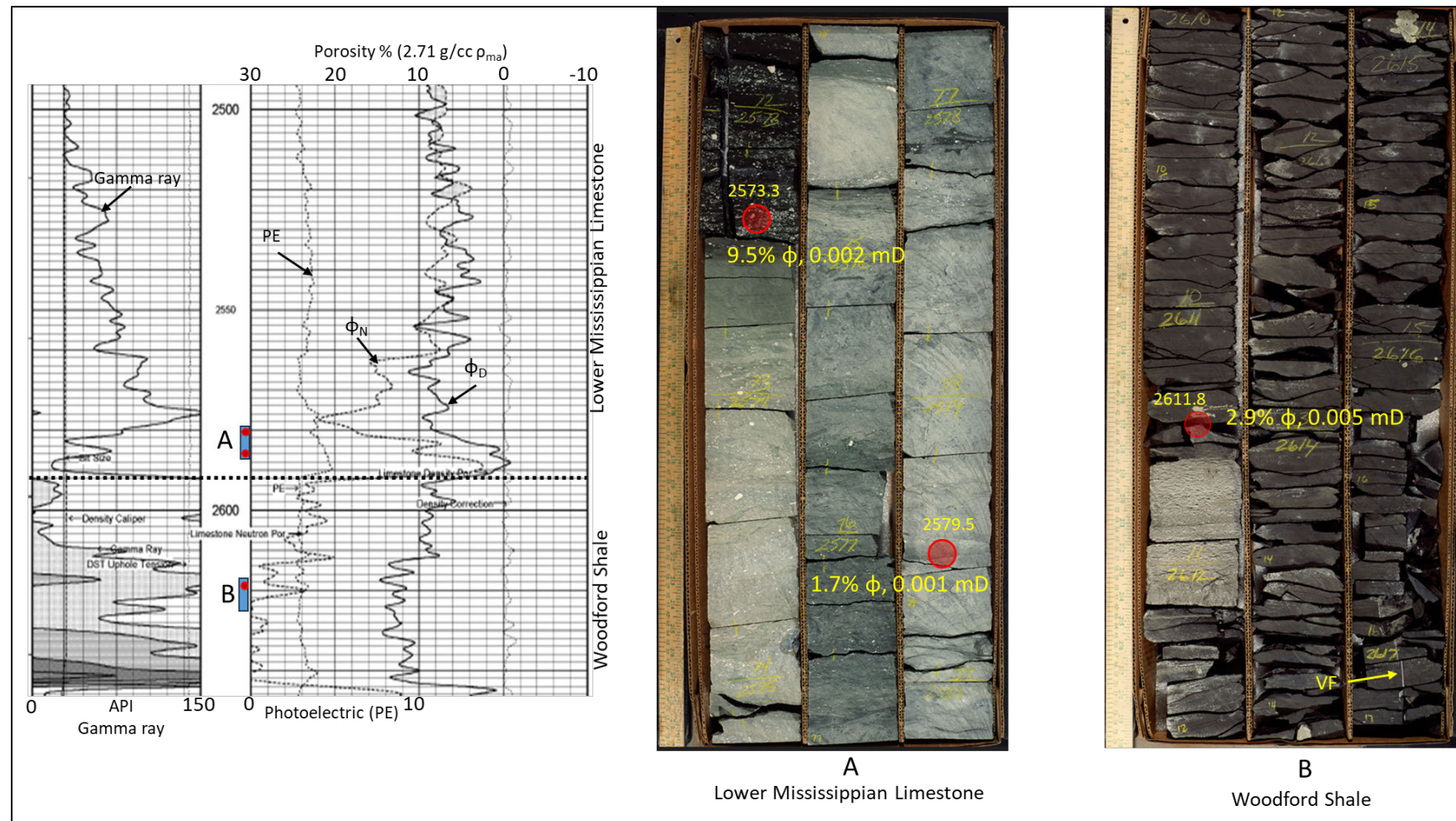


Figure 2.24—Wireline log responses and porosity and permeability measurements across the lower Mississippian Limestone and Woodford Shale intervals in the cored well in T.28N., R.9E. to the east of the Vanguard CCS Hub AoR (location shown in **Figure 2.41** and **Figure 2.43**). Note cemented vertical fracture (VF) in the Woodford core and porosity and permeability measurements for sample depths in yellow and marked by red circle. Delaminated core indicates Woodford Shale preferentially separated along bedding surfaces over fractures. Core depths are 8 ft shallower than log depths.

Evidence of isolation of the upper Mississippian Limestone cherty limestone and Mississippian Chat reservoirs from the Arbuckle Group is provided by production data from oil- and gas-producing fields in western Osage County and the adjoining counties. The integrity of the upper confining unit is supported by several types of data including different pressures and fluid types in the Arbuckle and Mississippian Chat reservoirs, different salinities of the brines, and no evidence of vertical migration along fractures of faults. Upward migration of oil and gas along a fault conduit in the Mervine field in eastern Kay County is supported by the charging of ten (10) shallow reservoirs in thermally immature upper Pennsylvanian and lower Permian strata by deeper-sourced hydrocarbons (Davis, 1984). Most of the anticlinal fields in western Osage County show no indication of the widespread filling of shallow reservoirs by vertically migrated oil and gas from deeper reservoirs or source beds and produce almost entirely from the Mississippian Chat. The anticlinal folds in the townships containing the AoR all lack faults that transect the Mississippian section and extend into the Pennsylvanian (**Figure 2.64**). Furthermore, evidence collected during drilling of the Mississippian section in the Bird Creek 2A-15 well on the eastern edge of the AoR in Section 15, T.27N., R.7E. indicates the lower Mississippian Limestone confining unit and the Mississippian “Solid” interval above have minimal indication of oil and gas. The “mudlog” with a hotwire chromatography indicates the lower confining unit and dense “solid” interval are devoid of gas shows (**Figure 2.65**) indicating low to minimal saturation of oil and gas and the presence of a low porosity and permeability barrier separating the upper Mississippian section from the Woodford Shale source rock and Arbuckle reservoir.

Claimed as PBI

 Basement tectonic faults

Figure 2.25—Seismic section through Blackland field showing termination of basement rooted faults within the Arbuckle Group. Due to the absence of faults transecting the Mississippian and Pennsylvanian section, oil and gas production in Blackland field is limited to the Mississippian Chat reservoir with no charging of shallow Pennsylvanian reservoirs. Blackland anticline formed during the Pennsylvanian and has a uniform thickness of Arbuckle Group across the fold.

Plan revision number: 0

Plan revision date: 6/24/2025

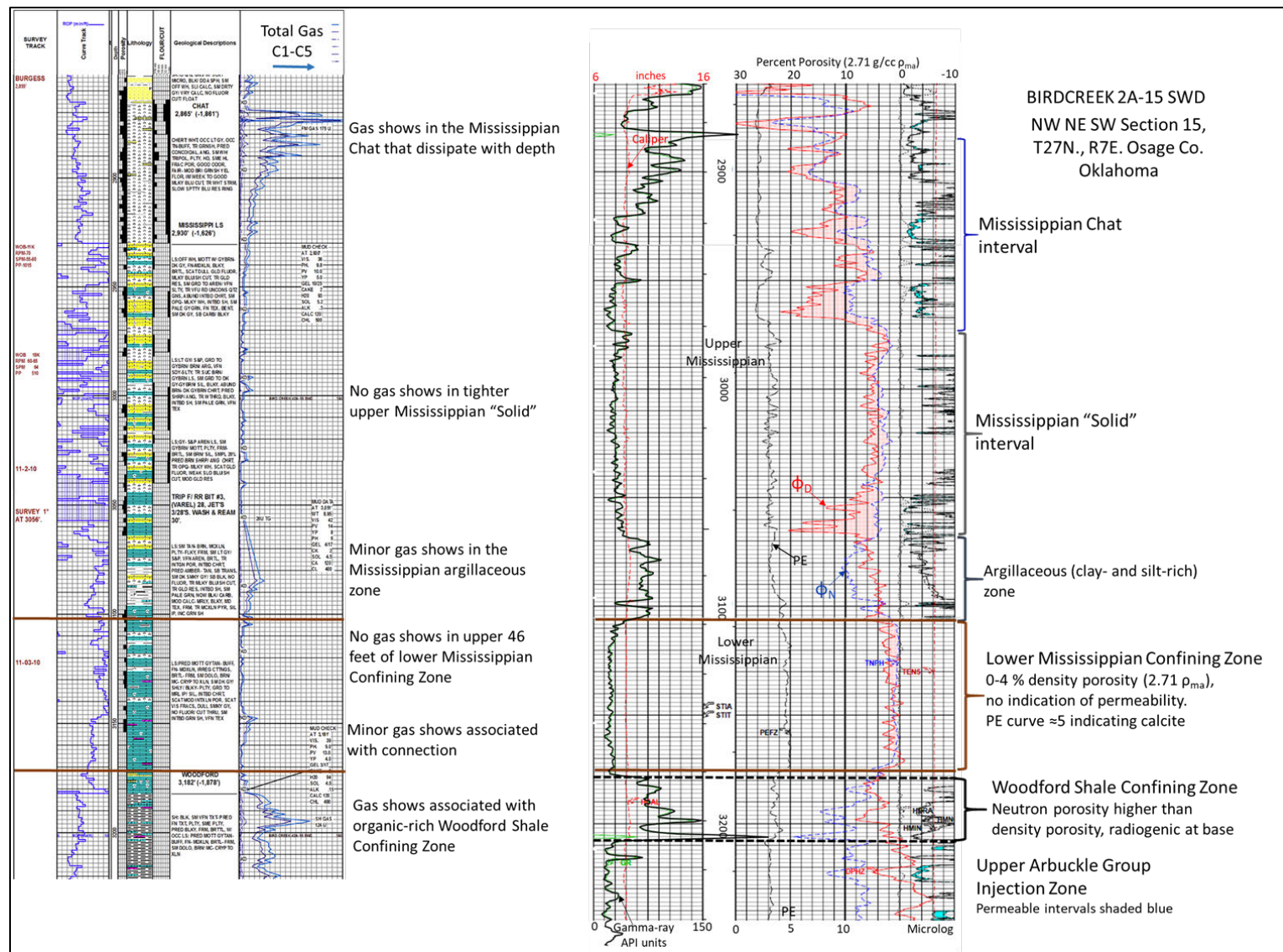


Figure 2.26—Gas chromatograph and porosity logs for the Bird Creek 2A-15 well in Sec. 15, T.27N., R.7E. on the eastern edge of the AoR. The lack of gas shows, low porosity, and absence of permeability in the lower Mississippian Limestone confirm the integrity of this confining zone.

2.4.2.1.2 Lower Baffle Zone in the Arbuckle Group

Arbuckle carbonate sediments were deposited in very shallow water on a carbonate platform. Arbuckle peritidal depositional facies form broad swaths that are subparallel to depositional strike. As a result of cyclic changes in sea level, gentle subsidence or a combination of factors, the generalized depositional facies developed: upper intertidal-supratidal, intertidal and subtidal. Carbonate sediments in each of these depositional settings have characteristics that facilitate their becoming reservoir or seal rocks. Research on numerous cores from wells across Oklahoma and the outcrops in the Arbuckle Mountains shows that thicker and cleaner intertidal and shallow subtidal carbonate are prone to become reservoirs and silty and more clay rich upper intertidal to supratidal facies and deeper open marine facies are prone to become seals. It is noteworthy that these facies can be traced for miles in outcrop and their different weathering patterns generated the famous “tombstone topography” of the Cotter Dolomite equivalent West Spring Creek Formation on the Arbuckle Uplift. Depositional cycles are expressed in gamma-ray profiles of surface and subsurface rocks as serrated-appearing gamma-ray profiles in which higher gamma-reading reflect more terrigenous input of clay and silt in upper intertidal, supratidal and open-marine settings, whereas lower gamma-ray values infer cleaner and water lower intertidal to shallow subtidal settings (Swinea et al., 2011). Cleaner carbonates are more susceptible to dissolution and fracturing, two key components to reservoir evolution in Arbuckle Group carbonates. In contrast, argillaceous carbonate resists dissolution and fracturing to become low-porosity and low-permeability baffles or seals that restrict vertical migration of fluid within the thick Arbuckle section.

Evidence for vertical permeability barriers in the Arbuckle Group in northern Oklahoma includes oil accumulations below brine-bearing intervals (**Figure 2.66**) and the successful reduction of seismic events when Arbuckle disposal wells were plugged back to exclude disposal close to the Arbuckle Group basement contact (Skoumal et al., 2024). The empirical evidence presented by Skoumal et al. (2024) showing the decrease in seismicity following plug back to prevent injection within or close to the basement contact supports the existence of effective baffles seals in the Arbuckle Group that would prevent the downward migration of pressure and fluid from the injection zone to the basement. Watney and Holubnyak (2017) presented several lines of evidence, including salinity and isotopic data from the Wellington field in southern Kansas that show isolation of the upper Arbuckle from the lower Arbuckle, and isolation of the Arbuckle Group saline aquifer from the upper Mississippian oil and gas reservoir. The Wellington field data support the premise that baffles within the Arbuckle Group prevent communication between upper and lower Arbuckle reservoir intervals and that confining units in the lower Mississippian, Woodford Shale and Simpson Shale effectively isolate the Arbuckle Group from the upper Mississippian reservoir interval.

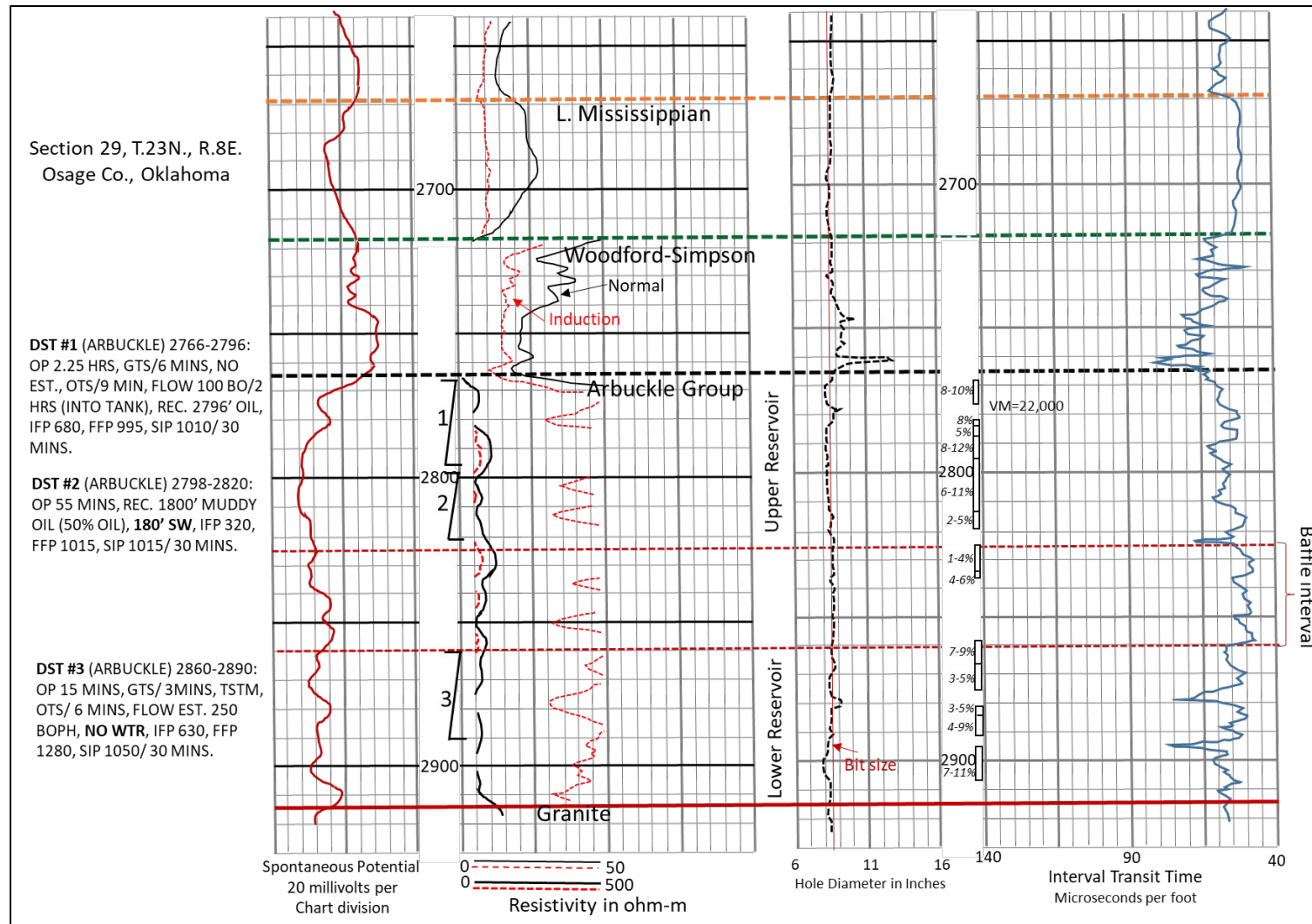


Figure 2.27—Evidence of a vertical permeability barrier in the Arbuckle Group. Results of drill-stem tests #1 and #2 delineate an upper reservoir with water-free oil and gas toward the top and oil and saltwater toward the base. The results of drill-stem test #3 below the baffle interval indicate a second reservoir without saltwater that is separated from the upper reservoir. Porosity measurements shown on the sonic porosity log are from Schlumberger and can be used to infer the baffle zone contains three separate zones of approximately 1-4 % porosity (VM = 22,000 ft/sec.).

Plan revision number: 0

Plan revision date: 6/24/2025

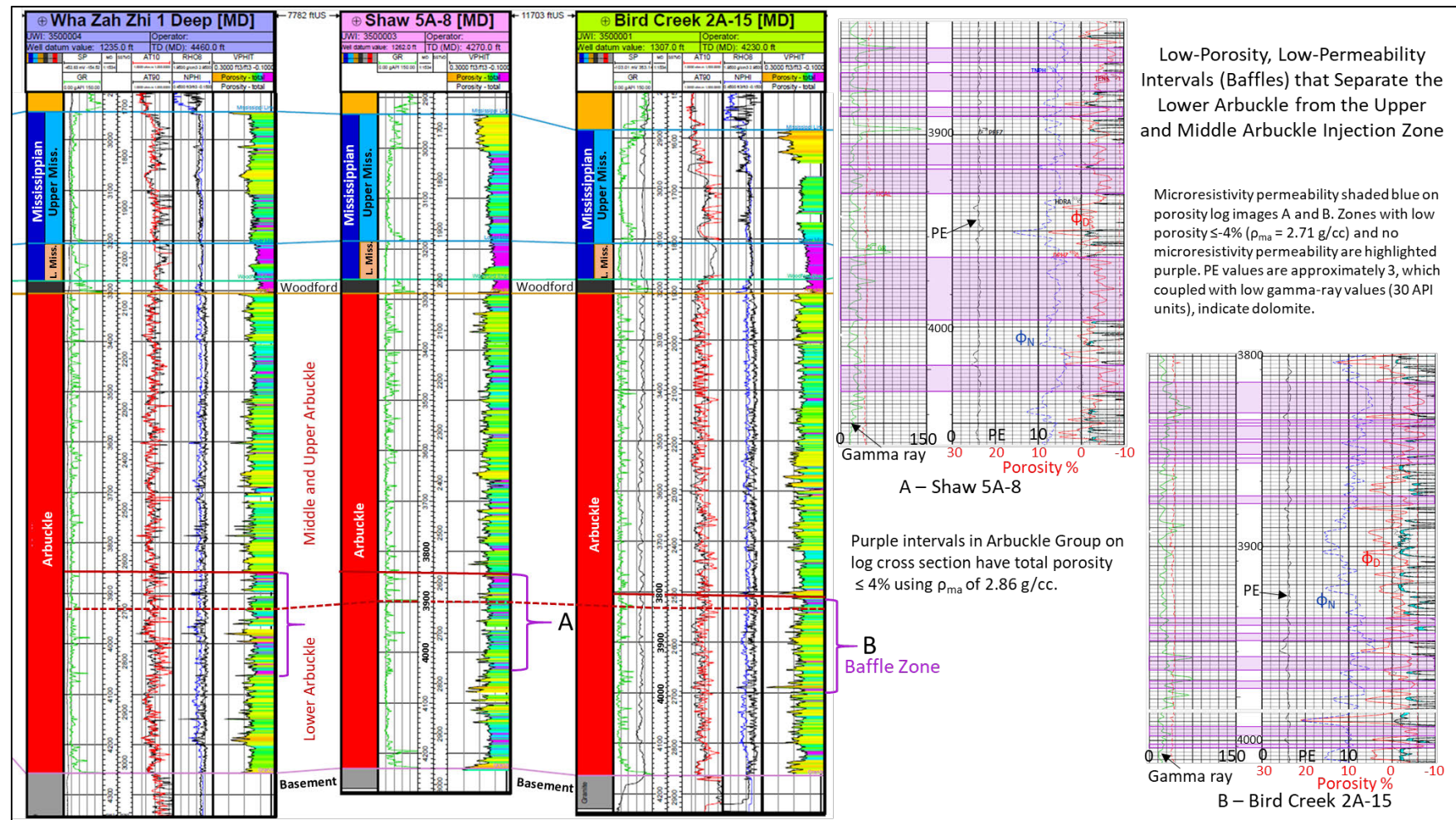


Figure 2.28—Flow baffles in the middle and lower Arbuckle Group that isolate the upper and middle Arbuckle injection and storage zone from the basement. Presence of baffles is supported by the isolation of oil and gas below water in the Arbuckle Group (Figure 2.66), and separate isotopic and salinity signatures within the Arbuckle in Wellington field, Kansas (Figure 2.68)

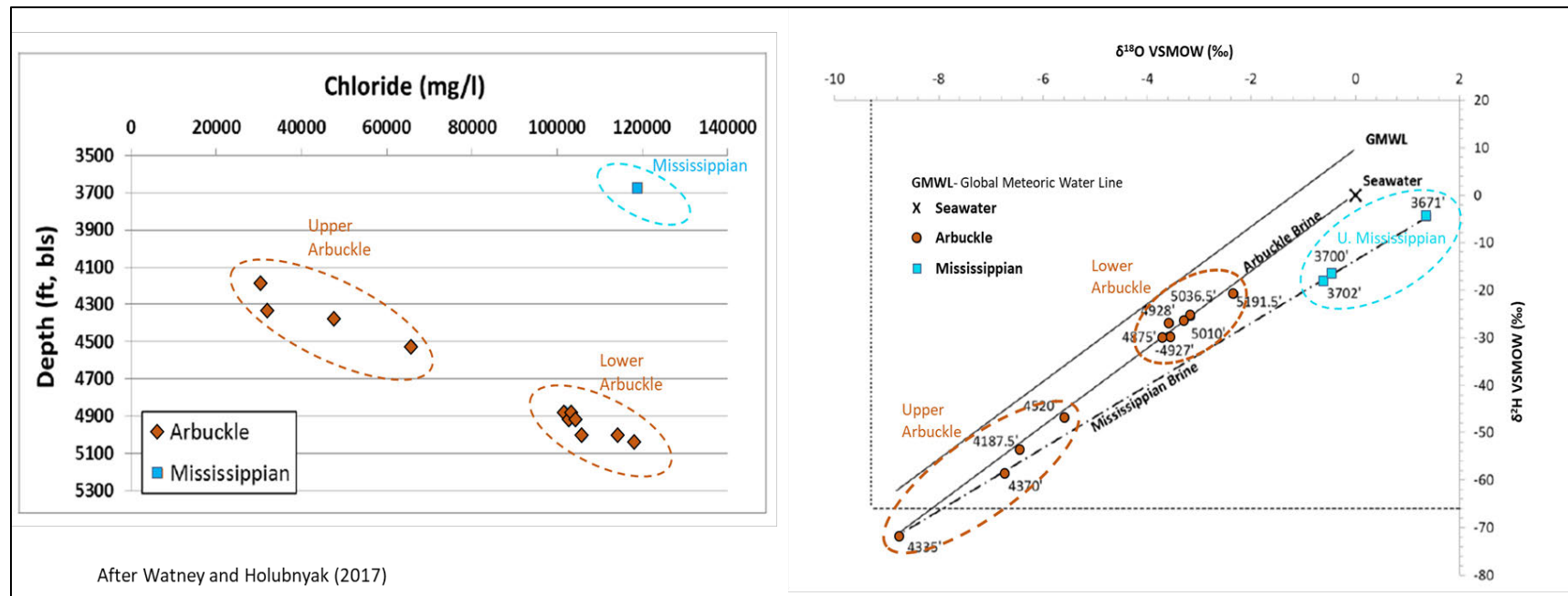


Figure 2.29—Salinity data (left) and isotopic data (right) from Wellington field, Kansas, after Watney and Holubnyak (2017). Salinity of water from the upper Mississippian reservoir is much higher than salinity in the upper Arbuckle, indicating isolation and separation by Mississippian/Woodford confining units. Similarly, hydrogen and oxygen isotopic data plot in three distinct fields, interpreted as separation of lower Arbuckle from upper Arbuckle and isolation of Arbuckle from upper Mississippian.

2.4.2.2 Porosity and Permeability

2.4.2.2.1 Upper Confining Zone

No cores of the Woodford and lower Mississippian Limestone were available for wells within the AoR, but core descriptions from the closest wells to core the Mississippian Limestone and Woodford Shale, were used. Core data from a well approximately 10 miles to the east of the Vanguard CCS Hub AoR were used to characterize porosity and permeability in the Woodford Shale and the lower Mississippian Limestone. These core data were calibrated to wireline log responses for the wells with modern log suites. Porosity from core and modern log suites were used to evaluate microresistivity log results so that vintage micrologs could be used to estimate reservoir thickness within the injection zone and thickness of negligible permeability intervals in the confining units and baffling interval.

As expected, porosity and permeability in the Woodford Shale are low. Because of the tendency of the shale to separate along bedding planes, acquiring core plugs is difficult and only one measurement was taken. Sample porosity was 2.9 percent, permeability to air of 0.012 mD, Klinkenberg permeability 0.005 mD, and grain density was 2.64 g/cm³. In addition to the single core plug from a conventional core, a single sidewall core plug was recovered from the Woodford Shale in the Shaw A5-8 well inside the AoR in Section 8, T.27N., R.7E. Porosity to gas (helium) in this sample was 0.1 percent, whereas the permeability to air was 0.231 mD, and grain density 2.63 g/cm³.

Plan revision number: 0

Plan revision date: 6/24/2025

Table 2.4.2a—Porosity and permeability results from sidewall cores of the Mississippian and Woodford intervals within the Aor. Shaw A5-8 well in Section 8, T.27N., R.7E.

Sample Number	Depth (ft)	Helium Porosity (%)	Grain Density (g/cm ³)	Air Permeability (md)	Stratigraphic Unit
37	2920	4.7	2.46	1.23	U. Miss. Cherty Zone
36	2926	4.3	2.54	fractured	U. Miss. Cherty Zone
35	2937	2.4	2.69	0.216	U. Miss. Cherty Zone
34	2943	6.8	2.59	0.57	U. Miss. Cherty Zone
33	2964	0.0	2.56	0.114	U. Miss. Cherty Zone
32	2969	6.5	2.59	0.229	U. Miss. Cherty Zone
31	2976	7.1	2.64	fractured	U. Miss. Cherty Zone
30	2982	0.9	2.57	0.149	U. Miss. Cherty Zone
29	2988	1.4	2.64	0.248	U. Miss. Cherty Zone
28	2996	2.4	2.57	0.368	U. Miss. Cherty Zone
27	3002	8.1	2.66	fractured	U. Miss. Cherty Zone
26	3011	1.5	2.62	0.156	U. Miss. Cherty Zone
25	3025	.05	2.68	0.0473	U. Miss. Cherty Zone
24	3027	1.0	2.61	0.409	U. Miss. Cherty Zone
23	3040	0.0	2.64	0.173	U. Miss. Solid
22	3046	0.0	2.65	0.153	U. Miss. Solid
21	3048	.02	2.67	0.0853	U. Miss. Solid
20	3056	.05	2.63	fractured	U. Miss. Solid
19	3076	.02	2.63	0.285	U. Miss. Solid
18	3083	.05	2.63	0.291	U. Miss. Solid
17	3096	0.0	2.66	0.115	U. Miss. Solid
16	3110	.04	2.58	fractured	U. Miss. Solid
15	3114	0.8	2.65	0.138	U. Miss. Solid
14	3126	0.2	2.58	fractured	U. Miss. Solid
13	3126	0.1	2.61	0.0812	U. Miss. Solid
12	3136	0.1	2.66	fractured	U. Miss. Solid
11	3144	0.1	2.63	0.567	U. Miss. Solid
10	3152	0.0	2.62	0.0948	U. Miss. Solid
9	3164	N/A	N/A	fractured	U. Miss. Solid
8	3177	0.3	2.63	0.281	Argillaceous Zone
7	3196	0.0	2.67	0.126	L. Miss. Confining Zone
6	3204	0.0	2.61	0.144	L. Miss. Confining Zone
5	3221	0.0	2.66	0.112	L. Miss. Confining Zone
4	3230	0.1	2.68	0.0618	L. Miss. Confining Zone
3	3240	8.9	2.71	2.44	L. Miss. porosity
2	3257	9.0	2.7	1.86	L. Miss. porosity
1	3266	0.1	2.63	0.231	Woodford Shale

Plan revision number:

Plan revision date: 6/24/2025

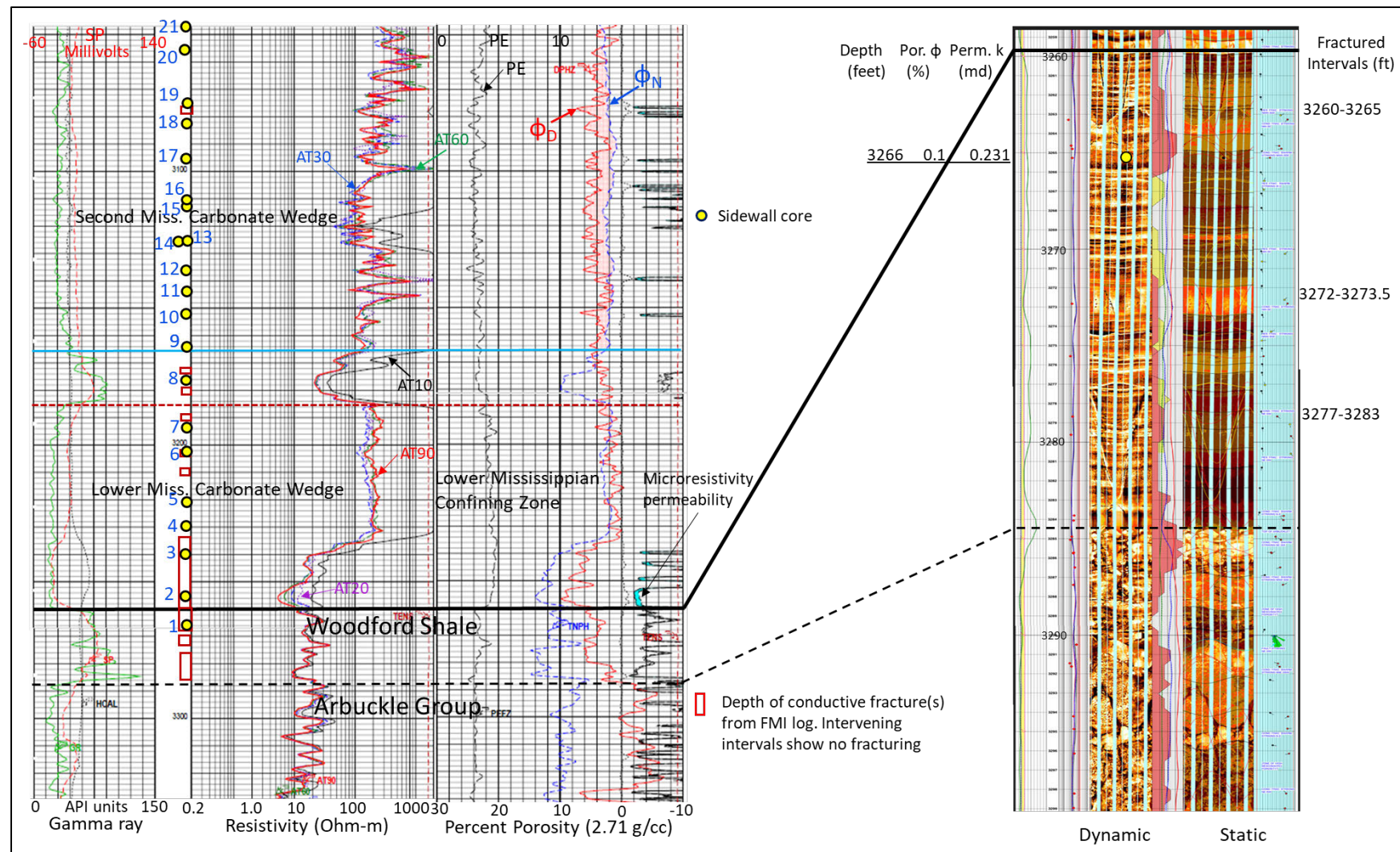
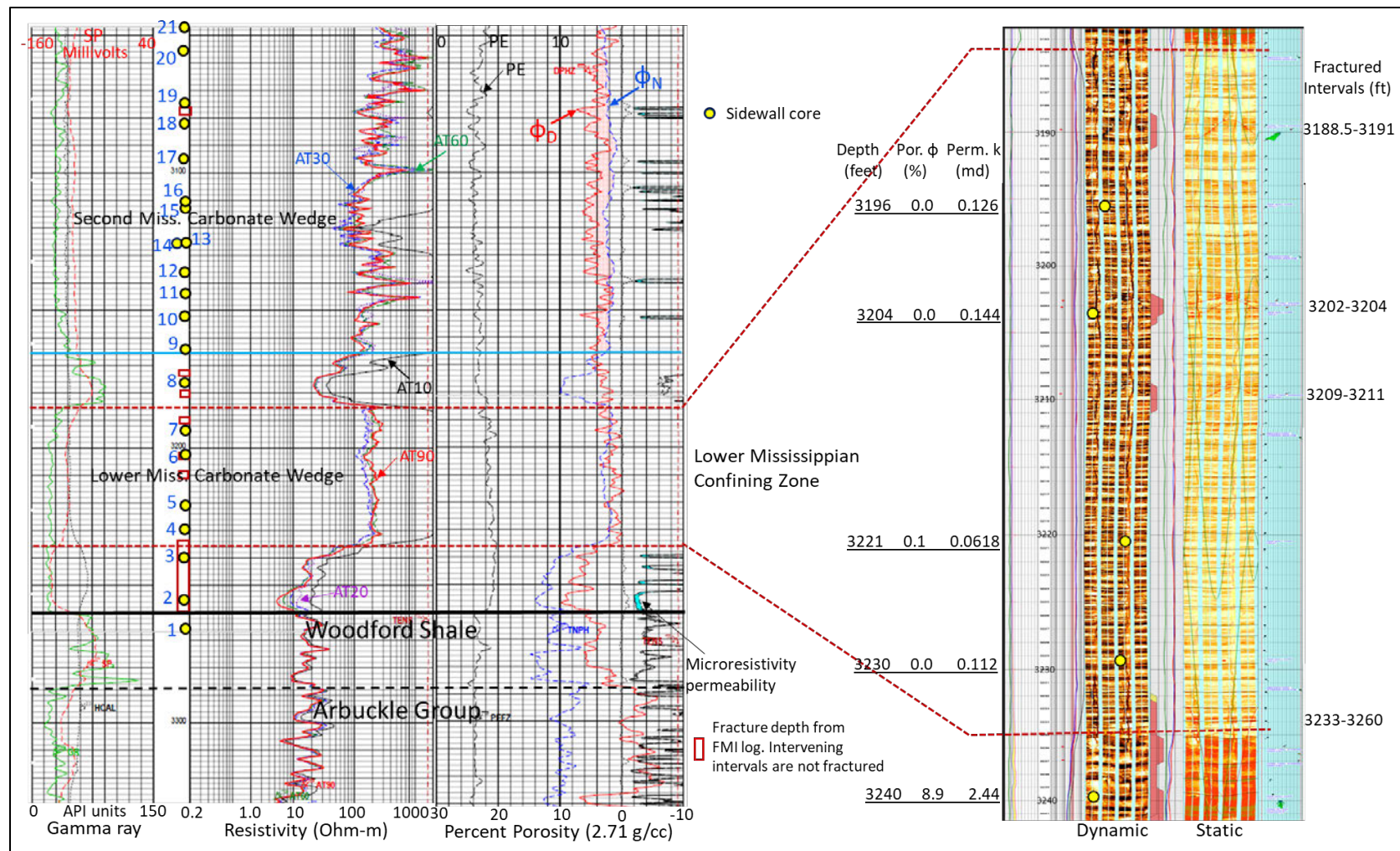


Figure 2.30—Open-hole geophysical logs and microresistivity formation image across the Woodford Shale showing the location of a sidewall core at 3266 ft. Fractures on formation microimage are mostly bed-bound and more frequent in calcite-cemented brittle intervals. Numbers in depth tract correspond to sidewall core plugs listed in **Table 2.4.2a**. Intervals with conductive fractures are contained in red rectangles. Shaw 5A-8 well within the AoR in Section 8, T.27N., R.7E.

The lower Mississippian Limestone in the cored well has low porosity and permeability as evidenced by petrophysical logs and a single measurement from a conventional core plug with 1.7 percent porosity and 0.001 mD permeability (**Figure 2.63**). The petrophysical log properties shown in a representative log (**Figure 2.43**) include low gamma-ray values (<30 API units) in clean non argillaceous limestone, photoelectric (PE) value of near 5 indicating calcite, values of density and neutron porosity between 0 and 4 percent (2.71 g/cc matrix density) and no indication of microresistivity separation to indicate permeability.

The conventional porosity and permeability measurements from the wells outside the AoR were supplemented by porosity and permeability measurements from sidewall cores taken across the Mississippian interval in the Shaw 5A-8 well in Section 8, T.27N., R.7E. within the AoR. The results from the sidewall core analyses are listed in **Table 2.4.2a** and shown in part on microresistivity images that cover intervals where sidewall cores were taken (**Figure 2.70**)

The average porosity for the four sidewall cores taken in the lower Mississippian Limestone confining zone is very low (<1.0%) with an average permeability to helium of 0.11md. The combination of low matrix porosity and the absence of bed-crossing fractures contribute to integrity of the lower Mississippian confining zone.



2.4.2.2.2 Arbuckle Group Baffle Interval

The Vanguard CCS Hub proposes to inject into the upper and middle sections of the Arbuckle Group above a series of low permeability and porosity beds (**Figure 2.67**) that we believe will prevent the downward migration of CO₂ into the Lower Arbuckle and the basement rocks. The proposed CCS site overlies the Washington Volcanic Group (WVG) north of the Labette Fault and Central Oklahoma Granite Group south of the Labette Fault, two basement rocks that have hosted numerous small injection-credited seismic events and a few large earthquakes in neighboring Noble and Pawnee counties (**Figure 2.75**). The goal of limiting injection to the upper and middle Arbuckle is to prevent pressure increase in basement rocks, and seismic events. Porosity measurement and the identification of low-permeability beds in the lower part of the Arbuckle Group is based on petrophysical logs as core is not available. Low-porosity and low-permeability intervals within the Arbuckle Group (**Figure 2.67**) have total porosity less than or equal to 4% using a 2.86 g/cc rock matrix and no indication of permeability as indicated by positive microlog separation (**Figure 2.67**). The cumulative effect of low-permeability intervals is a baffle zone that generates an effective seal to vertical migration of fluid.

2.4.2.3 Mineralogy

2.4.2.3.1 Upper Confining Zone

Currently, core data or visual imagery specific to the Woodford Shale within the Area of Review (AoR) are unavailable. The closest Woodford Shale core available for this proposal is a non-public core approximately 8 miles to the east (**Figure 2.59**). The Woodford Shale is intensely studied in Oklahoma and summarized in an Oklahoma Geological Survey review paper by Cardot and Comer (2021).

Core and petrophysical-log-derived mineralogy are similar for the Woodford Shale confining zone. The cored Woodford Shale is dominantly dark gray to black, silty and calcareous shale with a grain density of 2.64 g/cc. The Woodford contains calcite-cemented fractures that exhibit cohesivity that exceeds that of bedding planes as evidenced by separation of the core parallel to bedding (**Figure 2.63**). Photoelectric (PE) values between 3.0 and 3.5 are typical for shale where the dominant clay mineral is illite, with minor amounts of chlorite and kaolinite. Total rock x-ray diffraction analyses from northern Oklahoma (**Figure 2.71**) confirm that the dominant components are quartz and the clay mineral illite, which comprises 90-95 percent of the clay content (Snider, 2014). Quartz occurs as clay- to silt-sized detrital grains and cement and is the dominant mineral except in samples of thin carbonate beds (Table 2.4a). Diffraction patterns for extracted clay samples of the Woodford Shale from cores of wells in neighboring Noble County and nearby Payne County indicate sharp crystalline clay-mineral peaks, with illite dominating minor amounts of chlorite and kaolinite (Snider, 2014). Scanning electron microscopy (SEM) images corroborate the distinct morphological features of these clay minerals. Discrete illite grains exhibit curled edges and laminated platy textures, consistent with the descriptions by Keller et al. (1986). Mixed layer illite/smectite (I/S), although present in small quantities in southern Oklahoma, was not detected by x-ray diffraction of Woodford Shale samples from Noble and Payne counties (Snider, 2014). Calcite and quartz cement commonly fill fractures in the Woodford Shale with fracture height limited to the thickness of brittle beds (**Figure 2.63**). Bedded carbonate are limestone and dolomitic limestone detritus that when sampled, give high values of carbonate compared to samples of the typical dark Woodford Shale (example Sample 15, Table 2.4b).

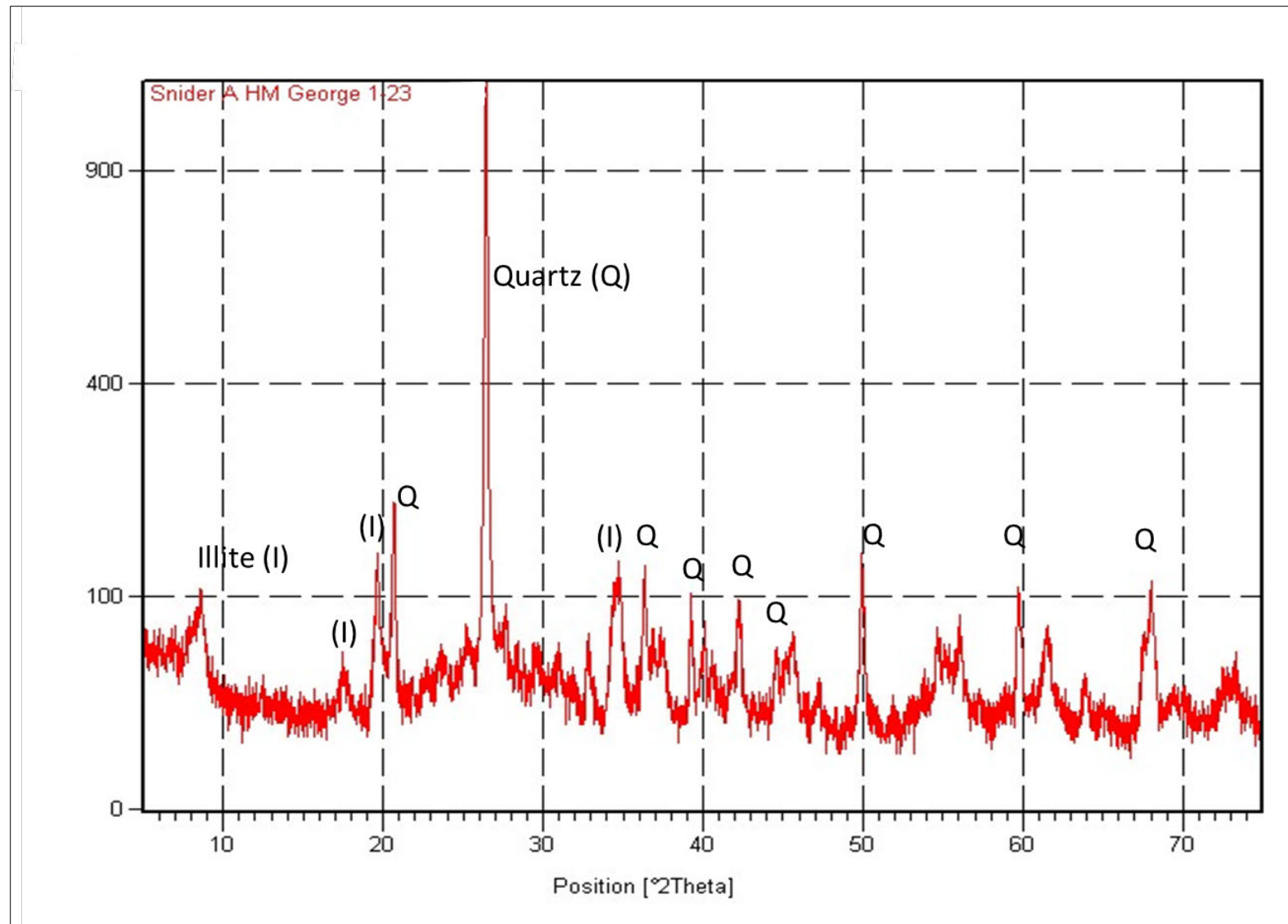


Figure 2.32—Total rock powder X-ray diffraction spectrum of Woodford Shale from Noble County, Oklahoma showing mineralogy dominated by illite (I) and quartz (Q).

Table 2.4b—Mineralogy of Non-Cherty Woodford Shale, Northern Oklahoma from X-ray Diffraction of Core from Noble County (percentages)

Sample Number	Silica	Clay	Sulfides	Carbonate
1	68	27.9	3.2	1.4
2	74.7	20.6	3.8	0.9
3	59.4	32.2	8.4	0
4	72.5	23.9	2.3	1
5	75.5	21.4	3.2	0
6	68.8	19.4	11.9	0
7	38.9	16.5	49	0
8	44.2	12.4	38.1	5.3
9	67.8	16.5	10.4	5.2
10	67	14	12.2	6.8
11	61.5	13.6	9.9	14.9
12	64.2	18.1	5.3	12.4
13	60.3	20.5	4.6	14.7
14	56.8	24	10.9	8.2
15	34	13	7.4	45.6
16	61.5	19.2	14.5	4.7
17	71.1	23.6	5.4	0
18	62.7	20.8	8	8.6
Average	61.6	19.6	11.6	2

Petrophysical evaluation of the Simpson Group indicates it is dominantly shale and thin low-porosity sandstone (**Figure 2.72**). The light gray to green shale characteristic of the Simpson Group was sampled in a core from a well located approximately 8 miles south of the AoR. The x-ray diffraction results showed the shale to be dominantly illite (**Figure 2.73**) a composition that can be confirmed during analysis of core recovered from a stratigraphic test well.

The illite-dominated mineralogy of Simpson Group shale is confirmed by its mechanical properties as the shale is prone to erode (“wash out”) during drilling resulting in an enlarged borehole as shown by the caliper curves on the open hole log sections shown in **Figure 2.72**.

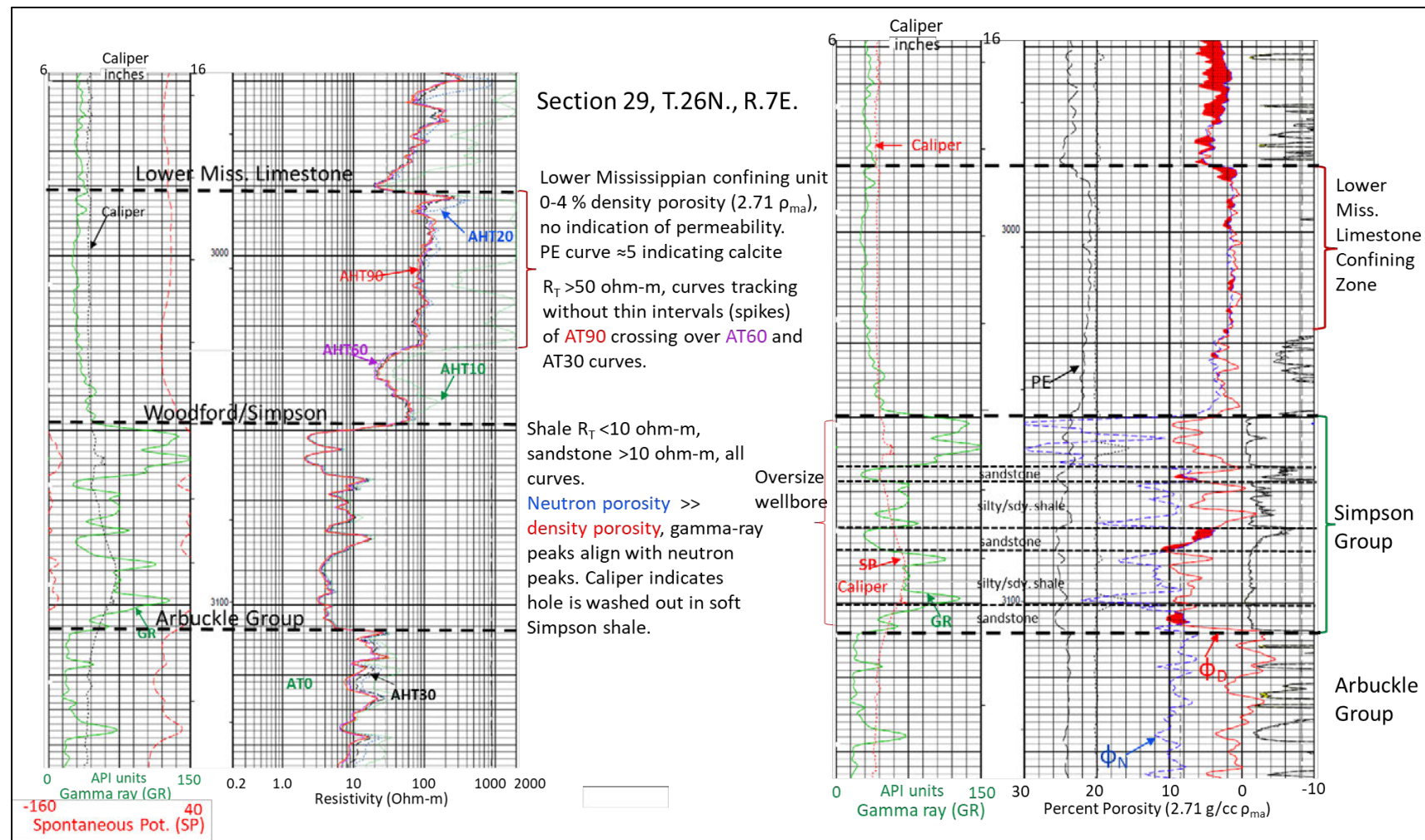


Figure 2.33—Geophysical log sections across the upper Arbuckle Group, Simpson Group and lower Mississippian Limestone show characteristics of the logged interval. Shale in the Simpson Group is prone to eroding during drilling resulting in an oversized hole as indicated by caliper curves. Arbuckle dolomite and lower Mississippian Limestone are more competent resulting in a close to in-gauge hole. Mineralogy of the lower Mississippian Limestone confining zone is indicated by PE curve values between 4 and 5 b/e that are typical for dolomitic limestone. PE curve values across Simpson Group are approximately 3 b/e in clay-rich shale and approach 2 b/e in silt- and sand-rich intervals.

Plan revision number: 0

Plan revision date: 6/24/2025

Petrophysical logs and the core of the lower Mississippian Limestone confirm the mineralogy of the carbonate as primarily calcite with lesser amounts of dolomite. The PE curve shown in **Figure 2.68** reads approximately 4.5 b/e and the neutron porosity curve is tracking the density curve, both indicators of a calcite dominated mineralogy. Shaly intervals with more clay minerals are recognized by increasing neutron and density porosity, coupled with increasing gamma-ray values and decreasing PE measurements.

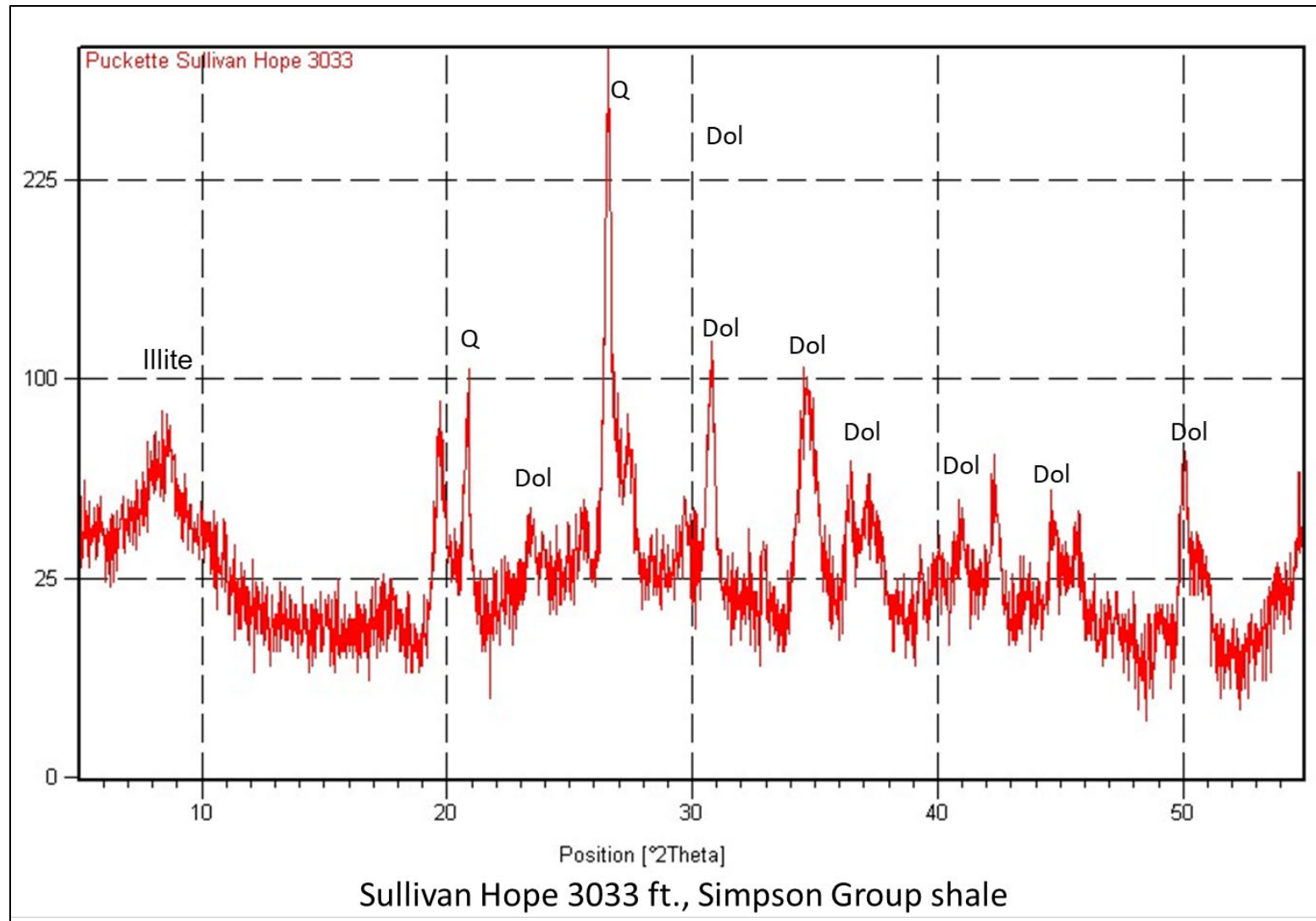


Figure 2.34—Whole rock powdered sample x-ray diffraction mineralogy of the light gray to green shale in the Simpson Group show quartz as the dominant mineral and lesser amounts of dolomite and the clay mineral illite. Example is from Sullivan Co. Hope well located approximately 8 miles south of the AoR (see location on Figure 2.58)

2.4.2.3.2 Lower Baffling Zone

The Arbuckle Group in Osage County is overwhelmingly dolomite, with minor amounts of quartz, calcite and clay minerals. Lynch (1990) analyzed Arbuckle core samples from two wells, the Oliphant Lafortune in Section 8, T.25N., R.6E. approximately 3 miles to the west of the AoR, and the Oliphant Nate in Section 15, T.24N., R.7E., approximately 4 miles south of the AoR. X-ray diffraction of these samples showed the Arbuckle was more than 95% to 100% dolomite in carbonate samples, which was confirmed by additional x-ray data collected from the same cores for this application (**Figure 2.74**). Photoelectric absorption (PE) curves on the set of modern petrophysical logs (**Figure 2.51 and Figure 2.55**) indicate the Arbuckle carbonate is overwhelmingly dolomite with most quartz occurring as thin sandstone beds within the thick carbonate interval.

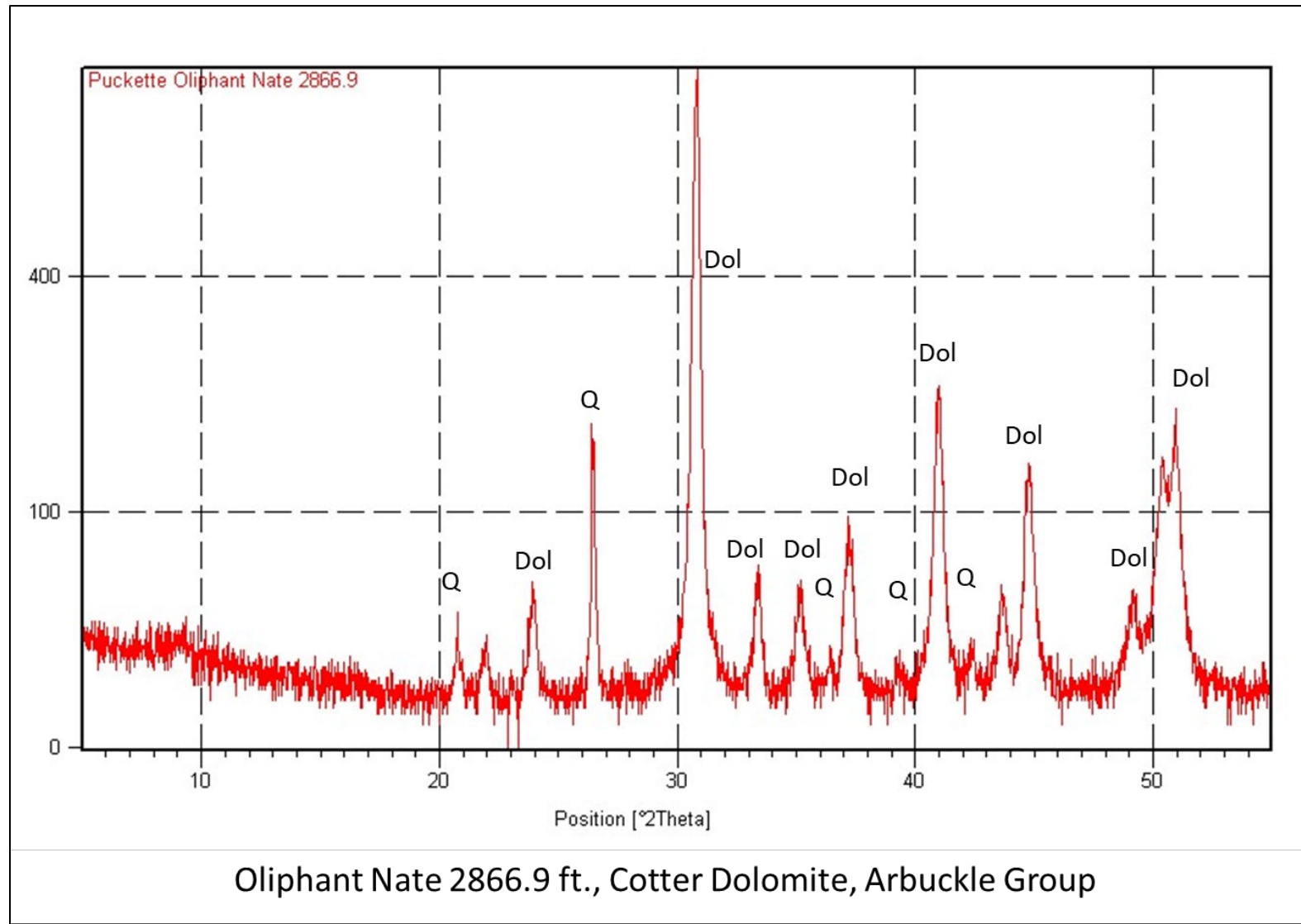


Figure 2.35—Mineralogy of the Cotter Dolomite, upper Arbuckle Group showing dolomite (Dol) as the dominant mineral and a lesser amount of quartz (Q) that could be detrital sand grains or chert. Example is from Oliphant Nata well located approximately 4 miles south of the AoR (see location on Figure 2.16).

2.4.2.4 Potential for Geochemical Interactions

2.4.2.4.1 Upper Confining Zone

The Woodford Shale and shale beds in the Simpson Group being primarily illite clay and quartz silt (**Figure 2.71** and **Figure 2.73**) are not prone to react with carbonic acid generated by the mixing of CO₂ and water. Calcite cementing the small fractures in the Woodford Shale and lower Mississippian Limestone would react to acidic fluids. However, the fractures in the Woodford Shale core are mostly vertical or at a high oblique angle to bedding and have short vertical heights that result from these fractures terminating in more-ductile beds adjacent to the fractured beds. Dissolution along a vertical fracture would likely cease when the calcite-cemented fracture terminates at the ductile bed.

The lower Mississippian Limestone is more reactive to carbonic acid than the Woodford Shale and if acidic fluids reach the limestone, some dissolution would be expected. The extent of dissolution would be minor because as the formation imaging surveys show, the limestone lacks high-height fractures that transect multiple beds. Instead, imaged fractures are seldom more than 1-2 ft in height and are separated by non-fractured intervals with low permeability that would prevent significant penetration of the unit.

2.4.2.4.2 Arbuckle Baffling Interval

Injection of CO₂ into brine-filled carbonate aquifers is expected to generate carbonic acid that will dissolve the rock matrix. Studies on injection of CO₂ into porous and permeable limestone and dolomite carbonates indicate no detrimental results (Seyeddi et al., 2020; Mathis and Sears, 1984) beyond enhancing the existing permeability and porosity and precipitation of calcite that could reduce microporosity. The low permeability dolomite beds that make up the lower baffling interval would resist fluid invasion and reduce rock-fluid interaction. In addition to reactions between CO₂ injectate and rock, injectate will also contact tubulars and cement of the stratigraphic test well/deep monitoring well that will penetrate the lower baffling zone. Therefore, these interactions will be expected and mitigated using specialty steel and cement that is less reactive to CO₂ and or carbonic acid. Details of the type of material to be used are provided in the section on well design.

2.4.2.5 Capillary Pressure and Integrity of the Confining Zone

Capillary pressure results from interactions of forces acting within and between fluids and their bounding solids. As with measurements of capillary pressure in other areas, it is expected that the cohesive forces and nanometer to micron pore throat size in the Woodford Shale and shale in the Simpson Group will result in high values. Capillary pressure curves for the Woodford Shale are available for samples of outcrops in southern Oklahoma and subsurface samples distal to AoR where Woodford Shale rock properties are different from those for the Woodford in northern Oklahoma. The core analyses of the Mississippian and Woodford intervals from the wells closest to the AoR did not report capillary pressure. Capillary pressure for the Woodford Shale, lower Mississippian Limestone, and lower Arbuckle baffling zone will be determined from core recovered during the drilling of the stratigraphic test well.

2.4.2.6 Additional Data Collection Plans

NexGen Carbon Oklahoma, LLC-Project Vanguard will acquire additional site-specific data through coring and downhole measurements during the drilling of a stratigraphic test well and the injection wells.

2.5 Geomechanical and Petrophysical Information [40 CFR 146.82(a)(3)(iv)]

2.5.1 Fractures

Evaluation of fractures and faults within the AoR relied on petrophysical logs and more specifically resistivity profiles and formation microimaging surveys. Two microresistivity image logs, one in the northern part of the Vanguard CCS Hub AoR, and a second immediately east of the AoR, surveyed approximately 90 ft in the Arbuckle injection zone, the Woodford Shale primary confining zone, the Mississippian Limestone including the lower Mississippian Limestone secondary confining zone, and the lower part of the Pennsylvanian Cherokee Group. These microimaging logs were interpreted by Schlumberger and the results included in Section 2.0.1 Faults and Fractures. The provided interpretation indicated that conductive fractures are mostly low-height and bed bound with a WNW-ESE orientation (azimuth 320 or 140 degrees). The dominant strike of faults is SW-NE though a significant NW-SW trend is also evident. Fractures induced during drilling have an ENE-WSW orientation that indicates maximum horizontal stress (σ_H) in the AoR is similar to the maximum horizontal stress proposed by Lund Snee and Zoback (2022).

Geomechanical properties for the Arbuckle dolomite can be inferred from examination of the two cores outside the AoR and mineralogical data provided by powder x-ray diffraction. Uniaxial compressive strength is porosity and mineralogy dependent, so we infer that relative uniaxial compressive strength increases with decreasing porosity and increasing P-wave velocity (Benevente et al., 2021). Core acquired during the drilling of the stratigraphic test will be sampled and tested for uniaxial compressive and tensile strength using conventional techniques. Less-invasive/destructive estimates of uniaxial compressive strength such as rebound hardness testing, microdrilling resistance force and P-wave velocity may also be used to estimate rock strength (Benvente et al., 2021) for the Arbuckle injection zone, Woodford-Simpson confining zone, lower Mississippian Limestone and middle and lower Arbuckle baffling interval.

2.5.2 Pore Pressure

Three (3) wells within the model domain (see *Section 3*) which had shut-in fluid levels were used to evaluate the pore pressure gradient within the Arbuckle Group. These data show the current average pore pressure gradient of 0.41 psi/ft.

2.5.3 Stress

Principal horizontal stress direction was determined from drilling induced fractures as described in Section 2.3.1 - Faults and Fractures. Minimum horizontal stress was estimated as insufficient data were available to make confident calculations of the magnitude of minimum horizontal stress from fluid injection pumping rates and leak-off pressures (White et al., 2002). The orientation of

Plan revision number: 0

Plan revision date: 6/24/2025

minimal horizontal stress is NNW – SSE or normal to the WSW – ENE orientation of σ_H . A discussion of the calculation of vertical stress follows.

2.5.3.1 Vertical Stress

Overburden stress, or vertical stress, was calculated from bulk density (Equation 2.1). The density is converted to pressure below ground level. A density (ρ) of 2.5 g/cm³ was used for shallow, missing values. To convert bulk density to pressure, 1 kg/cm is the equivalent of 14.22 psi. The overburden gradient for the project area is estimated to be approximately 1.12 psi/ft.

Equation 2.1—Bulk density.

$$\sigma_V = \rho_a \times g \times Z$$

Where,

ρ_a = average density per foot (where 1 kg/cm² = 14.22 psi)

g = acceleration due to gravity, 32.174 ft/sec²

Z = true vertical depth (ft)

2.5.3.2 Minimum Horizontal Stress (Fracture Gradient)

As no data from the AoR are available for experimentally determining the minimum horizontal stress nor the fracture gradient within the injection or confining zones, it was estimated empirically using Eaton's method (Eaton, 1969).

2.5.3.2.1 Eaton's Method Calculation

Eaton's method (see Equation 2.2) estimates fracture gradient using the overburden stress gradient (see Section 2.5.3.1), the reservoir pressure gradient, (see Section 2.5.2), and Poisson's ratio (see Section 2.5.4).

Equation 2.2—Eaton's method (Eaton, 1969) calculation for estimating fracture gradient.

$$FG = \frac{\nu(\sigma_V - P_p)}{(1 - \nu)} + P_p$$

Where,

FG = Fracture gradient (psi/ft)

P_p = pore pressure (psi)

ν = Poisson's ratio

σ_V = overburden pressure (psi)

2.5.3.2.2 Arbuckle Group

Based on the estimated input values for each parameter described in the sub-sections listed above, the fracture gradient within the Arbuckle Group is estimated to be 0.706 psi/ft:

$$0.706 \frac{\text{psi}}{\text{ft}} = \frac{0.3(1.1 \frac{\text{psi}}{\text{ft}} - 0.41 \frac{\text{psi}}{\text{ft}})}{(1 - 0.3)} + 0.41 \frac{\text{psi}}{\text{ft}}$$

2.5.3.2.3 *Upper Confining Zones*

As discussed in Section 2.5.4, Poisson's ratio has been estimated in the upper confining zones based on dipole sonic log data in the Conservancy 11-3W well located in Section 31, T.28N., R.9E. approximately 10 miles northeast of the AoR. This calculation indicates a relatively wide uncertainty in the calculated value and thus the calculated fracture gradient for both zones, as shown in **Table 2.2**.

Table 2.4—Eaton's (1969) method estimated fracture gradients for the Lower Mississippian and Woodford Shale confining zones based on the uncertainty range of Poisson's ratio for each zone derived from dipole sonic logs in the Conservancy 11-3W well.

Zone	<u>Percentile</u>		
	P10	P50	P90
Lower Mississippian			
Poisson's Ratio	0.247	0.296	0.332
Frac. Gradient (psi/ft)	0.53	0.61	0.67
Woodford Shale			
Poisson's Ratio	0.309	0.351	0.371
Frac. Gradient (psi/ft)	0.63	0.71	0.75

2.5.3.3 Additional Data Collection Plan

A stratigraphic well, Vanguard I-5 will be drilled in order to gather additional data including core and geophysical logs. These efforts will provide data to better characterize mechanical rock properties of the confining and injection zones. Cored material will be used for lab measurements to include bulk density, Young's modulus, Poisson's ratio, bulk modulus, bulk compressibility and Biot's coefficient which will be used to characterize the mechanical properties of the confining and injection zones. Resistivity and Sonic image logs will be run over the confining and injection zones in order to characterize and quantify any fracturing as fractures may affect the sealing capacity of the confining zone and modify the flow characteristics of the injection zone.

2.5.3.3.1 *Maximum Horizontal Stress*

Maximum horizontal stress can be estimated from mechanical tests on core or from wellbore breakout using poro-elastic strain modeling. Core and required geomechanical properties for estimating maximum horizontal stress including Poisson's ratio, Young's modulus, vertical stress and petrophysical properties obtained by open-hole well logging that will be acquired during the drilling of the stratigraphic test well Vanguard I-5.

2.5.3.3.1.1 *Stress Orientation*

Stress orientation within AoR was determined from analysis of the formation imaging log for the Shaw A5-8 well. Principal horizontal (σ_H) stress of WSW – ENE was determined based on the strike of drilling-induced fractures (see Figure 2.45). Minimum stress is normal to principal horizontal stress and is manifested by borehole breakout.

2.5.4 Ductility

Petrophysical log based estimates of Poisson's ratio are available from the Conservancy 11-3W well (**Table 2.2**). The log-based estimates of Poisson's ratio for the Lower Mississippian and Woodford Shale average 0.296 and 0.351 respectively suggest both intervals are not brittle and therefore unlikely to support extensive fracturing. These values will be confirmed by core collected from the upper confining zones and injection zone in Vanguard I-5. Resistivity image logs run in Vanguard I-5 will further quantify the presence of fracture networks and physical properties including fracture orientation, fracture density, and fracture aperture. When interpreted in conjunction with sonic imager data, any observed fracture networks can be classified as open (permeable) or closed (impermeable).

2.5.5 Rock Strength

Rock strength data for the confining zone and injection zone will be characterized by lab measured values of Young's modulus of core recovered from Vanguard I-5. Core plugs will be used to quantity tensile strength. Geophysical logs will be run in order to provide additional estimates of Young's Modulus over the confining and injection zones and provide additional vertical coverage beyond the cored interval.

2.3.1 In-Situ Fluid Properties

In-situ fluid properties such as temperature, salinity, density and viscosity of formation fluids can be difficult to obtain downhole, but sampling and quick analysis of fluid collected during drilling of the stratigraphic well will provide values for these properties at close to in-situ conditions. Temperature corrections to the values obtained for density and viscosity should yield values that approach those for in-situ conditions.

2.3.2 Geothermal Gradient

Drilling mud temperatures were gathered from open hole well log header data, and mud circulation time was considered. Plotting available temperature data with depth yielded a regional thermal gradient of 0.0144°F/ft, which was adopted for the area.

2.6 Seismic History [40 CFR 146.82(a)(3)(v)]

2.6.1 Summary of Seismic History and Available Data

The region encompassing Oklahoma and its surroundings experiences notable seismic activity. Analysis of data from the Oklahoma Geological Survey Earthquake Catalog, updated through March 2024, seismic since events between 1981 and 2023, with **Table 2.6** summarizing these occurrences. **Figure 2.75** highlights a subset of events with magnitudes of 2.5 or higher from 2000 to 2019 attributed to water injection. The USGS documented 3 small magnitude (1.3, 1.3 and 1.48) earthquakes to the west of the AoR between 2013 and February 2025 (**Figure 2.76**). While such small-magnitude events were occasionally recorded previously, catalog completeness typically includes earthquakes with magnitude thresholds of ~2.4 for local magnitude (ml) and 2.7 for moment magnitude (Mwe) since 1980. Within the AoR, there are no recorded seismic events meeting these thresholds, contrasting sharply with elevated seismicity rates in central and

Plan revision number: 0

Plan revision date: 6/24/2025

northcentral Oklahoma and southcentral Kansas, as well as areas adjacent to southwestern Osage County since 2010. As a result, the AoR within Osage County is considered seismically inactive, with neither natural nor anthropogenic seismic activity observed.

Claimed as PBI

Figure 2.36—Locations of historic 1897 to 2002 earthquakes in Oklahoma and earthquakes attributed to water injection during the seismically active period of 2009 to 2019. Earthquake locations and magnitude are from the Oklahoma Geological Survey. The obvious absence of historic seismic events and recent injection-induced events infers stability within the AoR (outlined and shaded red).

Table 2.5—Seismic Events for Osage County from the Oklahoma Geological Survey Earthquake Catalog

Year	Number of Events	Maximum Magnitude	Average Magnitude	Depth (km)
1882 – 1969	0	0	0	ND
1970 – 1979	0	0	0	ND
1980 – 1989	2	1.8	1.7	ND
1990 – 1999	2	2.1	1.75	ND
2000 – 2009	1	1.3		ND
2010 – 2013	0	0	0	
2014	3	2.4	1.8	ND
2015	4	2.9	1.9	5.97
2016	3	2.9	2.0	6.55
2017	1	2.2		4.68
2018	6	2.5	1.78	4.33
2019	14	1.8	0.95	3.97
2020	16	2.3	1.23	5.39
2021	11	2.1	1.45	7.1
2022	6	1.7	1.45	6.98
2023	16	1.8	1.26	5.8

ND – Depth not determined or arbitrarily assigned 5 km. All data from Oklahoma Geological Survey Earthquake Catalog.

Table 2.6—Seismic Events >1.0 M from the United States Geological Survey (USGS) Earthquake Catalog for Osage County between February 2013 and February 2025. Event numbers correspond to numbers shown on Figure 2.76.

Event Number	Magnitude	Depth (km)	Latitude	Longitude	Year
1	2.1	16.2	36.855	-96.288	2021
2	1.48	10.7	36.641	-96.652	2020
3	1.3	1.4	36.805	-96.711	2023
4	1.3	1.6	36.798	-96.705	2023
5	1.7	4.9	36.494	-96.879	2016
6	2.6	4.3	36.500	-96.943	2015
7	2.5	4.8	36.500	-96.950	2015
8	1.2	3.7	36.495	-96.970	2019
9	2.9	8.0	36.487	-96.976	2016
10	1.5	6.1	36.483	-96.990	2024
Average	1.86	6.17			

All data from Oklahoma Geological Survey Earthquake Catalog.

<https://earthquake.usgs.gov/earthquakes/search/>

Plan revision number: 0

Plan revision date: 6/24/2025

Claimed as PBI

Figure 2.37—Seismic events >1.0 M for Osage County and adjacent areas from the United States Geological Survey (USGS) Earthquake Catalog. Numbers for events correspond to tabulated data in **Table 2.7**.

The absence of seismic activity in western Osage County is in part attributable to Arbuckle Group properties (Milad et al., 2024). Subregional karst features within the Arbuckle provide ample permeability and storage potential. Attributes from 3D seismic reflection volumes identify large-relief karst features near the Arbuckle's top (Aboaba and Liner, 2021) and delineate a dense fracture network oriented at approximately N5E and S60E (Elebiju et al., 2011). The N5E fractures are generally sealed under the prevailing east-west maximum stress field, whereas the S60E trend aligns favorably for hydraulic conductivity. Though fracture density decreases with depth in the Arbuckle, the combined fracture systems create a polygonal network in the Arbuckle's upper portion, potentially filled with porous chert, as suggested by seismic coherence attribute (Elebiju et al., 2011).

The sharp increase in seismicity in northcentral Oklahoma since 2010 is attributed to anthropogenic activities, particularly wastewater disposal from hydrocarbon production. High volumes of brine associated with oil extraction are disposed of in the Arbuckle, which underlies most producing zones. Although Arbuckle pore pressures are naturally sub-hydrostatic (Puckette, 1996, Murray and Holland, 2014, and Walsh and Zoback, 2015), fluid injection increases these pressures, potentially perturbing stresses on basement faults, leading to seismic slip. However, Osage County remains anomalously quiet despite similarities in geologic setting, basement rock types and injection practices compared to neighboring seismically active areas.

Crain et al. (2017) suggest that dense intrusions beneath Osage County may have altered the basement's seismogenic potential, limiting fault activation. Gravity and magnetics data indicate the presence of dense intrusions that could reduce permeability and alter stress conditions. These geologic features, combined with lithologic variations, appear to influence seismic hazard on a local scale.

While fluid injection has been linked to regional seismicity (Ellsworth, 2013; Weingarten et al., 2015), local factors, including basement composition and structural history, play a critical role in determining seismic response. For example, areas with thick sedimentary cover or large, minimally fractured intrusions exhibit reduced seismicity, underscoring the importance of geologic controls on induced earthquakes.

2.6.2 Seismic Risk

A preliminary evaluation of seismic risk has been conducted for the NexGen CCS project area in Osage County. This location is characterized by the absence of known faulting in the Paleozoic section and exhibits a very low overall seismic risk based on the following factors:

- **Low incidence of natural (historic) earthquakes** near the CCS site (**Figure 2.75 and Figure 2.76**).
- **Minimal intensity of seismic events**, with maximum surface ground motion not exceeding an intensity of MMI=IV.
- **Sparse population density** in the vicinity of the CCS site, reducing potential exposures and impacts.
- **No history of injection-induced seismicity** associated with Class I or Class II wells in the site vicinity (**Figure 2.75, Figure 2.76 and Figure 2.77**).
- **Absence of identified faults** within the Paleozoic section of the AoR.

The local geology is typified by gently westward-dipping Lower Paleozoic sedimentary rocks that thicken to the south and west, a feature typical of this geological province. The seismicity in this

portion of Oklahoma is unusually quiet compared to other areas of the state, which is attributed to stable intrusion within the basement rock and the location of Osage County to the east of the Nemaha Uplift where long-lived basement-rooted faults generate structures such as the Dillworth and Mervine anticlines (Davis, 1984).

Seismic events are caused when tectonic forces acting on brittle rocks exceed their strength, resulting in sudden rupture. Several factors control a fault's susceptibility to sudden slippage and energy release including orientation of the fault to the direction of maximum horizontal stress, fault surface roughness, rock strength and pore fluid pressure (Birdie et al., 2017). The ratio of the three principal stresses: vertical stress [SV], maximum horizontal principal stress [SHmax], and minimum horizontal stress [Shmin], determines the type of movement along a fault plane (Simpson, 1997). The present stress field and type of expected fault movement are well established in northern Oklahoma and southern Kansas (Lund Snee and Zoback, 2022; Birdie et al., 2017) (**Figure 2.46**). The orientation of the Labette fault at a 45-degree angle to the present stress field diminishes the risk of it becoming seismically active. Basement and carbonate rocks generally have high rock strength, which favors resisting failure while at the same time favoring brittle deformation. Little is known regarding fault roughness and its importance is considered secondary compared to orientation to maximum horizontal stress, a relative importance justified by the orientation of seismogenic faults in northern Oklahoma and the lack of movement along known large faults including the Labette fault (**Figure 2.77**). Information provided by the Oklahoma Geological Survey's Oklahoma Earthquake Catalog clearly shows the majority of recent anthropogenic-induced seismic events are generated in the basement and that the few earthquakes occurring above the basement are located in areas of thicker sedimentary strata. A summary of all seismic events located in Osage County is provided in **Table 2.6**. Though the NexGen CCS site is in an area with low historic seismic activity (**Figure 2.75** and **Figure 2.77**), the surge in injection-induced earthquakes with basement foci (Hu, 2019) warrants isolating injectate and pressure from the sedimentary/basement contact.

Claimed as PBI

Figure 2.38—Correlation of earthquake moment magnitudes (Mw) to known and inferred faults from Hu (2019). Seismic activity is associated with secondary faults associated with major faults and seldom involves principal southwest-northeast trending faults. Major fault trends are labeled and color coded. Abundant Mw 2.5-3.5 earthquakes align with faults subparallel to maximum horizontal stress.

Plan revision number: 0

Plan revision date: 6/24/2025

Given the low historic seismic risk despite years of water injection, a dedicated earthquake response plan is not anticipated to be necessary. However, NexGen Carbon Oklahoma, LLC-Project Vanguard will implement an **Emergency and Remedial Response Plan** to address potential incidents, including natural events such as wildfires, tornadoes, floods, and earthquakes. The plan is detailed in *Section 11* and will include the following elements:

1. **Shutdown procedures** to ensure operational safety during emergencies.
2. **Emergency reporting protocols**, including a clear hierarchy of authority.
3. **Evacuation procedures**, including specific routes and methods for evacuation.
4. **Employee accountability procedures** to ensure all personnel are accounted for after evacuation.
5. **Operational continuity procedures** for staff remaining on-site for critical operations prior to evacuation.
6. **Contact information** for employees responsible for managing and communicating emergency procedures.

Additionally, evaluations have been performed to assess the potential effects of natural events on:

1. The structural integrity of well construction materials.
2. The integrity of the Injection and Confining Zones beneath the NexGen CCS site.

A review of data from the National Earthquake Information Center (Figure 2.55 and Figure 2.56) confirms that Osage County has a low likelihood of seismic activity, further supporting the site's suitability for the proposed CCS project.

Claimed as PBI

Figure 2.39—National Seismic Hazard Model (2023) map displaying the likelihood of damaging earthquake shaking in the United States over the next 100 years (after [Petersen et al., 2023](#)). The red star indicates the location of the AoR.

Plan revision number: 0

Plan revision date: 6/24/2025



Figure 2.40—Simplified seismicity hazard map representing the 2% in 50-year probability of a fixed VS30 760 m/s ground acceleration event¹⁰.

¹⁰ <https://www.usgs.gov/media/images/hazard-map-2023-50-state-update-national-seismic-hazard-model-project> (accessed 1/25/2025)

2.7 Hydrologic and Hydrogeologic Information [40 CFR 146.82(a)(3)(vi), 146.82(a)(5)]

The principal objective of the USEPA injection well program is the safeguarding of human health and the environment, particularly through the protection of potential underground sources of drinking water (USDWs). According to EPA guidelines, a USDW is defined as an aquifer that supplies a public water system and contains less than 10,000 mg/L of total dissolved solids (TDS). The subsequent sections provide a detailed examination of both regional and site-specific hydrogeology and hydrostratigraphy to demonstrate compliance with these standards. [40 CFR 146.82(a)(3)(vi), 146.82(a)(5)]

2.7.1 Hydrostratigraphy and Underground Sources of Drinking Water

The hydrostratigraphy of the AoR and adjacent areas was established using petrophysical logs integrated with surface geology. Cross sections constructed using vintage logs with shallow surface casing and exposed USDWs facilitated determining the distribution of aquifer sandstone and evaluation of water quality in the Vamoosa-Ada aquifer. Examination of these petrophysical logs also allowed a search for minor aquifers that might occur in the Vanoss Group beneath the Vanguard CCS Hub AoR. Petrophysical logs within and adjoining the AoR were analyzed for estimated total dissolved solids (TDS) and solute concentration in parts per million (ppm) using the spontaneous potential (SP) curve and true resistivity (R_t) curve. In areas where no low salinity water was evident on the well log below surface casing, the base of treatable groundwater is assigned the same value as the depth of the base of surface casing.

Assessing groundwater quality in the subsurface is best achieved by sampling. When water analyses from sampling are not available, wireline well log acquired data can be used. Once the wireline well log characteristics of brine-bearing and freshwater bearing aquifers were established, well logs across 11 townships that contain the Vanguard CCS Hub AoR were reviewed to locate the depth of deepest treatable water and cross sections showing the transition from freshwater to moderately saline water or brine in the Vamoosa-Ada aquifer were constructed (**Figure 2.30** and **Figure 2.32** and **Figure 2.29**).

The Class VI permit requires identification of all USDWs within the AoR, especially the lowermost USDW, which is most likely closest to the injection zone. The USDW is defined strictly on the basis of water quality (TDS < 10,000 mg/l). NaCl salinity was estimated from formation water resistivity (R_w) determined using two techniques: (1) true resistivity (R_t) and (2) spontaneous potential (SP). The resistivity method involves first calculating R_{wa} from porosity using the Archie equation (Archie, 1942) and second converting the calculated R_w to salinity (NaCl, mg/L). Formation water resistivity was calculated using 100% water filled pores in shale-free sandstone bodies in which $R_{wa} = R_w$, and since no hydrocarbons are known or expected in the Vamoosa Formation or the Ada Group in western Osage County the equation is simplified to Equation 2.3.

Equation 2.3— R_w calculated from R_t and porosity

$$R_w = \phi^2 * \frac{R_t}{a}$$

Plan revision number: 0

Plan revision date: 6/24/2025

Where,

ϕ = porosity in decimal,

R_t = true formation resistivity,

m = cementation exponent that is 2 for consolidated sandstone, and

α = tortuosity factor that is assigned 0.81 for consolidated sandstone.

R_w is converted to salinity using Equation 2.4.

Equation 2.4—conversion of R_w to NaCl salinity.

$$NaCl = \left((3647.5/(R_w - 0.0123)^{\frac{1}{0.9558}}) \right) * \frac{81.77}{T_f + 6.77}$$

Where,

T_f = formation temperature, and

R_w = Resistivity of formation water.

The calculation of R_w from the spontaneous potential deflection requires knowing the temperature of the formation T_f , resistivity of the drilling mud filtrate at formation temperature R_{mf} , equivalent formation water resistivity R_{we} . Temperature of formation T_f is calculated using Equation 2.5. Resistivity of mud filtrate at surface temperature from the low header is converted to R_{mf} at T_f using formula Equation 2.6. Equivalent formation water resistivity R_{we} is calculated using SP deflection and Equation 2.7. R_{we} is converted to R_w at formation temperature using Equation 2.8.

Equation 2.5—calculation of formation temperature using AMST and BHT.

$$T_f = \left(\frac{BHT - AMST}{TD} \right) (FD) + AMST$$

Where,

BHT = bottom hole temperature from log header,

TD = total depth,

FD = depth of formation being used for calculation,

T_f = formation temperature, and

AMST = annual mean surface temperature (60° F for Osage County) (Oklahoma Climatological Survey (2023).

Equation 2.6—calculation of resistivity of mud filtrate (R_{mf}) at formation temperature (T_f).

$$R_{mf} = \left(\frac{R_{mfsurf}(T_{surf} + 6.77)}{T_f + 6.77} \right)$$

Where,

R_{mf} = R_{mf} at formation temperature,

R_{mfsurf} = R_{mf} at measured surface temperature from log header, and

T_{surf} = measured surface temperature from log headers.

Equation 2.7—calculation equivalent water resistivity (R_{we}) from spontaneous potential (SP)

$$R_{we} = R_{mf} * 10^{\frac{SP}{(61 + 0.133 * T_f)}}$$

Plan revision number: 0

Plan revision date: 6/24/2025

Where,

R_{we} = equivalent R_w , and

SP = deflection of spontaneous potential from shale baseline.

Equation 2.8—conversion of R_{we} is to R_w .

$$R_w = (R_{we} + 0.131 * \frac{10^{\left(\left(\frac{1}{\log(\frac{T_f}{19.9})}\right)^{-2}\right)}}{(-0.5 * R_{we}) + 10^{\log(\frac{T_f}{50.8})}})^{\frac{0.0426}{0.0426}}$$

Porosity values used in the resistivity method were from density-neutron porosity logs and porosity measurements from outcrop samples of the Gypsy (Vamoosa) Sandstone (Doyle and Sweet, 1995). Based on mean values of 22% from the Gypsy Sandstone and similar values from modern logs suites that logged the Vamoosa-Ada aquifer, 22% porosity was used in calculating R_w for the Vamoosa Sandstone on vintage logs without porosity curves. Calculating R_w requires close attention to formation temperature (T_f). At T_f for the Vamoosa-Ada aquifer, a R_w of 0.395 ohm-m will yield a water of \approx 10,000 ppm NaCl. At T_f of 72 degrees Fahrenheit and 22% porosity, R_w of 0.395 yields an R_t of about 7 ohm-m using the resistivity method. If porosity decreases with depth to 20%, the R_t for \approx 10,000 ppm NaCl increases to 8 ohm-m.

Based on the parameters used to separate brine from freshwater with $<$ 10,000 ppm NaCl, available logs within the NexGen Carbon Oklahoma: Project Vanguard site area were analyzed and the results mapped as shown in Appendix A. The mapped base of water $<$ 10,000 ppm NaCl closely matches a map prepared by the USGS and shown in **Figure 2.80** along with cross sections depicting the change in resistivity and SP response in the Vamoosa-Ada aquifer as groundwater transitions from freshwater to saline water (**Figure 2.30 and Figure 2.31**).

As evidenced by cross-sections and maps, much of the AoR is not in an area where USDWs are detected on wireline logs. Deeper treatable water occurs to the east of the NexGen land position in T.27N. and T.28N., whereas in T.26N., it is evident in the eastern part of R.7E. and parts of R.8E. In T.25N., freshwater is evident in the eastern one-half of R.7E. and R.8E. In all areas, USDWs if evident, are separated from the Arbuckle Group injection zone by thick interval of shale-dominated Pennsylvanian strata, the Mississippian Limestone including the lower Mississippian Limestone confining unit and the Woodford Shale. This interval ranges from around 2,000 ft thick in the southeastern part of the Vanguard CCS Hub AoR, to more than 3,000 ft in the northern and western areas. With respect to surface water hydrologic units in Osage County, the AoR is mostly situated on the divide that separates the Salt Creek and Bird Creek/Hominy Creek drainage basins (**Figure 2.80**) (Abbott and Tortorelli, 1999). Streams are scarce and water for livestock is mostly collected and stored in small impoundments or ponds. A small part of the land position is drained directly to the Arkansas River.

2.7.2 Springs

Springs occur when the water table intersects the ground surface. Since the Vamoosa-Ada bedrock aquifer beneath the AoR dips to the west and becomes confined by overlying shale-rich strata, no springs are expected to discharge from the aquifer within the AoR. The top of the saturated zone (water table) in unconfined soil and regolith aquifers follows topography and the AoR is situated along a topographically high drainage divide. Any water saturating pores in the soil or regolith will drain downgradient/downslope to topographically lower areas where discharge into streams may occur.

2.7.3 Water Wells Within the Area of Review

Five (5) domestic-use bedrock groundwater wells occur within the AoR along with three (3) groundwater test wells and two (2) cathode protection wells (OWRB, 2023) (**Figure 2.27**). The closest groundwater monitoring wells associated with the Burbank oil field are approximately three miles west of the AoR (**Figure 2.27**). These wells monitor the Oscar and Vanoss bedrock aquifers as part of ongoing oil recovery operations in the Burbank oil field.



Figure 2.41—Location of most of the AoR on the drainage divide between the Salt Creek and Bird Creek/Hominy Creek drainage basins, resulting in the absence of perennial surface streams within the AoR. Map from Abbott and Tortorelli (1999).

2.8 Geochemistry [40 CFR 146.82(a)(6)]

2.8.1 Fluid Chemistry

Saline brines are present throughout the porous intervals beneath the Vamoosa-Ada aquifer, treated as the lowermost USDW, down to the contact between the Arbuckle Group and basement. Jorgenson and Signor (1996) (**Figure 2.58**) showed the TDS in the Arbuckle aquifer in western Osage County to range from 100,000 to 200,000 ppm. The lack of Arbuckle oil and gas production within the NexGen Carbon Oklahoma: Project Vanguard site prevented acquiring water samples from the Arbuckle saline aquifer within the AoR to determine water chemistry and a TDS value to include in the application. Samples were collected from the Arbuckle Group outside the AoR

Plan revision number: 0

Plan revision date: 6/24/2025

and compared with values reported in the USGS National Produced Waters Geochemical Database (<https://www.usgs.gov/tools/us-geological-survey-national-produced-waters-geochemical-database-viewer>).

2.8.1.1 Methodology for Salinity Determination

The approach used to determine salinity closely parallels the method for identifying Underground Sources of Drinking Water (USDWs). This methodology hinges on calculating the formation water resistivity (R_w) through the application of the Archie equation (Schlumberger, 1972). For the Archie equation (see Equation 2.9) to apply, it is necessary that the formation being evaluated is fully saturated with water, free from clay or shale contaminants (i.e., clean sand), and sufficiently thick to prevent interference from shoulder beds or mud filtrate invasion on resistivity logging tools.

Equation 2.9—Archie equation for calculating water saturation S_w .

$$S_w = \{a * R_w / R_t * \phi^m\}^{1/n}$$

Where:

S_w = water saturation of the formation

n = saturation exponent, typically 2.0 (varies from 1.8 to 4.0)

R_w = formation water resistivity

ϕ = porosity

m = cementation exponent, typically 2.0 (varies from 1.7 to 3.0)

R_t = true resistivity of the formation, adjusted for environmental factors

a = tortuosity factor, typically 0.81 for consolidated sandstones (varies from 0.62 to 2.45)

In shaly formations, the Archie equation tends to overestimate water saturation. Modified equations account for shale volume (V_{shale}) and reduce to the Archie equation when V_{shale} is zero (Asquith and Krygowski, 2004).

In a fully water saturated clean formations such as the Elgin Sandstone of the Vamoosa Formation, the true resistivity (R_t) equals R_o (resistivity of 100% saturated rock) and used to calculate apparent water resistivity (R_{wa}). In this case, the value of R_{wa} approaches and is minimally different from R_w . Furthermore, at the shallow depth of the USDWs, SP values change quickly with changes in salinity making the determination of R_w from SP difficult (Schlumberger, 1972). Therefore, the calculation of R_{wa}/R_w , especially when working with vintage electrical logs, becomes more confident when the resistivity method is used. Induction logging tools, designed to minimize the effects of borehole conditions and invaded zones, provide a highly accurate measure of formation resistivity for values ≤ 2 ohm-meters (Schlumberger, 1987) and can better estimates of R_{wa}/R_w in high salinity brines.

The resistivity of formation waters (R_w) in 100% water saturated shale-free formations was calculated using the R_{wa} formula for the reasons outlined above. This relationship is defined by Equation 2.3.

$$R_w = \phi^2 * \frac{R_t}{a}$$

Plan revision number: 0

Plan revision date: 6/24/2025

Where

ϕ = porosity in decimal,

R_t = true formation resistivity,

m = cementation exponent that is 2 for consolidated sandstone, and

α = tortuosity factor that is assigned 0.81 for consolidated sandstone.

Since the salinity of formation water is overwhelmingly NaCl salinity, R_w is converted to salinity using Equation 2.4:

$$NaCl = \left(\left(\frac{3647.5}{(R_w - 0.0123)} \right)^{\left(\frac{1}{0.9558} \right)} \cdot \frac{81.77}{T_f + 6.77} \right)$$

Where

T_f = formation temperature, and

R_w = Resistivity of formation water.

All calculations of R_w and salinity from wireline logs based on the Archie (1942) equation rely on the aquifer/reservoir being 100% water saturated and shale-free. Natural materials are seldom ideal and therefore, when possible, water samples should be acquired to accurately characterize salinity.

2.8.1.2 Formation Water Properties

As of the initial submission for this Class VI permit application, no wells have been drilled within Osage County to directly sample formation fluids. Fluid samples from the injection interval will be collected and analyzed in accordance with the procedures outlined in the "Pre-Operational Testing and Logging Plan," submitted in *Section 6*. This plan specifies the geological data to be obtained during the drilling and testing phases of the stratigraphic and injection wells.

Table 2.7—Summary table of measured and calculated TDS values for formation waters from relevant zones within a 6-mile buffer of the Vanguard CCS Hub AoR.

Zone	Significance	Depth to Top of Zone (TVD, ft)	Measured TDS (mg/L)	Log Calc. NaCl Equivalent (mg/L)
Vamoosa-Ada	USDW	750	NA	1,260
Vamoosa-Ada	USDW	900	2290	1,809
Tonkawa Ss.	Non-USDW	1260	NA	81,145
Cottage Grove Ss.	Non-USDW	1910	NA	166,360
Mississippian Chat	First Permeable Zone Above the Confining Layer	2950	186497	NA*
Arbuckle Group	Injection Zone	3250	NA	72,110

*Microporosity with high immovable water and oil content prevent meaningful log calculations

Plan revision number: 0

Plan revision date: 6/24/2025

2.8.1.2.1 Injection Zone—Arbuckle Group

Water analyses for the Arbuckle saline aquifer were not published by Jorgenson et al. (1996). During the drilling of the stratigraphic test well, water samples from the Arbuckle Group will be collected and analyzed. Petrophysical log calculated NaCl equivalent salinity was consistently under 100,000 TDS projected by the Jorgenson et al. (1996). A water sample from an Arbuckle producing well located 19 miles to the east of AoR tested a TDS of 115, 829 mg/L, whereas a second water sample located 10 miles east of the AoR tested a TDS of 141, 637 TDS, values that are consistent with the values projected by Jorgenson et al. (1996) and indicates a significant difference in Arbuckle water chemistry from Mississippian water, which has a higher salinity (**Table 2.8b**).

Table 2.8—Salinity Measurements from Water Samples, Osage County, Oklahoma

Lease Name	Well Number	Latitude	Longitude	Reservoir	TDS (mg/L)
Howell	05-2	36.668616°	-96.143998°	Arbuckle	115,829.4
Arsaga	#25-2	36.883231°	-96.494898°	Mississippian Chat	178,731.3
Conservancy	#31-4	36.860121°	-96.369386°	Mississippian Chat	174,568.8
Little Chief	#C-3	36.614431°	-96.624409°	Mississippian Chat	196,322.1
Kern Downey	#M-12	36.635991°	-96.625331°	Mississippian Chat	196,365.5

2.8.1.2.2 Upper Confining Layers

Water analyses for Woodford Shale formation water are not available. In southern Oklahoma, the Woodford Shale produces water where it is chert-rich and fractured, but generally the shale is not known for producing water and in most oil and gas producing areas, it tends to imbibe fracture treatment water.

2.8.1.2.3 First Permeable Zone Above the Confining Layer—Upper Mississippian Limestone

Water samples for Mississippian Chat reservoirs were collected for 4 wells located within 6 miles of the AoR (**Table 2.9**). Salinity calculations for the Mississippian Chat were not attempted because porous and permeable Mississippian Chat contains microporosity within weathered chert that contains immovable formation water and often oil and gas. The salinity values for the Mississippian Chat average 186,497 mg/L, which is considerably higher than the salinity of the Arbuckle sample. Similar differences in water salinity were noted by Watney and Holubnyak (2017) in the Wellington field in southern Kansas (Figure 2.43) and support the premise that Mississippian Chat reservoirs are isolated from the Arbuckle aquifer by low permeability confining zones in the Woodford-Simpson and/or lower Mississippian Limestone.

2.8.1.2.4 USDWs Within the Area of Review

The one published chemical analysis from D'Lugosz et al. (1986) for the Vamoosa-Ada aquifer within the AoR is a 900 ft deep sample from a well in Section 29, T.28N., R.7E. The water is sodium bicarbonate with a high concentration of sulfate and chloride, and slightly saline with a TDS of 2290 mg/L. Calculated NaCl equivalent salinity from vintage logs in the offsetting sections ranged from 1176 to 2442 mg/L.

Plan revision number: 0

Plan revision date: 6/24/2025

Table 2.8c—Water chemistry for the Vamoosa-Ada USDW within the AoR from D'Lugosz et al. (1986)

Loc.	Date	Depth	Ca	Mg	Na+K	HCO ₃	SO ₄	Cl	TDS	Br	Spec. Cond.
28N-7E-29	3-1975	900	8.1	3.4	860	560	860	200	2290	4.5	4000

2.8.2 Solid Phase Geochemistry

An evaluation of regional geochemical data sources, including Department of Energy regional partnership studies, regional analogues, and the USGS produced water database, was undertaken to preliminarily assess CO₂ compatibility with the mineral composition of the target injection zones. This review indicates no anticipated compatibility concerns within the reservoir formations. This preliminary evaluation will be further validated using site-specific geochemical data obtained from rock samples during the drilling of a stratigraphic test or injection well. The procedures for gathering and analyzing this data are detailed in the "Pre-Operational Testing and Logging Plan".

The data collection initiative described in the "Pre-Operational Testing and Logging Plan" will be implemented to thoroughly characterize the mineralogy of both the injection and confining zones. Regional studies conducted for the Department of Energy's partnerships and analysis of comparable formations have not indicated any potential compatibility issues with the reservoir mineralogy.

2.8.2.1 Injection Zone

Four of the five upper Arbuckle Group samples analyzed by Lynch (1990) were more than 95% dolomite with one sample being 49% quartz/chert. In the four samples with high dolomite concentration, quartz was less than 5%. Calcite was present in only two samples and its highest concentration was 4% (Table 2.8d). Published studies of the interaction of CO₂ with minerals in brine filled calcite aquifers shows porosity enhancement close to the injection site but little reaction distally (Seyyedi et al., 2020) Core analysis of injection zone dolomite showed that the reaction of CO₂ and minerals in a dolomite reservoir in West Texas did not generate noticeable changes to the dolomite, though dissolution of sulfate was evident (Mathis and Sears, 1984).

Table 2.9—Measured XRD mineralogy Upper Arbuckle injection zone from Lynch (1990)

Cotter Dolomite (n=5)		
	Average	
Mineral	wt. %	Maximum wt. %
QUARTZ	11.4	49
DOLOMITE	80.8	100
CALCITE	1.2	4

NexGen does not anticipate any adverse chemical reactions from CO₂ injection in the Arbuckle Group. X-ray fluorescence results from 20 measurements collected from the upper Arbuckle (Cotter Dolomite) cores examined by Lynch (1990), indicate the Arbuckle does not contain trace metals that could be liberated by dissolution of formation solids by the injectate. The framework grain mineralogy of the Arbuckle is largely non-reactive or has very slow kinetics under injection conditions.

Plan revision number: 0

Plan revision date: 6/24/2025

Table 2.8e--Chemical Analysis of the Upper Arbuckle Group: Oliphant Nate and Oliphant Lafortune cores. LOD is the limit of detection.

Element	Symbol	Average Concentration (ppm)	Number of Samples with Element	Average Concentration carbonate rocks (ppm)
Barium	Ba	199	17	30–200 ¹
Antimony	Sb	<LOD		
Tin	Sn	<LOD		
Silver	Ag	<LOD		
Uranium	U	3.8	4	1–5 ²
Thorium	Th	<LOD		
Molybdenum	Mo	<LOD		
Niobium	Nb	<LOD		
Zirconium	Zr	5.3	1	
Strontium	Sr	78	17	20–70 ³
Bromine	Br	4.7	16	2–5 ⁴
Arsenic	As	<LOD		
Gold	Au	<LOD		
Lead	Pb	<LOD		
Zinc	Zn	12.4	11	70 ⁵
Copper	Cu	47	17	27 ⁵
Nickel	Ni	<LOD		
Cobalt	Co	<LOD		
Titanium	Ti	134	2	
Phosphorus	P	<LOD		
Vanadium	V	40	16	20 ⁶
Chromium	Cr	26	16	4–10 ⁷

1. Foregs Geochemical Atlas of Europe: [/http://weppi.gtk.fi/publ/foregsatlas/text](http://weppi.gtk.fi/publ/foregsatlas/text)

2. Bell (1963) USGS Professional Paper, 474A.

3. Banner (1995) Sedimentology, 42, 804-824.

4. Panno et al. (1983) Economic Geology, 78, p. 150-156.

5. Brugger (2016) Encyclopedia of Earth Sciences: https://doi.org/10.1007/978-3-319-39193-9_212-1

6. Fischer and Ohl (1968): USGS Bulletin 1316.

7. USGS: https://pubs.usgs.gov/sir/2017/5118/elements/Chromium/Cr_txt.html

2.8.2.2 Upper Confining Zone and Arbuckle Baffle Interval

The Simpson-Woodford Shale confining zone and lower Mississippian Limestone have low permeability that limits the contact of injectate to mineral components. The Woodford Shale is mostly quartz silt and clay-size detrital quartz, illite and calcite as discrete thin beds, fracture filling cement and matrix cement. Since most fractures in the Woodford Shale have low vertical height and tend to terminate against more clay-rich beds, propagation of dissolution along these small fractures would be difficult. The lower Mississippian Limestone is dominantly calcite, but contains

Plan revision number: 0

Plan revision date: 6/24/2025

silt, clay and dolomite. Some reaction with the calcite is expected but contact is restricted by the low permeability.

The Arbuckle Group baffle zone contains low-porosity and low-permeability beds that impede vertical migration and were shown by Watney and Holubnyak (2017) to isolate the upper and lower sections of the Arbuckle Group in the Wellington field, Kansas. Petrophysical logs indicate these beds are dolomite that is with relatively low solubility.

2.8.2.3 First Permeable Zone Above Confining Layer

The first permeable zone above the Simpson-Woodford Shale primary confining layer and lower Mississippian confining zone is porous Mississippian Chat in the upper part of the Mississippian Limestone. Mississippian Chat is mostly silica in the form of chert clasts, small chert grains and quartz cement. These forms of silica are unreactive to acidic fluids and would be stable if contacted by CO₂ and carbonic acid.

2.8.2.4 Underground Source of Drinking Water - Vamoosa-Ada Aquifer

The Vamoosa-Ada aquifer is a quartz-rich sandstone based on thin -section petrography and PE response on petrophysical logs. Chert content increases to the south, toward Arbuckle and Ouachita source areas, but both chert and quartz are unreactive to forms of silica and stable under acidic environments.

2.8.3 Temperature

Determining accurate temperature data from regional sources, rather than directly from a stratigraphic test well, presents challenges. Burke et al. (2020) indicate bottomhole temperature (BHT) measurements are valuable for subsurface thermal regime characterization but have limitations. These include cooling effects from drilling mud infiltration and borehole geometry, as well as the time lag between drilling completion and temperature measurement (Poulsen et al., 2012). Consequently, measured BHTs are frequently lower than actual formation temperatures, as the mud column may not achieve thermal equilibrium.

Cheung (1978) suggested that heat from depths exceeding 600 miles cannot reach the upper crust solely through conduction and that processes such as igneous intrusion and volcanism contribute significantly to geothermal anomalies observed at the surface. Factors influencing geothermal gradients include:

- Climate
- Thermal conductivity
- Abnormal pore pressure
- Fluid migration
- Tectonics
- Distribution of radioactive isotopes

Thermal gradient maps serve as correction tools to approximate true bottomhole temperatures. The geothermal gradient, or the temperature increase with depth, is typically calculated by applying corrections to raw BHT data. These corrected gradients are then smoothed and contoured to generate maps (Ruppel et al., 2005).

Plan revision number: 0

Plan revision date: 6/24/2025

Cheung (1978) utilized equilibrated temperature data, including temperature logs, shut-in gas well pressure tests, and air-drilled wells, to study geothermal gradients in Oklahoma. Corrections for BHT discrepancies were applied by comparing BHT and equilibrated temperature differences as a function of depth. A near-surface temperature, extrapolated from reliable data, was used as a control point to construct linear gradients for areas with single-depth data. Harrison et al. (1983) identified two distinct geothermal gradient patterns in Oklahoma: one for normally pressured formations and another for abnormally pressured formations in deep Anadarko and Ardmore basins. The low gradients in these basins reflect their thick sedimentary sections and abnormally pressured formations, which restrict upward heat flow. Conversely, high gradients in the Arkoma Basin suggest a tectonic origin associated with a continental margin or rift zone.

In areas outside the Arkoma Basin, geothermal gradients are primarily linked to basement topography and fluid migration. Notably, several geothermal anomalies correlate with oil and gas accumulations, particularly in abnormally pressured formations. These findings suggest that Oklahoma's geothermal gradients are significantly influenced by basement relief.

For the Arbuckle Group within the Area of Review (AoR), the Harrison et al. (1983) geothermal gradient map indicates a gradient of approximately 15 degrees F per 1,000 ft. However, gradients of 16 degrees F per 1,000 ft are calculated from using bottom hole temperatures from well logs. Using a mean annual surface temperature of 60 degrees F, a gradient of 16 degrees/1000 ft, bottom hole temperature of approximately 108 degrees F at 3,000 ft below ground. This estimate aligns well with observed BHT data, which indicate temperatures of approximately 110 degrees F at the same depth. Many temperatures recorded during logging are slightly less as a result of transient cooling effects from drilling fluids. In the Arbuckle Group, recorded bottomhole temperatures range from 10 degrees F (upper interval) to 125 degrees F (lower interval), consistent with these gradient estimates. For the NexGen CCS site, preliminary estimates place the BHT at 124 degrees F at 4,000 ft. This estimate will be refined with site-specific data collected during the drilling of a stratigraphic test or injection well.

2.8.4 Salinity

A regional salinity distribution map from Jorgensen et al., (1996) highlights Arbuckle aquifer salinity values, which range from <1000 TDS in recharge areas to 100,000 to 200,000 TDS near the Vanguard CCS Hub AoR. To obtain more accurate local data, fluid samples will be collected from a stratigraphic test well drilled prior to injection operations.

2.8.5 Viscosity

Viscosity measures a fluid's resistance to flow. Since viscosity is density and temperature dependent, no effort to calculate viscosity was attempted. When water samples are collected from the stratigraphic test well, brine density and viscosity will be determined.

2.8.6 Additional Properties

Additional geochemical and reservoir properties of the Arbuckle Group will be determined through a stratigraphic test well to be drilled. This data collection effort will refine understanding of the reservoir characteristics relevant to carbon sequestration.

2.87 Compatibility of CO₂ with Subsurface Fluids and Minerals

Although no direct studies of CO₂-brine interactions have been conducted at the NexGen CCS site, a relevant analog exists 55 miles northwest in the Wellington Field, Sumner County, Kansas

Plan revision number: 0

Plan revision date: 6/24/2025

(Holubnyak et al., 2017). In this small-scale sequestration project, CO₂ was injected into the upper Mississippian reservoir from January to June 2016, with 20,000 metric tons of CO₂ successfully sequestered. Although Arbuckle injection was planned, permitting constraints limited injection to the Mississippian Formation. Key findings from the project included:

- **Injection Details:** 1,101 truckloads delivered 19,803 metric tons of CO₂, averaging 120 tons per day.
- **Production Impact:** CO₂ injection increased average oil production by ~68%, with ~18% of the injected CO₂ recovered.
- **Retention & Monitoring:** The high CO₂ retention and effective monitoring techniques provide valuable insights into reservoir behavior and risks for long-term CO₂ storage.

At the NexGen site, CO₂-rock interactions will be evaluated in terms of both short-term injection dynamics and long-term storage. Key concerns include the risk of exceeding the capillary entry pressure of the confining shale, which could enable CO₂ migration out of the reservoir. However, the small pore size and viscous drag of shale provide natural resistance to upward migration. Acidification of brine by CO₂ could also alter pore structures, depending on the reaction kinetics and heterogeneity of the caprock (Espinoza & Santamarina, 2017).

Short-term interactions during and immediately after injection will be evaluated through direct observation, while long-term interactions will rely on modeling and predictive tools. The primary factors influencing CO₂-rock interactions include:

- Dissolution of CO₂ in brine
- Acid-induced reactions with reservoir rocks
- Reactions driven by changes in brine concentration
- Clay desiccation
- Interactions with other non-CO₂ gases in the injection stream

Claimed as PBI

Figure 2.42—Regional distribution of salinity in the Arbuckle aquifer after Jorgenson et al. (1996). Approximate location of the Vanguard CCS Site AoR is shown by the yellow star.

A comprehensive sampling program has been designed to analyze both injection interval and caprock geochemistry. This program will examine geochemical parameters, including potential reactions at operational interfaces such as wellbore, cements, host rock, and caprock. This approach ensures a thorough evaluation of the site's compatibility with CO₂ storage requirements.

2.9 Other Information (Including Surface Air and/or Soil Gas Data, if Applicable)

2.10 Site Suitability [40 CFR 146.83]

2.10.1 Structural and Tectonic Suitability

The NexGen CCS project site in Osage County is situated on the Cherokee Platform that dips gently at less than 2 degrees to the west toward the Nemaha Uplift. Regionally, the platform extends across much of northeastern Oklahoma, southeastern Kansas and southwestern Missouri (Charpentier, 1995). In Osage County, the platform is underlain by the Osage High, a large igneous intrusion located southeast of the site. The Vanguard CCS Hub AoR is located in an area of gentle westerly dip between the Nemaha Fault Zone to the west and the Osage High. The area is tectonically stable and has not experienced the induced seismicity observed in neighboring counties with higher frequencies of basement faulting. The AoR is structurally monotonous without frequent large-offset basement-rooted faults that extend into the Mississippian and Pennsylvanian section like the Nemaha Fault zone, or anticlinal structures such as the folds over the basement hills on the Osage High. The AoR does straddle the basement-confined Labette Fault, which based on all evidence is inactive and has not hosted seismicity.

2.10.2 Storage Reservoir Suitability (Injection Zone)

The Arbuckle Group on the platform in Kansas and Oklahoma has been extensively studied and identified as a premier saline aquifer sequestration zone (Milad et al., 2024; Holubnyak et al., 2017). This regional saline aquifer is essentially continuous across the Midcontinent region and only absent over where it thins and ultimately truncated over the geographically small, buried hills such as those on the Osage High.

Osage County has a long history of hydrocarbon exploration dating back to the early 20th century, though production from the Arbuckle Group in western Osage County off the Osage High is uncommon compared to Upper Mississippian “chat” and Pennsylvanian sandstone reservoirs such as the Burbank Sandstone. The NexGen CCS site lies to the east of the giant Burbank field and to the west-northwest of the Osage High that is populated with buried granite hills that form structural traps in the overlying Arbuckle Group and Mississippian Chat reservoirs.

As a result of sparse Arbuckle Group production in western Osage County few exploratory wells are drilled to the Arbuckle. The AoR features relatively limited shallow well density and only 16 deep penetrations. The Arbuckle Group, a dolomite dolomitic limestone-rich interval, is proposed as the primary injection zone. Found at depths of 3,420 to 4,520 ft, this porous and permeable interval offers approximately 900 to 1,000 ft of brine-bearing rocks of which the upper 50-60% is the proposed injection zone. Deposited during the late Cambrian to middle Ordovician, the Arbuckle Group is predominantly dolomite divided into formations based on insoluble residues, paleontology and geochemistry. The Arbuckle thickens southwest of the site and dips gently west-southwest. An in-zone monitoring well will be constructed east of the injection site to observe pressure changes and the CO₂ plume's interaction with potential regional up-dip flow paths. Karsted intervals within the Arbuckle are expected to have enhanced porosity and permeability, increasing CO₂ storage capacity. The Arbuckle contains only saline water zones, and a stratigraphic test well will provide detailed geomechanical and petrophysical data for both confining and reservoir strata.

Plan revision number: 0

Plan revision date: 6/24/2025

Multiple confining units above and a flow boundary below the injection zone have been identified and will be further evaluated with stratigraphic testing. The primary upper confining unit is the combined Simpson Group shale and Woodford Shale, while the basal flow boundary consists of permeability baffles within the Arbuckle Group. A secondary upper confining zone is dense carbonate in the lower Mississippian Limestone. Regional permeability data indicates values <1 mD for these confining units. Core samples from the stratigraphic test well will confirm the geomechanical, and sealing properties of these zones. The Woodford Shale is regionally extensive, whereas the Simpson Group shale is distributed across the southern part of the site. Permeability baffles that separate the Arbuckle Group into upper, middle and lower intervals are stacked low-porosity and low-permeability zones evident on density-neutron porosity logs and microresistivity permeability logs. Baffles evident in the site area are also identified in southern Kansas in similar stratigraphic positions (Holubnyak et al., 2017). These upper and basal seals, which are not transected by mappable basement-rooted faults, will confine the CO₂ plume to the upper and middle Arbuckle injection zone and prevent vertical migration.

While research on the reaction of CO₂ and the Arbuckle dolomites is not available, CO₂ injection for tertiary oil recovery has been successfully conducted in dolomite reservoir facies of the Permian San Andres Formation in West Texas, which has similar lithologies and saline characteristics. Studies of closely spaced cores in the San Andres dolomite study demonstrated minimal reaction between host rock and CO₂ injectate (Mathis and Sears, 2024). Data from successful CO₂ sequestration in the upper Mississippian Limestone in a pilot study in Kansas help demonstrate the efficacy of the lower Mississippian confining unit and isolation of the upper Mississippian from the Arbuckle Group (Holubnyak et al., 2017). This study and data from San Andres CO₂ floods demonstrate that the NexGen site expects minimal compatibility issues with the injection and confining intervals. These findings suggest a low likelihood of detrimental CO₂-rock interactions, a hypothesis to be validated by testing injection and confining intervals during the project's pre-construction phase.

Preliminary modeling of the CO₂ plumes predicts minimal movement after cessation of injection due to the area's low formation dip rate. Of the 224 Arbuckle penetrations drilled within the AoR between the 1960s and mid-1980s, evaluations have been conducted to determine whether additional wellbore isolation or replugging is necessary.

2.10.3 Storage Capacity of the Injection Zone

The NexGen's static model—built on reservoir characteristics captured during site characterization—and the storage-capacity methodology of Bachu (2006) demonstrate that the Arbuckle Group can accommodate substantially more than the 71 million metric tons of CO₂ planned for Phase 1. Given the Arbuckle's basin-wide continuity, high porosity (7–12 %) and permeability (tens to $>1,000$ mD), and absence of stratigraphic or structural spill points, the maximum theoretical storage capacity extends well beyond our initial 71 M t. This conservative planning target reflects operational constraints and pressure-front management considerations, not the formation's in-place pore volume.

Plan revision number: 0

Plan revision date: 6/24/2025

Equation 2.10—CO₂ storage volume calculation (after Bachu 2006).

$$V_{CO_2} = (A \times H \times \emptyset \times (1 - Sw_{irr}) \times \rho_{CO_2} \times EF) \times 10^{-6}$$

Where:

V_{CO_2} = CO₂ Storage Volume (Mt)

A = area (m²)

H = net thickness (m)

\emptyset = porosity (v/v)

Sw_{irr} = irreducible water saturation

ρ_{CO_2} = density of CO₂ (reservoir conditions)

EF = Efficiency Factor – defined here as the ratio of the volume of CO₂ injected to the net pore volume (pore volume excluding irreducible water) at the final storage pressure.

Solid-phase geochemical literature on the Arbuckle Group, as well as pore water chemistry data, indicates no significant potential for interactions between the carbon dioxide steam and the formation or dissolved minerals that could impact storage capacity.

2.10.4 Summary of Site Suitability

The site's suitability is supported by regional data from company-owned oil and gas operations and thorough evaluations of available information. Key conclusions include:

- 1. Absence of USDWs within the AoR:** Limited underground sources of drinking water are located within the southern and eastern parts of the AoR.
- 2. Robust confining zones:** Multiple layers restrict vertical fluid migration out of the injection zone.
- 3. Low seismic risk:** The geologic setting minimizes the potential for induced seismicity due to injection operations.
- 4. Sufficient injection zone capacity:** The Arbuckle Group can accommodate the expected CO₂ injection volumes.

Regional petrophysical data underpin preliminary reservoir modeling, and subsequent data acquisition will confirm these results.

Prior to construction, surveys will be conducted to identify archaeological or cultural sites and assess the presence of threatened or endangered species. No mines, quarries (Oklahoma Department of Mines, 2022), or subsurface cleanup sites exist within or near the AoR; NexGen will maintain full access to the injection site during all project phases. The site, while located in Osage County and within Osage Nation tribal lands, is situated on private property owned by NexGen, with the Osage Nation retaining only mineral rights. Proximity to existing CO₂ pipeline infrastructure and industrial CO₂ emitters enhances the site's logistical advantages.

The site's geological attributes, including the properties of its confining and injection zones, make it highly suitable for carbon sequestration while protecting USDWs. The absence of major basement-rooted faulting that extends into the Paleozoic section within the AoR, and the Arbuckle depositional processes that generated internal baffles within the Arbuckle Group that insulate the basement from injected fluids, will maintain the region's seismic stability. Together, these factors support the NexGen CCS project as a promising site for safe and effective CO₂ storage.

2.11 References

Abbott, M. M., and R. L. Tortorelli, 1999, Surface-water characteristics and quality on the Osage Reservation, Osage County, Oklahoma, 1999, Water-Resources Investigations Report 02-4060, 60 p.

Aboaba, O., and Liner, C., 2021, Mississippian Chat and tripolite zones in Osage County, Oklahoma: Paleokarst interpretation based on 3D seismic and well logs. Interpretation, 9(3), T711-T726.

Ajayi, T., Gomes, J. S., and A. Bera, 2019, A review of CO₂ storage in geological formations emphasizing modeling, monitoring, and capacity estimation approaches: Petroleum Science, v. 16, p. 1028-1063.

Akin, R., 1964. Map of Arbuckle pools in Osage County: Tulsa Geological Society Digest, v. 32, p. 36. https://archives.datapages.com/data/tgs/digest/data/032/032001/36_tgs320036.htm?q=%2BauthorStrip%3Aakin

Al Atwah, I., Puckette, J., Pantano, J., Arouri, K., and J. M. Moldowan, 2019, Organic Geochemistry and Crude Oil Source Rock Correlation of Devonian-Mississippian Petroleum Systems in Northern Oklahoma: AAPG Memoir 122. p. 301-321.

Al-Shaieb, Z., Puckette, J., Abdalla, A., and P. Ely, 1995. Megacompartment complex in the Anadarko basin: A completely sealed overpressured phenomenon, in P. Ortoleva (ed.), Basin compartments and seals, AAPG Memoir 61, p. 55-68. <https://store.aapg.org/detail.aspx?id=748>

Archie, G. E., 1942, The electrical resistivity log as an aid in determining some reservoir characteristics: Journal of Petroleum Technology, v. 5, p. 54-62.

Asquith, G., and D. Krygowski, 2004, Spontaneous potential, in G. Asquith and D. Krygowski, Basic well log analysis: AAPG Methods in Exploration 16, p. 21-30.

Bachu, S. and Adams, J.J., 2003, Sequestration of CO₂ in Geological Media in Response to Climate Change: Capacity of Deep Saline Aquifer to Sequester CO₂ in Solution. Energy Conversion and Management, 44, 3151-3175.

Bachu, S., 2006, The potential for geological storage of carbon dioxide in northeastern British Columbia: Summary of Activities, 2006, B.C. Ministry of Energy, Mines and Petroleum Resources, p. 1-48.

Banner, J. L., 1995. Application of the trace element and isotope geochemistry of strontium to studies of carbonate diagenesis: Sedimentology, 42, p. 805-824. <https://www.jsg.utexas.edu/banner/files/Application-of-isotope-and-trace-Sedimentology-1995.pdf>

Bell, K. E., 1963. Uranium in carbonate rocks: USGS Professional Paper 474A, 29 p. <https://pubs.usgs.gov/pp/0474a/report.pdf>

Benavente, D., Fort, R., and M. Gomez-Heras, 2021. Improving uniaxial compressive strength estimation of carbonate sedimentary rocks by combining minimally invasive and non-destructive technique: International Journal of Rock Mechanics and Mining Sciences, v. 147, p. 1-9. <https://doi.org/10.1016/j.ijrmms.2021.104915>

Birdie, T., Holubnyak, E., Watney, L., Bidgoli, T., Hallenbach, J., and M. Fazelalavi, 2017, Assessing induced seismicity risk at the Wellington geologic sequestration site: <https://www.netl.doe.gov/sites/default/files/event-proceedings/2017/carbon-storage-oil-and-natural-gas/posters/Tiraz-Birdie-Seismic-Risk-Evaluation-at-the-Wellington--Kansas--CO2-Geologic-Storage-Site.pdf>

Boardman, D. R., II, Puckette, J. O., Watney, W. L., Cemen, I., Cruse, A. M., and D. D. Hurst, 2009, The Eagles Bluff Shale: a new upper Devonian black shale formation in the Ozark Uplift of northeastern Oklahoma, northwestern Arkansas, and southwestern Missouri: Geological Society of America Abstracts with Programs, v. 41, no. 2, p. 12.

Boardman, D. R., II, Nestell, M. K., and L. W. Knox, 1995, Depth-related microfaunal biofacies model for Late Carboniferous and early Permian cyclothemic sedimentary sequences in Mid-Continent North America, in Sequence Stratigraphy of the Mid-Continent, N. J. Hyne, ed., p. 93-118.

Boyd, D. T., 2008, Stratigraphic guide to Oklahoma oil and gas reservoirs: Oklahoma Geological Survey Special Publication 2008-1, 2 p.

Brugger, J., 2016. Encyclopedia of Earth Science Series, zinc. https://doi.org/10.1007/978-3-319-39193-9_212-1

Burke, L. A., Pearson, O. N., and Kinney, S. A., 2020, New method for correcting bottomhole temperatures acquired from wireline logging measurements and calibrated for the onshore Gulf of Mexico basin, U.S.A.: U.S. Geological Survey Open-File Report 2019-1143, 12 p.

Cain, C. L., 2018, Deciphering the Cleveland Sandstone Stratigraphic Framework: Differentiating the Kiefer and Owasso Sandstone Complexes, North-Central and Northeastern Oklahoma: unpublished M.S. thesis, Oklahoma State University, 118 p. <https://openresearch.okstate.edu/entities/publication/4756697b-f34b-4940-9841-be4c051666e0>

Callner, S. A., 2014, An integrated approach to understanding sedimentary structures and depositional processes in Devonian-Mississippian black shale: the Woodford Shale and associated strata in the southern Midcontinent: unpublished M.S. thesis, Oklahoma State University, 91 p.

Campbell, J. A., and J. L. Weber, 2006, Wells drilled to basement in Oklahoma: Oklahoma Geological Survey Special Publication 2006-1, 6 p.

Cardott, B. J. and J. B. Comer, 2021, Woodford Shale (Upper Devonian to Lower Mississippian): from hydrocarbon source rock to reservoir: Oklahoma Geological Survey Bulletin 152, 100 p.

Cardott, B. J., 2018, Bibliography of Oklahoma hydrocarbon source rocks: Oklahoma Geological Survey

Cheung, P. K. S., 1978, Geothermal Gradient in Sedimentary Rocks in Oklahoma: unpublished M.S. thesis, Oklahoma State University, 55 p.

Childress, M., and G. M. Grammer, 2019, Characteristics of debris flows and outrunner blocks - evidence for Mississippian deposition on a distally steepened ramp, in G. M. Grammer, J. M. Gregg, J. O. Puckette, P. Jaiswal, S. J. Mazzullo, M. J. Pranter, and R. J. Goldstein, eds., Mississippian reservoirs of the midcontinent: AAPG Memoir 122, p. 131-150.

Comer, J. B. and H. H. Hinch, 1987, Recognizing and quantifying expulsion of oil from the Woodford Formation and age-equivalent rocks in Oklahoma and Arkansas: AAPG Bulletin, v. 71, No. 7, p 844-858.

Cope, C. C., 2003, Grain size and mineralogic characteristics of alluvium and terrace deposits, Osage Reservation, Oklahoma: unpublished M.S. thesis, Oklahoma State University, 155 p.

Crain, K., Chang, J. C., and J. I Walter, 2017, Geophysical anomalies of Osage County and its relationship to Oklahoma seismicity: American Geophysical Union, Fall Meeting 2017, abstract #S23C-0816.

Davis III, H. G., 1984, Wrenching and oil migration, Mervine field area, Kay County, Oklahoma, the Shale Shaker Digest XI, vols. XXXIII-XXXV (1982-1985), 145-158.

Denison, R. E., 1981, Basement rocks in northeastern Oklahoma: Oklahoma Geological Survey Circular 84, 84 p.

Denison, R. E., Lidiak, E. G., Bickford, M. E., and Kisvarsani, E. B., 1984, Geology and geochronology of Precambrian rocks in the central interior of the United States: U. S. Geological Survey Professional Paper 1241-C, 20 p.

Derby, J. R., Raine, R. J., Runkel, A. C., and M. P. Smith, 2012, Paleogeography of the great American carbonate bank of Laurentia in the earliest Ordovician (early Tremadocian): The Stonehenge transgression, in J. R. Derby, R. D. Fritz, S. A. Longacre, W. A. Morgan, and C. A. Sternbach, eds., The great American carbonate bank: The geology and economic resources of the Cambrian-Ordovician Sauk megasequence of Laurentia: AAPG Memoir 98, p. 5-13.

Dille, A. C., 1956, Paleotopography of the Precambrian surface of northeastern Oklahoma: unpublished M.S. thesis, University of Oklahoma.

Plan revision number: 0

Plan revision date: 6/24/2025

D'Lugosz, J. J., McClafin, R. G., and M. V. Marcher, 1986, Geohydrology of the Vamoosa-Ada Aquifer east-central Oklahoma: Oklahoma Geological Survey Circular 87, 42 p.

Doyle J. D. and M. L. Sweet, 1995, Three-dimensional distribution of lithofacies, bounding surfaces, porosity, and permeability in a fluvial sandstone-Gypsy Sandstone of northern Oklahoma: AAPG Bulletin 79, p. 70-95.

Eaton, B. A., 1969. Fracture gradient prediction and its application in oilfield operations: Journal of Petroleum Technology, v. 21, no. 10, p. 1353-1360. <https://doi.org/10.2118/2163-PA>

Elebiju, O. O., Matson, S., Keller G. R., and K. J. Marfurt, 2011, Integrated geophysical studies of the basement structures, the Mississippi chert, and the Arbuckle Group of Osage County region, Oklahoma: AAPG Bulletin v. 95, no. 3, p. 371-393.

Ellsworth, W. L., 2013, Injection-Induced Earthquakes. Science, Vol 341, Issue 6142.

Ethington, R. L., and R. I. Dresbach, 1990, Ordovician conodonts in the Arbuckle Group, southern Arbuckle Mountains, Oklahoma, in Early to Middle Paleozoic conodont biostratigraphy of the Arbuckle Mountains, southern Oklahoma, S. M. Ritter ed., Oklahoma Geological Survey Guidebook 27, p. 33-38.

Ethington, R. L., Repetski, J. E., and J. R. Derby, 2012. Ordovician of the Sauk megasequence in the Ozark region of northern Arkansas and parts of Missouri and adjacent states, in J. R. Derby, R. D. Fritz, S. A. Longacre, W. A. Morgan, and C. A. Sternbach, eds., The great American carbonate bank: The geology and economic resources of the Cambrian-Ordovician Sauk megasequence of Laurentia: AAPG Memoir 98, p. 275-300. <https://doi.org/10.1306/13331496M983496>

Firkins, M., 2021. Seismic characterization of intra-basement deformation and its influence on the overlying sedimentary strata: implications for tectonic evolution and induced seismicity inn northern Oklahoma.

Fischer, R. P., and J. P. Ohl, 1970. Bibliography on the geology and resources of vanadium to 1968: USGS Bulletin 1316, 168 p. <https://doi.org/10.3133/b1316>

Foltz, K., Snider, A., and J. Puckette, 2016, Composition and mechanical properties of the Woodford Shale, northern Oklahoma: AAPG Search and Discovery Article #51220.

Foregs, 2005. Foregs Geochemical atlas of Europe, R. Salminen (chief-editor). <http://weppi.gtk.fi/publ/foregsatlas/text>

Fritz, R. D., Medlock, P. M., Kuykendall, M. J. and J. L. Wilson, 2012, Fritz, R. D., Medlock, P. M., Kuykendall, M. J. and J. L. Wilson, 2012, The geology of the Arbuckle Group in the midcontinent: Sequence stratigraphy, reservoir development, and the potential for hydrocarbon exploration, in J. R. Derby, R. D. Fritz, S. A. Longacre, W. A. Morgan, and C. A. Sternbach, eds., The great Amercian carbonate bank: The geology and economic resources of the Cambrian-Ordovician Sauk megasequence of Laurentia: AAPG Memoir 98, p. 203-273.

GSA, 2022, Geologic Time Scale version 6.0. <https://www.geosociety.org/GSA/gsa/timescale/home.aspx>

Gerhard, L. C., 2004, A new look at an old petroleum province: Current Research in Earth Sciences, Bulletin 250, part 1, p. 1-27.

Gilbert, C., 2014, The Wichita Mountains in Oklahoma, their story through time: Oklahoma Geological Survey Guidebook 39, 39 p.

Ham, W. E., 1973, Regional geology of the Arbuckle Mountains, Oklahoma, Oklahoma Geological Survey, Guidebook for Field Trip No. 5, The Geological Society of America 1973 Annual Meeting: Dallas, TX, p. 56.

Plan revision number: 0

Plan revision date: 6/24/2025

Harrison, W. E., Luza, K. H., Prater, M. L. and P. K. Cheung, 1983. Geothermal resource assessment in Oklahoma: Oklahoma Geological Survey Special Publication 83-1, 42 p. <http://ogs.ou.edu/docs/specialpublications/SP83-1.pdf>

Heckel, P. H., 1986, Sea-level curve for Pennsylvanian eustatic marine transgressive-regressive depositional cycles along midcontinent outcrop belt, North America: *Geology*, v. 14, p. 330-334.

Heran, W. D., Green, G. N., and D. B. Stoeser, 2003, A digital geologic map database for the State of Oklahoma: USGS Open-File Report OF-2003-247 <http://pubs.usgs.gov/publication/ofr03247>

Hill, E., 2017, Core and wireline log based, shelf to basin stratigraphic framework of Mississippian strata, east-central Oklahoma: unpublished M.S. thesis, Oklahoma State University, 292 p.

Holubnyak, Y., Watney, W. L., Birdie, T., Rush, J. and M. Fazelalavi, 2017, Reservoir Modeling of CO₂ Injection in Arbuckle Saline Aquifer at Wellington field, Sumner County, Kansas: Kansas Geological Survey Open-File Report 2016-29, 10 p.

Houseknecht, D., 1986, Evolution of a passive margin to foreland basin: the Atoka Formation of the Arkoma basin, south-central U.S.A: Special publications International Assoc. Sediment, v. 8, p. 327-345.

Hu, X., 2019, Faults in northeastern Oklahoma: their occurrence and relationship to hydrocarbon production and modern seismic activity: unpublished M.S. thesis, Oklahoma State University, 56 p.

Hunt, J., 2017, Conodont biostratigraphy in middle Osagean to upper Chesterian strata, north-central Oklahoma, USA: unpublished M.S. thesis, Oklahoma State University, 179 p.

Hurd O., and M. D. Zoback, 2012, Intraplate earthquakes, regional stress and fault mechanics in the central and eastern U.S. and southeastern Canada: *Tectonophysics* 581 (2012) p. 182-192.

Ireland, H. A., 1944, Regional correlation and subsurface studies of the Arbuckle Group of rocks in Oklahoma: Tulsa Geological Society Digest, v. 13, (1944-1945), p. 57-60.

Jakucs, L., 1977. Morphogenetics of karst regions: New York, John Wiley and Sons, 284 p. https://books.google.com/books/about/Morphogenetics_of_Karst_Regions.html?id=5ciEAAAAIAAJ

Jennings, C. J., 2014, Mechanical Stratigraphy of the Mississippian in Osage County, Oklahoma. Graduate Theses and Dissertations Retrieved from <https://scholarworks.uark.edu/etd/2347>

Johnson K. S., 2008, Geologic Cross Section of Oklahoma, in Earth sciences and mineral resources of Oklahoma, K. S. Johnson and K. V. Luza eds., Oklahoma Geological Survey Education Publication 9, p. 7.

Johnson, K. S. and B. J. Cardott, 1992, Geologic framework and hydrocarbon source rocks of Oklahoma, in K.S. Johnson and B.J. Cardott, eds., Source rocks in the southern Midcontinent, 1990 symposium: OGS Circular 93, p. 21-37.

Jorgenson, D. G., Helgensen, J. O., Signor, D. C., Leonard, R. B., Imes, J. L., and S. C. Christenson, 1996, Analysis of regional aquifers in the central Midwest of the United States in Kansas, Nebraska, and parts of Arkansas, Colorado, Missouri, New Mexico, Oklahoma, South Dakota, Texas, and Wyoming: Summary: USGS Professional Paper 1414, 67 p.

Jorgenson, D. G., and D. C. Signor, 1981, Plan of study for the central midwest regional aquifer system analysis in parts of Arkansas, Colorado, Kansas, Missouri, Nebraska, New Mexico, Oklahoma, South Dakota and Texas: USGS Water Resources Investigation, Open-File Report 81-206, 28 p.

Kampman N., Bickle M., Wigley, M., and B. Dubacq, 2014, Fluid flow and CO₂-fluid-mineral interactions during CO₂-storage in sedimentary basins: *Chemical Geology*, v. 369, p. 22-50.

Keeling, R. M., 2016, Stratigraphic interpretation and reservoir implications of the Arbuckle Group (Cambrian-Ordovician) using 3D seismic, Osage County, Oklahoma. Graduate Theses and Dissertations Retrieved from <https://scholarworks.uark.edu/etd/1557>

Keller, W., Reynolds, R., and A. Inoue, 1986, Morphology of clay minerals in the smectite-to- illite conversion series by scanning electron microscopy. *Clays and Clay Minerals*, 34(2), 187- 197.

Keller, G. R., 2014, The Southern Oklahoma Aulacogen: It's a classic: Oklahoma Geological Survey Guidebook 38, N. Suneson ed., p. 389-391.

Kleinschmidt, R. E., and P. B. Lorenz, 1976, North Burbank Unit tertiary recovery pilot test - Annual Report: May 1975- May 1976, BERC/TPR-76/2 (July 1976).

Kolawole, F., Morgan, C. B., Chang, J. C., Marfurt, K. J., Lockner, D. A., Reches, Z., B. M. Carpenter, 2019. The susceptibility of Oklahoma's basement to seismic reactivation. <https://www.nature.com/articles/s41561-019-0440-5>

Krumme, G. W., 1981, Stratigraphic Significance of Limestones of the Marmaton Group (Pennsylvanian, Desmoinesian) in Eastern Oklahoma, Oklahoma Geological Survey, OGS Bulletin 131, p. 1-60.

Lillie, R. J., Nelson, K. D., Voogd, B.D., Brewer, J. A., Oliver, J. E., Brown, L. D., and S. Kaufman, 1983, Crustal Structure of Ouachita Mountains, Arkansas a Model based on integration of COCORP reflection profiles and regional geophysical data: AAPG Bulletin, v. 67, pp. 907-931.

Lund Snee, J.-E., and M. D. Zoback, 2022, State of stress in areas of active unconventional oil and gas development in North America: AAPG Bulletin, v. 106, no. 2, p. 355–385.

Luza, K. V., 2009, Earthquakes of Oklahoma, in Earth sciences and mineral resources of Oklahoma, K. S. Johnson and K. V. Luza, eds., Oklahoma Geological Survey Education Publication 9, p. 9.

Lynch, M. T., 1990, Evidence of paleokarstification and burial diagenesis in the Arbuckle Group of Oklahoma: unpublished M.S. thesis, Oklahoma State University, 163 p.

Lynch M. T., and Z. Al-Shaieb, 1991, Paleokarstic features and thermal overprints observed in some of the Arbuckle cores in Oklahoma, in Arbuckle Core Workshop and Field Trip, K.S. Johnson, ed., Oklahoma Geological Survey Special Publication 91-3, p. 31-68.

Marsh, S., and A. Holland, 2016, Comprehensive Fault Database and Interpretive Fault Map of Oklahoma: Open File Report OF2-2016. 15 pages.

Mashburn, S. L., Cope, C. C., and M. M. Abbott, 2003, Aquifer Characteristics, Water Availability, and Water Quality of the Quaternary Aquifer, Osage County, Northeastern Oklahoma, 2001-2002, USGS Water-Resources Investigations Report 03-4235.

Mathis, R. L., and S. O. Sears, 1984, Effect of CO₂ Flooding on dolomite reservoir rock, Denver Unit, Wasson (San Andres) field, TX: Soc. Pet. Eng. AIME, Pap.; (United States), Vol. SPE13132; Conference: 59. annual Society of Petroleum Engineers of AIME technical conference, Houston, TX, USA, 16 Sep 1984.

Mazzullo, S. J., Wilhite, B. W., Boardman, D. R., Morris, B. T., and C. Godwin, 2019, Lithostratigraphy, biostratigraphy, stratigraphic architecture, and depositional systems in Lower to Middle Mississippian strata on the western flank of the Ozark Dome, Midcontinent U.S.A., in G. M. Grammer, J. M. Gregg, J. O. Puckette, P. Jaiswal, S. J. Mazzullo, M. J. Pranter, and R. J. Goldstein, eds., Mississippian reservoirs of the midcontinent: AAPG Memoir 122, p. 25-58.

McCarthy, K., Rojas, K., Nieman M., Peters, K., and A. Stankiewicz, 2011, Basic Petroleum Geochemistry for Source Rock Evaluation: Schlumberger Oilfield Review 23, no. 2, p. 32-43.

Plan revision number: 0

Plan revision date: 6/24/2025

McCracken, E., 1955, Correlation of insoluble residue zones of upper Arbuckle of Missouri and southern Kansas: American Association of Petroleum Geologists, Bulletin, v. 39, p. 47-59.

McCullough, B. J., and R. M. Slatt, 2015, Paleotopographic control on the variability of Woodford Shale strata across the southern Cherokee Platform area of central Oklahoma: a mechanism for increased preservation-potential of organic content: AAPG Search and Discovery, Article # 51125.

McKnight E. T., and R. P. Fischer, 1970, Geology and ore deposits of the Picher field Oklahoma and Kansas: Geological Survey Professional Paper 588, 165 p.

Milad B., Moghanloo, R. G., and N. W. Hayman, 2024, Assessing CO₂ geological storage in Arbuckle Group in northeast Oklahoma: Fuel, v. 356, <https://doi.org/10.1016/j.fuel.2023.129323>.

Miser, H. G., 1954, Geologic Map of Oklahoma, <http://ogs.ou.edu/docs/geologicmaps/GeologicMapofOklahoma.pdf>

Morgan, B. C., and K. E. Murray, 2015, Characterizing small-scale permeability of the Arbuckle Group Oklahoma, Oklahoma Geological Survey Open File Report (OF-2-2015), 12 p.

Morris, A., Ferrell, D. A., and D. B. Henderson, 1996, Slip-tendency analysis and fault reactivation

Murray, K. E. and A. A. Holland, 2014, Subsurface fluid injection in oil and gas reservoirs and wastewater disposal zones of the Midcontinent: Search and Discovery Article #80377.

National Park Service, 2015, National Park Service, Vendome Well, https://www.nps.gov/chic/learn/nature/vendome_well.htm

Newell, K. D., Peterie, S. L., and R. D. Miller, 2024, Study to establish a measurement protocol for accurately estimating regional Arbuckle properties in south-central Kansas: Kansas Geological Survey Open-File Report 2024-12, 41 p.

Oklahoma Corporation Commission, 2024, Salt water disposal records: Oklahoma Corporation Commission, <https://oklahoma.gov/occ/divisions/oil-gas/induced-seismicity-and-uic-department/salt-water-disposal-records-by-county.html>

OCWP, 2012, Oklahoma Water Resources Board Oklahoma Comprehensive Water Plan Executive Report, 2012 update, 159 p.

Oklahoma Mesonet, 2024, Past data, <https://www.mesonet.org/past-data>

Osborn, N. I., and R. H. Hardy, 1999, Statewide groundwater vulnerability map of Oklahoma: Oklahoma Water Resources Board Technical Report 99-1, 15 p.

Over, D. J., 1992, Conodonts and Devonian-Carboniferous boundary in the upper Woodford Shale, Arbuckle Mountains, south-central Oklahoma: Journal of Paleontology, v. 66, no. 2, p. 293-311.

OWRB, 2011, Oklahoma Water Resources Groundwater Well Record Search, <https://oklahoma.gov/owrb/data-and-maps/interactive-maps.html>

Panno, S. V., Hardbottle, G., Sayre, E. V., and W. C. Hood, 1983. Genetic implications of halide enrichment near a Mississippi Valley-type ore deposit: Economic Geology, 78, p.150-156. <https://experts.illinois.edu/en/publications/genetic-implications-of-halide-enrichment-near-a-mississippi-vall>

Perdue Petroleum, 2020, North Burbank Unit (NBU) CO₂ Monitoring, Reporting, and Verification (MRV) Plan, 88 p.

Plan revision number: 0
Plan revision date: 6/24/2025

Perry, W. J., Jr., 1989, Tectonic Evolution of the Anadarko Basin Region, Oklahoma: U.S. Geological Survey Bulletin 1866A, p. 1-28.

Peterson, M. D., Shumway, A. M., [...] and R. C. Witter and 51 others, 2023. The 2023 US 50-State National Seismic Hazard Model: Overview and implications: *Earthquake Spectra*, Sage Journals, v. 40, issue 1, p. 5-88. <https://doi.org/10.1177/87552930231215428>

Puckette, J. O., 1996, Evaluation of underpressured reservoirs as potential repositories for liquid wastes: unpublished Ph.D. dissertation, Oklahoma State University, 273 p.

Rascoe, B., Jr., and N. J. Hyne, 1988, Petroleum geology of the Mid-Continent: Tulsa Geological Society Special Publication No. 3, 162 p.

Reeves, K. T., Johnson, I. W., Guo, G., Sharma., B., Chen, K. C., and H. B. Carroll, 1999, Exploration 3D seismic field test, Native Tribes Initiative: U.S. Department of Energy, p. 1-74.

Roberts, M. T., 2005, Geologic profiles derived from seismic data west and east of the Arkansas-Oklahoma State line, Arkoma basin and frontal Ouachita Mountains, in Stratigraphic and Structural Evolution of the Ouachita Mountains and Arkoma Basin, Southeastern Oklahoma and West-Central Arkansas: Application to Petroleum Exploration: Oklahoma Geological Survey, Circular 112b, N. H. Suneson, I. Cemen, and R. M. Slatt, eds., p. 17-24.

Rogers, S., 2001, Deposition and diagenesis of Mississippian Chat reservoirs, north-central Oklahoma, AAPG Bulletin, v. 85, no. 1, p. 115-129.

Rountree, J. H., 1980, Petroleum geology of the Arbuckle Group, southern Osage and eastern Pawnee counties, Oklahoma: unpublished M.S. thesis, Oklahoma State Oklahoma, 71 p.

Ruppel, S.C., Jones, R.H., Breton, C.L., and Kane, J.A., 2005, Preparation of maps depicting geothermal gradient and Precambrian structure in the Permian Basin. Contract report to the U.S. Geological Survey Order No. 04CRSa0834.

Saadatpoor, E., Bryant, S. L., and K. Seperhrnoori, 2010, New trapping mechanism in carbon sequestration: Transport in Porous Media v. 82, p. 3-17.

Schlumberger, 1987, Log Interpretation Principles/Applications, Schlumberger Educational Services, Houston, Texas, p. 198.

Schlumberger, 1972, Determination of R_w , in Log Interpretation, Volume I - Principles, p. 77-80.

Sellars, R. B., Jr., 1967, The Siluro-Devonian rocks of the Ouachita Mountains: Tulsa Geological Society Digest, v. 35, p. 231-241.

Seyyedi, M., Mahmud, H. K. B., Verall, M., Giwelli, A., Estaban, L., Ghasemiziarani, M., and B. Clennell, 2020, Pore Structure Changes Occur During CO_2 Injection into Carbonate Reservoirs

Shelton, J. W., Ross, J. S., Garden, A. J. and J. L. Franks, 1985, Geology and mineral resources of Payne County, Oklahoma: OGS Bulletin 137, 85 p.

Simpson, R. W., 1997, Quantifying Anderson's fault types: *Journal of Geophysical Research*, v. 102, no. B8, p. 17909–17919.

Skoumal, R. J., Barbour, A. J., Rubinstein, J. L., and M. E. Glasgow, 2024, Reduced injection rates and shallower depths mitigated induced seismicity in Oklahoma: *The Seismic Record*, 4(4) p. 279-287.

Snider, A., 2014, Characterization of the Woodford Shale in southern Noble and northern Payne counties, Oklahoma: unpublished M.S. thesis, Oklahoma State University, 80 p.

Stein, S., Stein, C. A., Blavuscunas E., and J. Kley, 2015, Using Lake Superior parks to explain the Midcontinent Rift: Park Science, v. 32(1)- Summer 2015.

Stein, C., Kley, J., Stein, S., Hindle, D., and R. G. Keller, 2015, North America's Midcontinent Rift: when rift meets LIP: *Geosphere* v. 11 (5): GESO1183.1, p. 1607-1616.

Sweeney, R. E., and P. L. Hill, 2005. Nebraska, Kansas and Oklahoma aeromagnetic and gravity maps and data: a web site for distribution of data, Data Series 138, online report. <https://pubs.usgs.gov/ds/2005/138/neksok.html> <https://pubs.usgs.gov/ds/2005/138/neksok.html>

Swinea, T., Lopez, M., Bacon C. and J. Puckette, 2011, Spectral gamma ray investigation of the West Spring Creek Formation (Ordovician), Upper Arbuckle Group, southern Oklahoma; AAPG Search and Discovery Article # 90133.

Terrell, D. M., 1972, Trend and genesis of the Pennsylvanian Elgin Sandstone in the western part of the northeastern Oklahoma: unpublished M.S. thesis, Oklahoma State University, 79 p.

Thomas, W. A., 2014, The southern Oklahoma transform-parallel intracratonic fault system: Oklahoma Geological Survey Guidebook 38, N. Suneson ed., p. 375-387.

Thorman, C. H., and M. H. Hibshman, 1979, Status of mineral resource information for the Osage Indian Reservation, Oklahoma, Bureau of Indian Affairs Administrative Report BIA-47, 60 p.

United States Geological Survey. Chromium. https://pubs.usgs.gov/sir/2017/5118/elements/Chromium/Cr_txt.html

Vanden Berg, B., LeBlanc, S., and G. M. Grammer, 2019, Integrated reservoir characterization to provide insight into porosity and permeability in a mixed carbonate-siliciclastic reservoir, in G. M. Grammer, J. M. Gregg, J. O. Puckette, P. Jaiswal, S. J. Mazzullo, M. J. Pranter, and R. J. Goldstein, eds., Mississippian reservoirs of the midcontinent: AAPG Memoir 122, p. 227-270.

Walsh, F. R., and Zoback, M. D., 2015, Oklahoma's recent earthquakes and saltwater disposal: *Sci. Adv.* 1, e1500195 (2015).

Walter, J. I., Ogwari, P., Thiel, A., Ferrer, F., Woelfel, I., Chang, J. C., Darold, A. P., and A. A. Holland, 2020, The Oklahoma Geological Survey Statewide Seismic Network: *Seismol. Res. Lett.*, 91 (2A): 611–621.

Watney, W. L., and Y. Holubnyak, 2017, Small scale field test demonstrating CO₂ sequestration in Arbuckle saline aquifer and by CO₂-EOR at Wellington field, Sumner County, Kansas: Final Report prepared for NETL, Department of Energy under Award Number DE-FE00006821. 123 p.

Weingarten, M., Ge, S., Godt, J. W., Bekins, B. A., and Rubinstei, J. L., 2015, High-rate injection is associated with the increase in U.S. mid-continent seismicity. *Science*, 1336-1340.

West, A., 2015, Pennsylvanian subsurface sequence stratigraphy based on 3D seismic and wireline data in western Osage County, Oklahoma. Graduate theses and dissertations retrieved from <https://scholarworks.uark.edu/etd/1073>

White, A.J., Traugott, M.O. and R. E. Swarbrick, 2002. The use of leak-off test as means of predicting minimum horizontal in-situ stress, *Petroleum Geoscience*, Vol. 8 2002, p.189-193. <https://doi.org/10.1144/petgeo.8.2.189>

Xu, T., Apps, J. A., and K. Pruess, 2001. Analysis of Mineral Trapping for CO₂ Disposal in Deep Aquifers, Lawrence Berkely National Laboratory publications, 104 p. <https://escholarship.org/uc/item/6wv7v0gn>

Plan revision number: 0

Plan revision date: 6/24/2025

Yielding, G., 2002. Shale gouge ratio - calibration by geohistory, in Hydrocarbon Seal Quantification, A. G. Koestler and R. Hunsdale (ed.); NPF Special Publication 11, p. 1-15.
https://www.researchgate.net/publication/248596801_Shale_Gouge_Ratio-Calibration_by_Geohistory

Yielding, G., Freeman, B., and T. Needham, 1997. Quantitative fault seal prediction: AAPG Bulletin 81, p. 897-917.
<https://archives.datapages.com/data/bulletns/1997/06jun/0897/0897.htm?q=%2BauthorStrip%3Ayielding>

3.0 AoR AND CORRECTIVE ACTION

AoR and Corrective Action GSDT Submissions

GSDT Module: AoR and Corrective Action

Tab(s): All applicable tabs

Please use the checkbox(es) to verify the following information was submitted to the GSDT:

- Tabulation of all wells within AoR that penetrate confining zone *[40 CFR 146.82(a)(4)]*
- AoR and Corrective Action Plan *[40 CFR 146.82(a)(13) and 146.84(b)]*
- Computational modeling details *[40 CFR 146.84(c)]*

The complete Area of Review (AoR) and Corrective Action Plan Report has been submitted through the GSDT platform. All required data fields within the module have been appropriately filled and included in the submission.

This report provides a detailed overview of the computational modeling methods used to delineate the AoR, the Corrective Action Plan addressing existing well penetrations within the AoR, and the schedule for reevaluating the AoR once injection operations commence. A comprehensive review of the geology and hydrogeology of the site has been included as an appendix to the main report, accompanied by an extensive bibliography citing references utilized during the AoR modeling and reporting processes.

The AoR and Corrective Action Plan Report meets the regulatory requirements set forth in 40 CFR 146.82(a)(13), 146.84(b), and 146.84(c).

4.0 FINANCIAL RESPONSIBILITY

Financial Responsibility GSDT Submissions

GSDT Module: Financial Responsibility Demonstration

Tab(s): Cost Estimate tab and all applicable financial instrument tabs

Please use the checkbox(es) to verify the following information was submitted to the GSDT:

Demonstration of financial responsibility **[40 CFR 146.82(a)(14) and 146.85]**

NexGen Carbon Oklahoma, LLC (NexGen) is demonstrating financial responsibility in compliance with 40 CFR 146.85. NexGen anticipates utilizing one or a combination of the following mechanisms: (1) Surety Bonds, (2) Trust Accounts, or (3) Insurance, to ensure coverage of costs related to corrective action, emergency and remedial response, injection well plugging, post-injection site care, and site closure.

All required information has been submitted via the GSDT platform, with all relevant data fields within the module completed and included in the submission.

Plan revision number: 0

Plan revision date: 6/24/2025

5.0 INJECTION WELL CONSTRUCTION

All information satisfying 40 CFR §146.82(a)(9), (11), and (12) and 40 CFR §146.86 is described in **05_Construction_Details_NexGen_Vanguard-Merge.pdf**.

6.0 PRE-OPERATIONAL LOGGING AND TESTING

Pre-Operational Logging and Testing GSDT Submissions

GSDT Module: Pre-Operational Testing

Tab(s): Welcome tab

Please use the checkbox(es) to verify the following information was submitted to the GSDT:

Proposed pre-operational testing program ***[40 CFR 146.82(a)(8) and 146.87]***

All information satisfying 40 CFR 146.82(a)(8) and 146.87 is described in **06_Pre-Operational_Testing_NexGen_Vanguard.pdf**.

Plan revision number: 0

Plan revision date: 6/24/2025

7.0 INJECTION WELL OPERATION 40 CFR 146.82(7) & (10)

All information satisfying 40 CFR 146.82(a)(7) and (10) is described in **07_Inj_Well_Ops_NexGen_Vanguard.pdf**.

8.0 TESTING AND MONITORING

Testing and Monitoring GSDT Submissions

GSDT Module: Project Plan Submissions

Tab(s): Testing and Monitoring tab

Please use the checkbox(es) to verify the following information was submitted to the GSDT:

Testing and Monitoring Plan *[40 CFR 146.82(a)(15) and 146.90]*

All information satisfying 40 CFR 146.82(a)(15) and 146.90 is described in **08_TM_Plan_NexGen_Vanguard.pdf**

9.0 INJECTION WELL PLUGGING

Injection Well Plugging GSDT Submissions

GSDT Module: Project Plan Submissions

Tab(s): Injection Well Plugging tab

Please use the checkbox(es) to verify the following information was submitted to the GSDT:

Injection Well Plugging Plan ***[40 CFR 146.82(a)(16) and 146.92(b)]***

All information satisfying 40 CFR 146.82(a)(16) and 40 CFR 146.92(b) is described in **09_Plugging_Plan_NexGen_Vanguardpdf**.

10.0 POST-INJECTION SITE CARE (PISC) AND SITE CLOSURE

PISC and Site Closure GSDT Submissions

GSDT Module: Project Plan Submissions

Tab(s): PISC and Site Closure tab

Please use the checkbox(es) to verify the following information was submitted to the GSDT:

PISC and Site Closure Plan [*40 CFR 146.82(a)(17) and 146.93(a)*]

GSDT Module: Alternative PISC Timeframe Demonstration

Tab(s): All tabs (only if an alternative PISC timeframe is requested)

Please use the checkbox(es) to verify the following information was submitted to the GSDT:

Alternative PISC timeframe demonstration [*40 CFR 146.82(a)(18) and 146.93(c)*]

All information satisfying 40 CFR 146.82(a)(17) and 146.93(a) is described in
10_PISC_SC_Plan_NexGen_Vanguard.pdf.

11.0 EMERGENCY AND REMEDIAL RESPONSE

All information satisfying 40 CFR 146.82(a)(19) and 146.94(a)] is described in **11_ERRP_NexGen_Vanguard.pdf**.

Emergency and Remedial Response GSDT Submissions

GSDT Module: Project Plan Submissions

Tab(s): Emergency and Remedial Response tab

Please use the checkbox(es) to verify the following information was submitted to the GSDT:

Emergency and Remedial Response Plan **[40 CFR 146.82(a)(19) and 146.94(a)]**

12.0 INJECTION DEPTH WAIVER AND AQUIFER EXEMPTION EXPANSION

Not Applicable—No injection depth waiver nor aquifer exemption expansion is requested or required.

Injection Depth Waiver and Aquifer Exemption Expansion GSDT Submissions

GSDT Module: Injection Depth Waivers and Aquifer Exemption Expansions

Tab(s): All applicable tabs

Please use the checkbox(es) to verify the following information was submitted to the GSDT:

- Injection Depth Waiver supplemental report *[40 CFR 146.82(d) and 146.95(a)]*
- Aquifer exemption expansion request and data *[40 CFR 146.4(d) and 144.7(d)]*